OPTIXPLORER

Laboratory Tutorials
Hardware Operating Instructions
Software Operating Instructions

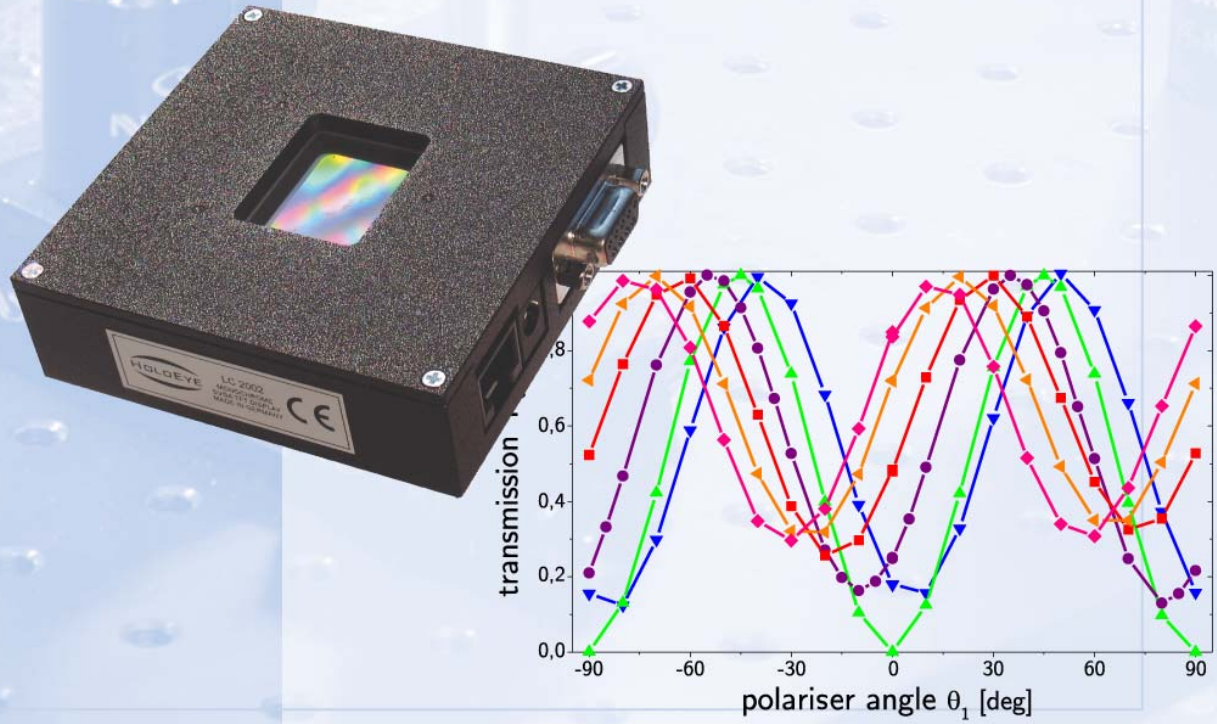

HOLOEYE

Pioneers in Photonic Technology

Note

The instructions provided in this document are required for the correct usage of the devices and serves the prevention of danger. All persons who apply or use, care for, maintain and control the components of the kit should read the instructions and follow them carefully. This document is an essential part of the 'OptiXplorer' kit and should always be at the user's disposal.

The provided laser is a class 3B laser, therefore special safety measures have to be taken. Both direct and indirect irradiation of this laser is dangerous for the eyes.

* * *

Copyright notice

This document is subject to alteration without notice.

Version of this document: 2.8f

Brief overview of the OptiXplorer

Six experimental modules with many tasks illustrate the wide area of physical phenomena, which can be investigated experimentally with the OptiXplorer. These are e.g. optical setup of a projector, properties of polarised light, optical properties of liquid crystals, phase modulation and amplitude modulation of light fields, diffraction of light at dynamically changing structures, diffractive optical elements (DOEs) and their interaction, spatial frequency filtering and phase-shifting interferometry.

Main component of the OptiXplorer is the spatial light modulator (SLM) 'LC2002'. The device is a general purpose and easy-to-use device for displaying images by use of a monochrome, transparent liquid crystal display (LCD). It simplifies the application of LCDs in experimental setups, e.g. for prototype development or in research labs. The small size of the device and its comfortable control interface are major characteristics for enabling an easy usage.

The device is designed to be plugged into the graphics board of a personal computer with a resolution up to SVGA format, i.e. 800 x 600 pixels. The device converts colour signals into corresponding grey level signals. The SLM can be plugged into a personal computer using the serial RS-232 port. After installing the LC2002 driver software, the image parameters of the LCD can be easily controlled by the computer. The driver software always saves the current setting of the image parameters. Hence, whenever the system is started this latest setting will be loaded automatically.

For the experimental realisation a diode laser module with integrated beam-expanding optics, two polarisers with rotatable mounts, several optomechanical components, and the required cables and power supplies are provided.

The provided 'OptiXplorer' software offers the tools to implement the named optical functions on the SLM. The LC2002 control software allows the comfortable configuration of the SLM via the serial RS232 port. Furthermore, two measurement control programmes, 'PhaseCam' and the LabView™ programme 'DynRon', are provided for the described experiments.

Thus, the OptiXplorer is suitable for introductory and advanced laboratory classes in physics and engineering study courses.

Acknowledgement of co-operation with universities

The theoretical introduction and the experimental tutorials have been created in cooperation with and incorporating feedback from several universities in Germany. We would like to thank our partners for their valuable contributions and suggestions for further improvement.

We would like to name the authors of the most substantial contributions:

Prof. Dr. Ilja Rückmann, Dr. Tobias Voß – Universität Bremen

PD Dr. Günther Wernicke, Humboldt-Universität zu Berlin

Dipl.-Phys. Stephanie Quiram (AG Prof. H.J. Eichler), Technische Universität Berlin

Dipl.-Ing. (FH) Sven Plöger (AG Prof. J. Eichler), Technische Fachhochschule Berlin

Of course we welcome further feedback and invite all users to contribute ideas for further experiments or to provide additions to the theoretical introduction. We are sure there are many more interesting laboratory experiments that can be done using the OptiXplorer.

Dr. Andreas Hermerschmidt, HOLOEYE Photonics AG

Components of the OptiXplorer

The following components are delivered with the OptiXplorer:

- 1 LCD image display device LC2002
- 1 Power supply 15V= / 0,8A
- 1 RS-232 adapter cable
- 1 VGA monitor cable
- 1 LC2002 mounting ring

- 1 Laser module with focus-adjustable beam expander
- 1 Mounting ring
- 1 Power supply 5V / 1A

- 1 OptiXplorer manual
- 1 CD-ROM with software

- 2 Power supply adapters (for local electricity sockets)

Extra components within the advanced version:

- 2 Rotary polarisers
- 4 Posts
- 4 Post holders
- 4 Rail carriers
- 1 Rail 30 cm

TABLE OF CONTENTS

1 Introduction to the topics of the OptiXplorer

The diffraction of light at dynamically adjustable optical elements as represented by the LC cells of a spatial light modulator can be described by the transmission through the LC material, which is characterized by its electro-optical properties, and the then following pattern formation due to propagation of the diffracted wave. Diffractive optical elements (DOEs) are used more and more in modern optical instruments. The optical function is caused by the diffraction and interference of light in contrast to refractive optical components. Spatial light modulators offer the dynamical realization of diffractive optical elements.

The usage of diffraction and interference requires tiny structures in the dimension of the optical wavelength. The fabrication of such small structures became possible in the context of modern methods of nanotechnology. Lithographical production technologies and replication processes have made it possible to mass produce DOEs. Thus diffractive optical elements, which can potentially replace lenses, prisms, or beam-splitters and can even be used to create image-like diffraction patterns, are easier to produce and more compact than their refractive counterparts, if these exist all.

A well-known visible application of DOEs in the consumer market is an optical head to be mounted on a laser pointer to create arrows, crosses and other patterns. It is less well-known that some digital cameras for the consumer market make use of a DOE and a weak (and therefore eye-safe) infrared laser diode for their autofocus system.

In more technical applications, DOEs are often used as viewfinder systems which enable to see at which point a device or tool is working, or as spot-array generators e.g. for 3-D surface measurements. Also, diffractive optical beam-splitters can create arrays of beams with the same intensity in a geometrical grid. Such elements are used for example to measure objectives and telescope mirrors faster and more precisely compared to measurements with one beam or with mechanical scan devices.

In the experiments a liquid crystal micro-display will be used as a spatial light modulator to create diffractive optical structures, for exploration of dynamical diffracting objects as well as the investigation of the functionality and the physical properties of the device itself.

Liquid crystal displays (LCDs) with pixel sizes significantly smaller than 100 µm are used nowadays in digital clocks, digital thermometers, pocket calculators, video and data projectors and rear projection TVs. Due to the low cost, robustness, compactness and the advantage of electrical addressing with low power consumption, LCDs are superior to other technologies.

I THEORETICAL FOUNDATIONS

2 Preliminary remarks

Six experiments have been chosen for the OptiXplorer, covering several topics in optics including the optical setup of a projector, properties of polarised light, optical properties of liquid crystals, the modulation of phase, amplitude and polarisation of light fields, the diffraction of light at dynamically changing structures, Diffractive Optical Elements (DOEs), and interferometry (phase shifter).

This chapter is dedicated to provide a introduction into fields, which are either not dealt with in a similar way in existing textbooks or may not be discussed in a way that makes certain connections between subjects which are considered necessary for understanding the experimental tutorials. Wherever the existing textbooks cover subjects in a way that was considered without a doubt to be sufficient (and of course often much more than that) for understanding the experiments, examples of such books will be given as reference. There will be, however, some sections in which content are presented which is well-covered in textbooks already, just in order to make some connections within this chapter and also to avoid a too much fragmented presentation of the subjects.

3 Electro-optical properties of liquid crystal cells

Liquid crystals (LCs) are considered a phase of matter, in which the molecule order is between the crystalline solid state and the liquid state. The LCs differ from ordinary liquids due to long range orders of their basic particles (i.e. molecules) which are typical for crystals. As a result they usually show anisotropy of certain properties, including dielectric and optical anisotropies. However, at the same time they show typical flow behaviour of liquids and do not have stable positioning of single molecules.

There are different types of liquid crystals, among which are *nematic* and *smectic* liquid crystals. Nematic liquid crystals show a characteristic linear alignment of the molecules, they have an orientation order but a random distribution of the molecule centres. Smectic liquid crystals additionally form layers, and these layers have different linear orientation directions. Therefore smectic liquid crystals have an orientational *and* a translational order.

For usage in LCD’s, liquid crystals are arranged in spatially separated cells with carefully chosen dimensions. The optical properties of such cell can be manipulated by application of an external electric field which changes the orientation of the molecules in a reversible way. Due to the long range order of the molecules and the overall regular orientation, a single LCD element features voltage-dependent birefringent properties. Therefore an incidental light field sees different refraction indices for certain states of polarisation. Therefore an LCD element can change the polarisation state of such a light field specifically by providing a well-defined voltage.

The LC cells have boundaries which are needed to firstly separate the cell and secondly to accommodate the wires needed for addressing each cell with an independent voltage value (i.e. the electric field). Because the cells are arranged in a regular two-dimensional array, the cell boundaries act as a two-dimensional grating and produce a corresponding diffraction effect.

3.1 Twisted nematic LC cell

The following discussion will focus on LCD based on *twisted nematic* liquid crystals. In the cells of such LCDs, the bottom and the top cover have alignment structures for the molecules which are typically perpendicular to each other. As a result of the long range

order of the LC, the molecules form a helix structure, which means that the angle of the molecular axis changes along the optical path of light propagating through the LC cell.

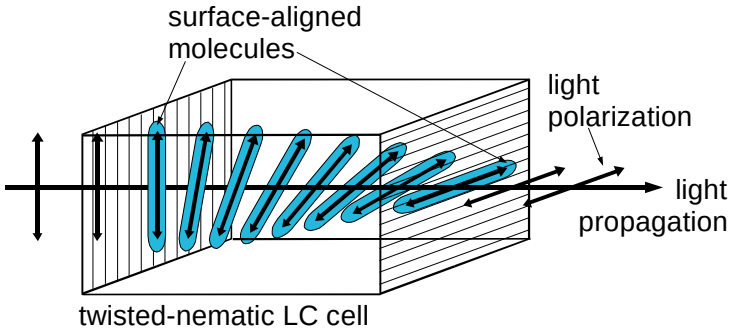

Figure 1: Polarisation-guided light transmission

The helix structure of twisted nematic crystals can be used to change the polarisation status of incident light. When the polarisation of the light is parallel to the molecules of the cell at the entrance facet, the polarisation follows the twist of the molecule axis. Therefore the light leaves the LC cell with a polarisation that is perpendicular to the incident polarisation.

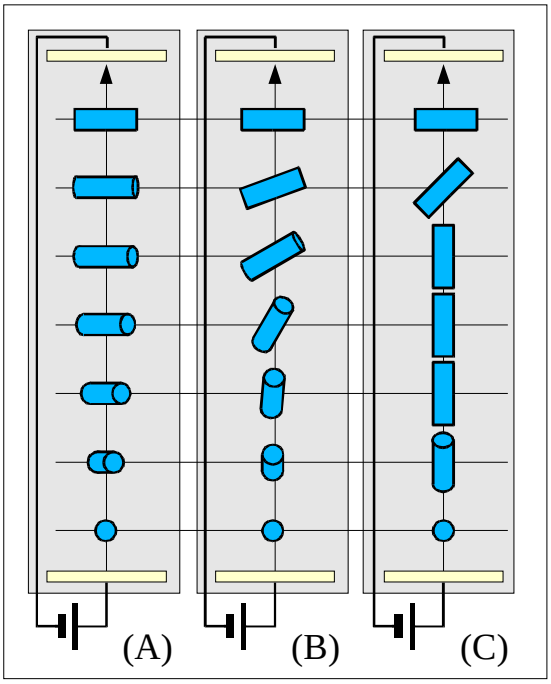

Figure 2: LC cells with different applied voltages: $V_A = 0$ with twisted, but untilted molecules, $V_B > V_{thr}$ with tilted, partially aligned molecules, $V_C \gg V_{thr}$ with aligned molecules in the central region of the cell.

In order to realize a dynamic optical element, a voltage is applied to the LC cell. This voltage causes changes of the molecular orientation, as is illustrated in Figure 1 for three voltages V_A, V_B, V_C . Additionally to the *twist* caused by the alignment layers (present already at $V_A = 0$), the molecules experience a voltage-dependent *tilt* if the voltage is higher than a certain threshold ($V_B > V_{thr}$). With increasing voltage ($V_C \gg V_{thr}$), only some

molecules close to the cell surface are still influenced by the alignment layers, but the majority of molecules in the centre of the cell will get aligned parallel to the electric field direction.

If the helix arrangement of the LC cell is disturbed by the external voltage, the guidance of the light gets less effective and eventually ceases to happen at all, so that the light leaves the cell with unchanged linear polarisation.

It is straightforward to combine such switchable element with a polariser (referred to as analyser) to obtain a 'light valve' for incident polarised light. For non polarised light sources, it is only necessary to place a second polariser in front of the LC cell to obtain the same functionality. To gain a more detailed insight, it is necessary to review the polarisation of light fields.

3.2 Polarisation of light

The polarisation of light is defined by orientation of its field amplitude vector. While *non polarised* light consists of contributions of all the different possible directions of the field amplitude vectors, polarised light can be characterized by either a single field component (*linear polarisation*) or by a superposition of field components in two directions. Partial polarised light is a mix of polarised and non polarised light. The polarisation state of such light can be described with the *Stokes parameters*.

For a completely polarised light field the state of polarisation of this light field propagating into the z direction can be expressed by a Jones vector representation

(1) $$\mathbf{V} = \begin{pmatrix} V_x \\ V_y \end{pmatrix}$$

where V_x and V_y are complex numbers which tell about the relative amplitudes and phases of the two basic linear polarisations. It is convenient to normalise this vector $\mathbf{V}$ so that $|\mathbf{V}|=1$ and the field strength (i.e. amplitude) is expressed in a separate variable.

A *linear* polarisation is given by vectors of the form

(2) $$\mathbf{V} = \begin{pmatrix} \cos\alpha \\ \sin\alpha \end{pmatrix}$$

which tells that the polarisation components in x and y direction do not have a mutual phase delay. Arbitrary states of polarisation are referred to as *elliptic polarisation* and are given by vectors

(3) $$\mathbf{V} = \begin{pmatrix} \cos\alpha & \exp(\mathrm{i}\Gamma/2) \\ \sin\alpha & \exp(-\mathrm{i}\Gamma/2) \end{pmatrix}$$

where Γ denotes the phase delay between the polarisation components.

The expression of polarisation states can be used to analyse the propagation of light in anisotropic media like solid state matter crystals or liquid crystals.

3.3 Propagation in anisotropic media

Materials which on the atomic level can be described as a regular arrangement of particles in a well-defined lattice are referred to as *crystals*. Liquid crystals can be described by the same model due to the translational order of the molecules.

If the material is not isotropic with respect to its optical properties, the refractive index and correspondingly the speed of light becomes polarisation dependent for most propagation directions. However, the highly ordered state of matter nevertheless leads to the existence of optical axes in the material. If a light wave propagates parallel to an *optical axis*, the material appears to be isotropic for that wave.

Light propagation along directions that are *not* parallel to an optical axis is characterized by two indices of refraction n_1 and n_2 valid for two orthogonal states of polarisation, which are usually different. This effect is referred to as *birefringence*.

Here the discussion shall be limited to *uniaxial* crystals, in which the polarisation states are referred to as *ordinary (o)* and *extraordinary (eo)* polarisation, with refractive indices n_o and n_{eo}. Along the optical axis, the refractive index is given by n_0 for all polarisation directions with the velocity c / n_0. For all other propagation directions the ordinary polarised light propagates with c / n_0, too. The velocity of the extraordinary polarised light depends on the angle between the direction of propagation and the optical axis:

(4)
$$\frac{1}{n_{eo}^2(\theta)} = \frac{\cos^2(\theta)}{n_o^2} + \frac{\sin^2(\theta)}{n_{eo}^2}.$$

The impact of a birefringent material on a transmitting light wave can be expressed by matrices which convert the Jones vector of the incident light (see previous section) to a new Jones vector, the so called *Jones matrices*. In its simplest form, the Jones-calculus is a systematic method of calculation to determine the effects of different, the polarisation condition affecting elements to a completely polarised light wave. When using this calculation the vector of the incident light wave will be multiplied one after another with characteristic matrices, the Jones matrices - one for each optical element. Finally, the result will be the vector of the electric field strength of the wave exiting the optical system.

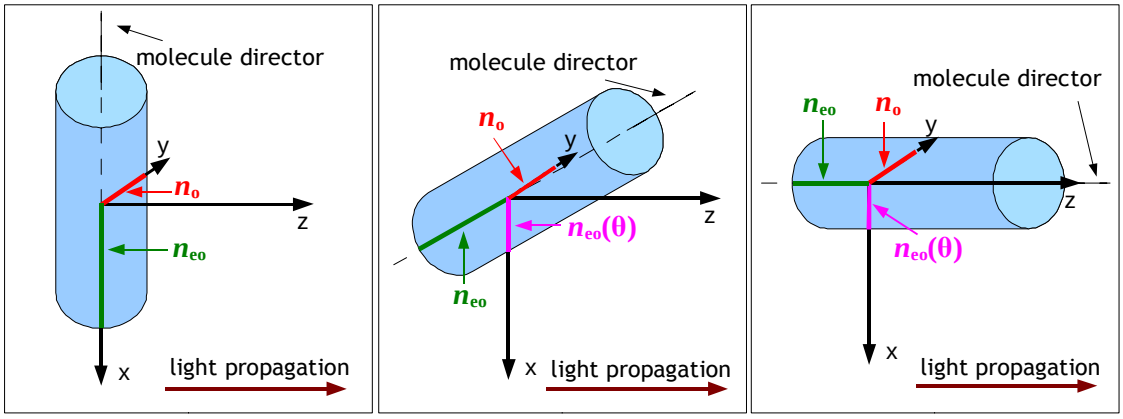

Figure 3: Refractive indices: ordinary n_o, extraordinary n_{eo} and resulting extraordinary refractive index $n_{eo}(\theta)$ for different direction of the molecules

The different refractive indices introduce a mutual phase delay between the two partials fields corresponding to the two linear polarisations which are propagating with the velocities c / n_o and c / n_{eo}. The transmitted light after a distance d (given by the thickness of the material) is therefore given by

(5)
$$\mathbf{V}' = \begin{pmatrix} V'_{eo} \\ V'_{o} \end{pmatrix} = \mathrm{W}_d \begin{pmatrix} V_{eo} \\ V_{o} \end{pmatrix},$$

where

$$W_d = \begin{pmatrix} \exp(-i\frac{n_{eo}\omega}{c}d) & 0 \\ 0 & \exp(-i\frac{n_o\omega}{c}d) \end{pmatrix}. \quad (6)$$

3.4 Wave plates

An optical component with parallel entrance and exit facets made from an uniaxial birefringent material with its optical axis perpendicular to the direction of light propagation is referred to as a wave plate. Such optical components can be described in different coordinate systems.

In the following, we will use the *x*-*y* coordinate system oriented on the optical table. The *u*-*v* coordinate systems for the optical components may be rotated around the optical axis with respect to the system of the optical table, as illustrated in Figure 4. For birefringent optical components we will assign the *u* axis to correspond to the extraordinary (eo) axis and the *v* axis to the ordinary (o) axis.

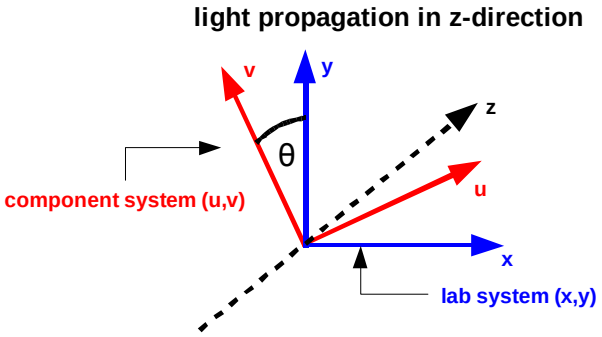

Figure 4: View of the coordinate systems: the *x*-*y*-coordinate system of the optical table and the *u*-*v* coordinate system of an optical component

The matrix W_d of a wave plate can be expressed in the form

$$W_d = e^{-i\Phi} \cdot \begin{pmatrix} \exp\left(-i\frac{\Gamma}{2}\right) & 0 \\ 0 & \exp\left(i\frac{\Gamma}{2}\right) \end{pmatrix}, \quad (7)$$

where the quantity Γ, describing the relative phase delay, is given by

$$\Gamma = (n_{eo} - n_o)\frac{2\pi}{\lambda}d \quad (8)$$

and the quantity Φ, describing the absolute phase, is defined by

$$\Phi = \frac{1}{2}(n_{eo} + n_o)\frac{2\pi}{\lambda}d\,. \quad (9)$$

The phase factor $\exp(-i\Phi)$ may be neglected in some cases, for example when there is no interference phenomena considered.

A *half-wave plate* is a particular example of a wave plate with a thickness

(10) $$d = \frac{\lambda}{2(n_{eo} - n_o)},$$

so that the mutual phase delay is given by $\Gamma = \pi$. This means that the optical path between the two waves with orthogonal polarisations differs by half the wavelength of the light field. The Jones matrix of a half-wave plate, whose extraordinary axis meets the x axis of the laboratory system x-y, is obtained as

(11) $$\mathrm{W}_{\mathrm{HWP}} = \begin{pmatrix} -\mathrm{i} & 0 \\ 0 & \mathrm{i} \end{pmatrix}.$$

In the following we assume that a wave plate is placed in an optical system so that the optical axis is perpendicular to the direction of light propagation z and has an angle δ with respect to the x axis. A state of polarisation can be written as a Jones vector in the coordinate system of the wave plate, or in the x-y coordinate system. The Jones vector of a polarisation state can be transformed from one system to the other by means of a rotation matrix $R(\delta)$ as

(12) $$\mathrm{R}(\delta) = \begin{pmatrix} \cos\delta & \sin\delta \\ -\sin\delta & \cos\delta \end{pmatrix}.$$

Any Jones vector $\mathbf{V}$ can be written in the x-y coordinate system as

(13) $$\mathbf{V} = \begin{pmatrix} V_x \\ V_y \end{pmatrix} = \mathrm{R}(-\delta)\begin{pmatrix} V_{eo} \\ V_o \end{pmatrix} = \begin{pmatrix} \cos\delta & -\sin\delta \\ \sin\delta & \cos\delta \end{pmatrix}\begin{pmatrix} V_{eo} \\ V_o \end{pmatrix}.$$

The matrix of a wave plate in the x-y coordinate system of the wave is then given by

(14) $$\mathrm{W}_{\mathrm{WP}} = \mathrm{R}(-\delta)\mathrm{W}_d\mathrm{R}(\delta).$$

A half-wave plate with an optical axis inclined by an angle of $\delta = 45°$ with respect to the x direction of the coordinate system can be described by the matrix

(15) $$\mathrm{W}_{\mathrm{HWP}}^{(45°)} = \begin{pmatrix} 0 & -\mathrm{i} \\ -\mathrm{i} & 0 \end{pmatrix}$$

This means that light polarised parallel to the x direction, which is assumed to have an angle of 45° with respect to the direction of ordinary polarisation, will have its Jones vector changed from

(16) $$\mathbf{V} = \begin{pmatrix} V_x \\ V_y \end{pmatrix} = \begin{pmatrix} 1 \\ 0 \end{pmatrix}$$

to

(17) $$\mathbf{V}' = \begin{pmatrix} 0 & -\mathrm{i} \\ -\mathrm{i} & 0 \end{pmatrix}\begin{pmatrix} 1 \\ 0 \end{pmatrix} = \begin{pmatrix} 0 \\ -\mathrm{i} \end{pmatrix} = \exp(-\mathrm{i}\frac{\pi}{2})\begin{pmatrix} 0 \\ 1 \end{pmatrix},$$

which corresponds to a rotation of the polarisation direction by an angle of 90°.

3.5 Jones matrix representation of a 'twisted nematic' LC cell

A twisted nematic LC cell can be described as a succession of a high number of very thin wave plates which change the orientation of their optical axis according to the change of the direction of the molecular axis. The total Jones matrix of the cell is then obtained by matrix multiplication of all the matrices of the assumed thin wave plates as

(18) $$\mathrm{W}_{\text{TN-LC}} = \mathrm{R}(\alpha)\cdot e^{-\mathrm{i}\cdot(\beta+\Phi_0)}\begin{pmatrix} \cos\gamma - \mathrm{i}\left(\frac{\beta}{\gamma}\right)\sin\gamma & -\left(\frac{\alpha}{\gamma}\right)\sin\gamma \\ \left(\frac{\alpha}{\gamma}\right)\sin\gamma & \cos\gamma + \mathrm{i}\left(\frac{\Gamma}{\gamma}\right)\sin\gamma \end{pmatrix},$$

where α is the twist angle of the molecules through the entrance and exit facets of the cell and the quantity γ is given by

(19) $$\gamma = \sqrt{\alpha^2 + \beta^2}\ .$$

The birefringence β is dependent on the refractive index difference $\Delta n = n_{\text{eo}}\text{-}n_{\text{o}}$, the thickness d of the LC display and the wavelength λ of the incident light:

(20) $$\beta = \frac{\Gamma}{2} = \frac{\pi\cdot d}{\lambda}\cdot\left(n_{\text{eo}} - n_{\text{o}}\right).$$

Because the extraordinary index of refraction n_{eo} is dependent on the orientation of the LC molecules and therefore on the voltage applied to the LC cell, the birefringence β is also voltage-dependent. The absolute phase Φ can be written as

(21) $$\Phi = \beta + \frac{2\pi}{\lambda} d\cdot n_{\text{o}} = \beta + \Phi_0\,.$$

The voltage-independent phase factor Φ_0 will be neglected in the following discussion. For the determination of the display parameters a different notation of the Jones matrix is recommended. Now in the x-y coordinate system we can write

(22) $$\mathrm{W}_{\text{TN-LC}}^{\text{fghj}} = \mathrm{R}(-\psi)\cdot\mathrm{W}_{\text{TN-LC}}\cdot\mathrm{R}(\psi) = e^{-\mathrm{i}\cdot\beta}\cdot\begin{pmatrix} f - \mathrm{i}\cdot\mathrm{g} & h - \mathrm{i}\cdot\mathrm{j} \\ -h - \mathrm{i}\cdot\mathrm{j} & f + \mathrm{i}\cdot\mathrm{g} \end{pmatrix},$$

where the Jones matrix components f, h, g and j are dependent on the display parameters:

$$
\begin{aligned}
f &= \cos\gamma\cdot\cos\alpha+\frac{\alpha}{\gamma}\cdot\sin\gamma\cdot\sin\alpha\\
h &= \cos\gamma\cdot\sin\alpha-\frac{\alpha}{\gamma}\cdot\sin\gamma\cdot\cos\alpha\\
g &= \frac{\beta}{\gamma}\cdot\sin\gamma\cdot\cos(2\psi-\alpha)\\
j &= \frac{\beta}{\gamma}\cdot\sin\gamma\cdot\sin(2\psi-\alpha)
\end{aligned}
\qquad (23)
$$

With the 'director' angle ψ describing the position of the long axis of the molecules at the front of the LC display in the *x*-*y* coordinate system. The Jones matrix components satisfy the condition $f^2+g^2+h^2+j^2=1$.

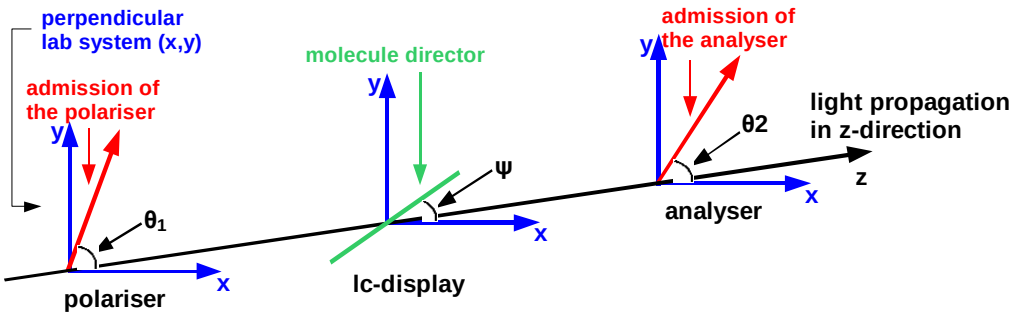

Figure 5: *x*-*y* coordinate system with the orientations of the polarisers (θ_1,θ_2) and the 'director' angle ψ, describing the position of the long axis of the molecules at the front of the LC display in the *x*-*y* coordinate system

For the determination of the Jones matrix components, the system comprising of polariser, light modulator and analyser shown in Figure 5 will be discussed. For the calculation of the transmission of the system polarisers with any rotation are used. The polarisers are described by the matrices $P_{\mathrm{rot}}(\theta_1)$ and $P_{\mathrm{rot}}(\theta_2)$ for any passage direction θ_1 and θ_2 in the *x*-*y* coordinate system. They results, analogue to the consideration of the wave plate above, from the matrix multiplication from a polariser with a horizontal passage direction

$$
\mathrm{P_h}=\begin{pmatrix}1 & 0\\ 0 & 0\end{pmatrix}, \qquad (24)
$$

with the rotation matrices

$$
\mathrm{P_{rot}}(\theta_i)=\mathrm{R}(-\theta_i)\cdot\mathrm{P_h}\cdot\mathrm{R}(\theta_i)=\begin{pmatrix}\cos^2(\theta_i) & \cos(\theta_i)\cdot\sin(\theta_i)\\ \cos(\theta_i)\cdot\sin(\theta_i) & \sin^2(\theta_i)\end{pmatrix}. \qquad (25)
$$

The transmittance $T(\theta_1, \theta_2)$ of the light which passes through an LC display can be calculated with the Jones formalism. The vector of a light field entering a system comprising of polariser, LCD and analyser can be written as

(26) $$\mathbf{E}_2 = E_2(\theta_1,\theta_2)\begin{pmatrix}\cos(\theta_2)\\ \sin(\theta_2)\end{pmatrix} = \mathrm{P}_{\mathrm{rot}}(\theta_2)\cdot \mathrm{W}_{\mathrm{TN-LC}}^{\mathrm{fghj}}\cdot E_1(\theta_1)\cdot\begin{pmatrix}\cos(\theta_1)\\ \sin(\theta_1)\end{pmatrix}.$$

The transmittance of the system is obtained by multiplication of the matrices as

(27) $$\begin{aligned} T(\theta_1,\theta_2) &= \frac{|E_2(\theta_1,\theta_2)|^2}{|E_1(\theta_1)|^2} \\ &= f^2\cos^2(\theta_1-\theta_2)+ fh\sin(2\theta_1-2\theta_2)+h^2\sin^2(\theta_1-\theta_2)\cdot \\ &\quad + g^2\cos^2(\theta_1+\theta_2)+ gj\sin(2\theta_1+2\theta_2)+ j^2\sin^2(\theta_1+\theta_2) \end{aligned}$$

With $|E_1(\theta_1)|\neq 0$ this function is well defined for all angles. To ensure this, in the case of linearly polarised light a wave plate with almost $\lambda/4$ can be used.

If a LC cell satisfies $\alpha \ll \beta$, which is the case for thick cells, the Jones matrix can be significantly simplified and permits an intuitive interpretation:

(28) $$W_{\mathrm{TN\text{-}LC}} \approx R(-\alpha)\begin{pmatrix}\exp(-\mathrm{i}\beta) & 0\\ 0 & \exp(\mathrm{i}\beta)\end{pmatrix}.$$

If the incident light is polarised parallel to the *x*- or *y* axis the polarisation axis will be rotated by the twist angle α between the directions of the alignment layers, as implied by the intuitive explanation illustrated in Figure 1.

3.6 Properties of a TN-LC cell with an applied voltage

If a voltage is applied to the cell, the molecules tend to align parallel to the electric field. Thereby the anisotropy of the liquid crystal is reduced because the angle between the direction of light propagation and the molecular axes gets smaller until eventually both directions are parallel, and the optical axis of the liquid crystal is parallel to the direction of light propagation (see Figure 2).

In terms of the analysis done here, the difference $\Delta n = n_{\mathrm{eo}}\text{-}n_{\mathrm{o}}$ gets smaller and therefore for sufficiently high voltages one gets $\beta \to 0$. For this situation the Jones matrix can be approximated as

(29) $$W_{\mathrm{TN\text{-}LC}} \approx R(-\alpha)\begin{pmatrix}\cos\alpha & \sin\alpha\\ -\sin\alpha & \cos\alpha\end{pmatrix} = \begin{pmatrix}1 & 0\\ 0 & 1\end{pmatrix}$$

which means that for a strong voltage applied to the LC cell the light polarisation is not changed.

The analysis of the intermediate cases in which the molecules are no more aligned in the helix structure but not yet parallel to the field can be done with the matrix $W_{\mathrm{TN\text{-}LC}}$ without one of the two approximations given above. With such analysis, the voltage-dependent optical properties can be obtained. As a result, incident light with linear polarisation leaves the cell with an elliptic state of polarisation.

However, the voltages applied to the LC cell are not directly accessible in the LC2002 device contained in this kit. The voltages applied to the cells can be controlled via a customized electronic drive board. This drive board receives information on what voltage should be applied to the cell as grey level values of the signal created by the VGA output of a graphics adapter of a common PC.

Although for the derivation of the given Jones matrix assumptions have been made that do not always hold, the theory based on this Jones matrix is completely sufficient for the understanding of most of the optical properties of liquid crystal cells. A more complex description of the LC displays using the Jones-formalism to include edge effects in the volume close to director plates can be found in the literature, see for example H. Kim and Y. H. Lee [7].

3.7 Amplitude and phase modulation using TN-LC cells

The voltages that are applied to the cells of the LC display are in a range that permits an almost continuous transition between the 'helix state' which rotates the incident polarisation to the 'isotropic state' in which the polarisation remains unchanged. It is obvious that by inserting an analyser behind the display the LC display one can achieve an *amplitude modulation* of a transmitting polarised light wave.

By examination of the Jones matrices $W_{\text{TN-LC}}$ one can also deduce that the phase of the light passing the analyser is changed dependent on the voltage-dependent parameter β. If the SLM is illuminated by a coherent light source (e.g. a laser) various diffraction effects that are based on this *phase modulation* can be observed. For the experiments it is important to note that the incident polarisation for obtaining a comparatively strong phase modulation with only weak amplitude modulation is *not* parallel or perpendicular to the alignment layers.

At the LC2002 amplitude and phase modulation are coupled. Using the position of polariser and analyser, however, different ratios of amplitude and phase modulation can be realized. A maximum amplitude modulation with minimal phase modulation is called an 'amplitude-mostly' configuration. A maximum phase and minimum amplitude modulation is called a 'phase-mostly' configuration

For doing experiments with the LC2002 dealing mainly with diffraction effects, it is not necessary to review the changes of the polarisation states in detail. It is sufficient to understand that the system which comprises of polariser, LCD and analyser can be seen as an optical component which can be used to introduce a *mutual voltage-dependent phase shift* between the waves passing through individual LC cells.

The main steps in the transition from a TN-LC cell to a LC-based micro-display are of course the arrangement of the cells in one-dimensional or two-dimensional arrays, and the establishment of an interface that permits individual addressing of the cells. This results not only the creation of phase or amplitude modulation, but also the creation of a desired spatial distribution of this modulation, resulting in the creation of a *spatial light modulator.*

A LCD sandwiched between polarisers can thus be used not only as an image source in a projection system, but also (with other polariser settings) as a switchable diffractive element which can be used to represent dynamically optical elements like Fresnel zone lenses, gratings and beam splitters, which can be modified by means of electronic components.

4 Scalar theory of light waves and diffraction — Fourier optics

4.1 Plane waves and interference

The ability of interference is a fundamental property of light, which is caused by its wave nature. Interference refers to the effects of mutual amplification and cancellation which are observed when two or more waves are superimposed. When monochromatic light waves of the same frequency interfere, the amplitudes of the resulting field at any place and at any time is given by the addition of the amplitudes of the involved waves.

In the following we will only review the interference of linearly polarised waves with amplitude vectors parallel to each other. Therefore, in the mathematical description of the interference one can use the notation of complex amplitudes instead of the summation of the complex vector field amplitudes.

Unlike sound waves, light waves have certain preconditions for their ability to create interference effects. These preconditions originate from the process of light emission, and are summarized in the term and the concept of *coherence*.

4.1.1 Interference of plane waves

A single plane wave can be written as

$$E^i(\mathbf{r},t) = A_0 \exp(\mathrm{i}(\mathbf{k}\cdot\mathbf{r} - \omega t + \delta)), \tag{30}$$

where ω denotes the frequency of the light and $\mathbf{k}$ is the wave vector, while δ denotes a constant phase-offset. For two overlapping light waves at an arbitrary time t, we get spatially dependent amplitudes

$$E_1(\mathbf{r}) = A_1 \exp(i\mathbf{k}_1\cdot\mathbf{r} + \delta_1) \tag{31}$$

and

$$E_2(\mathbf{r}) = A_2 \exp(i\mathbf{k}_2\cdot\mathbf{r} + \delta_2). \tag{32}$$

For any position $\mathbf{r}$ the resulting complex amplitude is given by

$$E(\mathbf{r}) = E_1(\mathbf{r}) + E_2(\mathbf{r}) = A_1 e^{i(\mathbf{k_1 r}+\delta_1)} + A_2 e^{i(\mathbf{k_2 r}+\delta_2)} \tag{33}$$

The intensity of the interference is obtained as

$$I(\mathbf{r}) \sim E(\mathbf{r})E^*(\mathbf{r}) = A_1^{\,2} + A_2^{\,2} + A_1A_2 e^{i[\mathbf{r}(\mathbf{k_1}-\mathbf{k_2})+(\delta_1-\delta_2)]} + A_1A_2 e^{-i[\mathbf{r}(\mathbf{k_1}-\mathbf{k_2})+(\delta_1-\delta_2)]}, \tag{34}$$

or

$$I = I_1 + I_2 + 2\sqrt{I_1 I_2}\cos\Phi. \tag{35}$$

The phase difference $\Delta\Phi$ of both interfering waves is

$$\Delta\Phi = \Phi_1 - \Phi_2 = \mathbf{r}(\mathbf{k_1} - \mathbf{k_2}) + (\delta_1 - \delta_2). \tag{36}$$

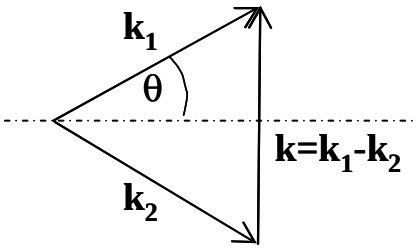

Figure 6: Difference $\mathbf{k}$ of two wave vectors $\mathbf{k_1}$ and $\mathbf{k_2}$ with enclosed angle 2θ

Considering two waves of equal amplitude ($A_1 = A_2 = A_0$), the intensity of the interference changes periodically between 0 and $4I_0$. Strict additivity of intensities applies only if the addend (the so called interference element)

$$2\sqrt{I_1 I_2}\cos\Delta\Phi$$

is zero. If this is the case, there is no interference. Interference means deviation from the additivity of intensities. For all spatial positions which satisfy

$$\Delta\Phi = 2N\pi \qquad \text{with } N = 0,1,2,...$$

a maximum intensity can be found

(37) $$I_{\max} = I_1 + I_2 + 2\sqrt{I_1 I_2}\ .$$

The positions with minimal intensity are

(38) $$I_{\min} = I_1 + I_2 - 2\sqrt{I_1 I_2}$$

and satisfy

(39) $$\Delta\Phi = 2(N+1)\pi\,.$$

It is important to note that the intensity as a whole is neither increased nor decreased. It is the nature of interference to merely distribute the energy differently, as the total energy must be preserved.

The intensity pattern with observable bright-dark contrasts is referred to as interference fringes. An important parameter for the characterization of their visibility is the contrast. It is defined as the sum of the maximum and minimum intensity normalised by the difference between maximum and minimum intensity:

(40) $$C = \frac{I_{\max} - I_{\min}}{I_{\max} + I_{\min}}.$$

For the superposition of two flat monochromatic waves we obtain

(41) $$C = \frac{2\sqrt{I_1 I_2}}{I_1 + I_2}.$$

4.1.2 Coherence of light

The previous explanations deliver only a rather vague description of the true nature of the interference of light waves and assume conditions (monochromatic waves, point light sources), which in reality are not met. As experience shows, it is in general not possible to observe interference effects by superposition of two waves emitted by different thermal light sources or from two different points of an extended thermal light source.

Although light emission is often treated as a continuous process, it can be described more accurately as a sequence of emissions of many short wave trains. Electrons in the atom move into excited states by absorption of energy. The duration of the irradiation corresponding to the limited lifetime of these states of about 10^{-8} s leads to the emission of short wave trains of about 3 m in length. Furthermore, the light emitted from different points of the thermal light source is statistically distributed, and the phase relationship between two successive wave trains emitted by a point source changes from emission event to emission event in an unpredictable way.

In the previous discussion, it was implicitly assumed that the difference of the phase constants δ_1 and δ_2 remains constant for the observation time t_b. However, the waves emitted from an extended light source have neither a spatially nor temporally stable phase relationship. As a result, many waves with statistically different phase relationships are superimposed successively during the observation time. The resulting interference pattern is not stationary but changes its appearance in intervals of 10^{-8} s. Only the time-averaged intensity

(42) $$\langle I \rangle_{t_b} = I_1 + I_2 + 2\sqrt{I_1 I_2}\,\frac{1}{t_b}\int_0^{t_b} \cos\Delta\Phi \; dt$$

can be measured, assuming that the amplitudes of the individual waves are constant over the time interval t_b.

If the phase relations of the superimposed waves vary in a way that during the observation time all phase differences between 0 and $2N\pi$ occur for equally long time intervals, the temporal average of the quantity $\cos(\Delta\Phi)$ is zero, and just the sum of the individual intensities I_1 and I_2 is measured. In this case, one can no longer speak of interference, and these light sources are referred to as *incoherent*.

If in contrast the difference (δ_1-δ_2) remains constant over the whole observation period, the participating waves are called *coherent*, which means that there exists is a fixed phase relationship between them. In this case, the measured intensity is indeed described by equation (42). The radiation emitted by real light sources is partially coherent, strictly coherent and incoherent light, respectively, is only obtained from the light of infinitely extended or punctual light sources.

In Section 4.1.1, the interference of monochromatic light waves was considered, emitted by ideal point light sources. These assumptions are obviously idealizations. Real light sources are always light emitting areas of finite size. The relationship between the size of the light source and the obtainable contrast in the interference fringes leads to the coherence condition, which tells that the product of the light source width b and the emission aperture $\sin\alpha$ (where 2α is the opening or aperture angle) has to be very small compared to half the wavelength of the emitted radiation. Although the individual point sources emit waves with statistically distributed phase relations, a certain extension of the light source for producing interference pattern is allowed.

Wave trains with fixed phase relationships can be generated by splitting the light of one light source into two or more partial waves. The coherent division can take place using one of the following two principles:

1. *Division of the amplitude*

   An interferometer, which is based on this method, is the Michelson interferometer.

2. *Division of the wavefront*

   This principle is used in the Young interferometer, for example.

As a result of the division, two waves are obtained, in which the phase changes in an unpredictable way, but in the *same* way. The difference (δ_1-δ_2) therefore remains constant.

After paths of different length, creating a phase difference, the partial waves will be reunited. With the help of Fourier's integral theorems, however, it can be shown that the wave trains are only quasi-monochromatic because of their limited length L_k. They have a finite spectral bandwidth. Only an infinitely extended wave would be monochromatic.

If the optical path difference between the two wave trains exceeds the length L_k, no interference can be observed, as the phase-correlated waves no longer overlap. The largest path difference, for which interference is still observed, is called *coherence length*.

The Michelson interferometer allows a very simple and rapid determination of the coherence length. For approximately equal paths, the contrast of the interference fringes is quite high. Increasing the optical path difference will decrease the contrast. If the retardation exceeds the coherence length, the contrast decreases to zero.

4.2 Diffraction theory

4.2.1 Kirchhoff's diffraction theory

A plane wave propagating into the z-direction can be written as

(43) $$E^i = E_0 e^{\mathrm{i}(kz-\omega t)}$$

where ω denotes the frequency of the light and

(44) $$k = \frac{2\pi}{\lambda}$$

is the absolute value of the wave vector $\mathbf{k}$, which is inversely proportional to the wavelength of the light λ. We will review a situation in which is wave is incident onto an object at $z = 0$. This object is assumed to be thin so that it can be described by a complex-valued transmission function $\tau(x,y)$. The transmitted field is

(45) $$E^t(x, y, z = 0) = \tau(x, y) E^i(x, y, z = 0)\,.$$

The resulting light propagation can be described by applications of *Huygens' principle*. According to this principle, a spherical wave is created by each point (x,y) at $z = 0$ of the diffracting object. All spherical waves must be added (i.e. integrated), to obtain the field amplitude from a point (x',y',z) behind the diffracting object.

This description contains also waves in negative z-direction, which are not observed. In the Fresnel-Kirchhoff diffraction theory a direction factor is therefore introduced, which excludes the waves in negative z-direction. The resultant field is obtained as

(46) $$E(x', y', z) = \frac{e^{\mathrm{i}kz}}{\mathrm{i}\lambda z} \int_{-\infty}^{\infty}\int_{-\infty}^{\infty} E^t(x, y, 0) e^{\mathrm{i}k((x'-x)^2+(y'-y)^2)} (1+\cos(\mathbf{e}_z\mathbf{r}))\,dx\,dy \quad .$$

In general this equation is too complicated to solve diffraction problems, but for many relevant situations suitable approximations can be used.

4.2.2 Fresnel approximation

The transversal dimension of the diffracting object should be small, compared to the distance between object and diffraction pattern (paraxial approximation).

In this case $\cos(\mathbf{e}_z\mathbf{r}) \approx 1$ and the distance can be written as

(47) $$r \approx z + \frac{(x'-x)^2}{2z} + \frac{(y'-y)^2}{2z}$$

As the amplitude is less sensitive than the phase, within the denominator the approximation with $r \approx z$ can be used. From this we have

(48) $$E(x',y',z) = \frac{e^{ikz}}{i\lambda z} \int_{-\infty}^{\infty}\int_{-\infty}^{\infty} E^t(x,y,0) e^{\frac{ik}{2z}\left((x'-x)^2+(y'-y)^2\right)} dxdy$$

This equation describes the convolution of the transmitted field with an impulse response of the structure. Multiplying the quadratic expression in the exponent results in

(49) $$E(x',y',z) = A(x',y',z)\mathcal{F}[E^t(x,y,0)e^{\frac{i\pi}{\lambda z}(x^2+y^2)}](\nu_x,\nu_y)$$

with

(50) $$A(x',y',z) = \frac{e^{ikz}}{i\lambda z} e^{\frac{ik}{2z}\left(x'^2+y'^2\right)}$$

and

(51) $$\nu_x = \frac{x'}{\lambda z}, \quad \nu_y = \frac{y'}{\lambda z}$$

The quantities ν_x and ν_y are referred to as *spatial frequencies* analogue to the frequencies of the Fourier transformation (above written as $\mathcal{F}$) of temporal signals.

The Fresnel diffraction covers the common situation in which the observation plane is at a finite distance behind the object. There is a continuous transition between the setups which are governed by Fresnel diffraction and the next approximation, referred to as Fraunhofer diffraction.

4.2.3 Fraunhofer diffraction

The Fraunhofer diffraction is a special case (and analytically a simplification) of the Fresnel diffraction, which is valid for large distances. The Fraunhofer approximation applies if

(52) $$\left(x^2+y^2\right)\frac{\pi}{\lambda} << z$$

is satisfied for (x,y) and (x',y') and the diffracting object is illuminated by a plane wave. In this case

(53) $$E(x',y',z) = A(x',y',z)\mathcal{F}[E(x,y,0)](\nu_x,\nu_y)$$

with

(54) $$A(x',y',z) = \frac{\exp(ikz)}{i\lambda z} .$$

The far-field in the Fraunhofer approximation is given by the Fourier transformation of the field directly behind the diffracting object. The spatial frequencies of the diffracting structure create waves, which propagate with angles

$$\alpha \approx \tan\alpha = \frac{x'}{z} = \lambda \nu_x$$
$$\beta \approx \tan\beta = \frac{y'}{z} = \lambda \nu_y \tag{55}$$

to the optical axis, respectively. With the help of a lens the far-field of the light propagation can be obtained in the focal plane of the lens (see section 4.5.1).

This means that in optics propagation of the light field realizes a Fourier transformation in a natural way simply by propagation. The Fourier transformation of a two-dimensional object

$$F(\nu_x, \nu_y) = \mathcal{F}[f(x,y)](\nu_x, \nu_y)$$
$$= \int_{-\infty}^{\infty}\int_{-\infty}^{\infty} f(x,y)\exp(-2\pi i(\nu_x x + \nu_y y))\,dxdy \tag{56}$$

can be observed directly as a function of the spatial frequencies, which can be associated with diffraction orders. These spatial frequencies can be manipulated and filtered. The Fourier filtering is a passive parallel image processing performed at the speed of light.

4.3 Symmetries of diffraction patterns

For certain diffracting objects, the observed diffraction patterns exhibit certain symmetries. It is obvious that rotationally symmetrical object creates a rotationally symmetrical diffraction pattern, and that mirror symmetries, for example with respect to the x- or the y-axis, are observed in the diffraction patterns again. The following sections will deal with symmetries, whose presence is not quite as obvious.

4.3.1 Fraunhofer diffraction at pure amplitude objects

Pure amplitude objects illuminated by a plane wave transmit an electric field $E^t(x,y,0)$, which can be written as a merely real-valued function. Under this condition the Fourier integral of the Fraunhofer diffraction pattern in equation (56) can now be easily separated in its real and imaginary part according to the Euler equation $\exp(ix)=\cos(x)+i\sin(x)$. It can be shown easily that in this case the diffraction pattern is described by a *hermitian function*, which is a function of symmetry

$$F(-\nu_x, -\nu_y) = F^*(\nu_x, \nu_y). \tag{57}$$

This means that the intensity distribution of diffraction patterns of pure amplitude objects always shows a two-fold rotational symmetry (equivalent to inversion symmetry) with respect to the optical axis. In other words, for each wave diffracted to the upper right a phase-conjugated wave of equal intensity will be diffracted to the lower left.

4.3.2 Fraunhofer diffraction at binary elements

Even for binary phase elements with the transmittance values $\exp(0) = +1$ and $\exp(i\pi) = -1$ a purely real-valued field is obtained. As a result, the far-field diffraction pattern exhibits the hermitian symmetry described in the previous section.

Even a diffracting object that can be represented by *any* two transmittance values τ_1 and τ_2 retains the hermitian symmetry of the diffraction far-field. This can be proven rather easily exploiting the linearity of the Fourier transformation, because diffracting objects represented by only two transmittance values can be obtained from a diffracting object

with the transmittance values $\exp(0) = +1$ and $\exp(i\pi) = -1$ by the linear transformation $\tau'(x,y)=a\tau(x,y)+b$, with $a=(\tau_2-\tau_1)/2$ and $b=(\tau_1+\tau_2)/2$.

The Fourier transform of the constant value b represents an undiffracted wave of the same amplitude. The undiffracted wave propagates in the far-field parallel along the optical axis (with spatial frequency 0) and is therefore often referred to as the zero diffraction order. The diffracted waves are obtained in the same way as by the original element, with a scaling factor a to the amplitudes.

This means that two binary elements whose transmission functions can be transformed into each other by such a linear transformation create very similar diffraction patterns. The only differences are the amplitude scaling factor to the diffracted waves and a different scaling factor to the undiffracted wave. The two scaling factors are mutually dependent, due to the conservation of energy.

Experimentally the transition between two binary elements occurs, for example, as soon as one of the grey scale values used for addressing binary elements to a spatial light modulator is modified. To implement a well-defined transmission function in the light modulator 'LC2002' a polariser and an analyser will be used. A change in the polariser orientation means usually a change of the transmittance values of an addressed diffracting structure and leads to the described effect.

A special case will now be reviewed which is relevant not only for spatial light modulators, but also for manufacturing static diffractive optical elements. For the realization of binary diffractive elements by using an ideally transmissive material both transmittance values τ_1 and τ_2 are phase-only values $\exp(i\Phi_1)$ and $\exp(i\Phi_2)$. Fully equivalent is a description by the transmittance values $\exp(0) = +1$ and $\exp(i\Delta\Phi)$ with $\Delta\Phi = \Phi_1-\Phi_2$.

For simplicity should we will also assume that the calculated diffractive element for the ideal phase stages $+1$ and $\exp(i\pi) = -1$ generates no undiffracted wave, meaning the Fourier integral of the transmission function for the spatial frequency 0 returns the amplitude 0. In this case we get

(58) $$\left|\left(\mathcal{F}[\tau']\right)(\nu_x,\nu_y)\right|^2 = \begin{cases} \cos^2(\Delta\Phi/2) & \text{for } \nu_x=\nu_y=0 \\ \left|\left(\mathcal{F}[\tau]\right)(\nu_x,\nu_y)\right|^2 \sin^2(\Delta\Phi/2) & \text{otherwise} \end{cases}.$$

This means that depending on the phase $\Delta\Phi$, the energy will be divided between the undiffracted wave and the diffracted waves. The extreme cases are $\Delta\Phi=0$ (here all the energy remains in the undiffracted wave and the phase factor is a de facto non-existent) and $\Delta\Phi=\pi$ (here no undiffracted wave is observed). Of course, the described behaviour is periodical in $\Delta\Phi$ in accordance with the equation given above, meaning that for all odd multiples of π the undiffracted wave disappears, too.

4.3.3 Diffraction at spatially separable diffracting objects

A spatially separable diffracting object is an object whose transmission function $\tau(x,y)$ can be expressed by the product

(59) $$\tau(x,y) = \tau_x(x)\cdot\tau_y(y).$$

Of course, all diffracting objects which can acquire this property by rotation around the optical axis are assumed to spatially separable, too. As shown in the equations for the diffraction pattern in the Fresnel approximation (see Section 4.2.2) and the Fraunhofer approximation (see Section 4.2.3), this property is transferred to the diffraction patterns which are given by a product of the two integrals for the two spatial directions.

This is important, for example, if the diffracting object is a dynamic DOE created with an SLM (see section LIN6 for details) that generates an additional undiffracted wave. If a linear diffracting object $\tau_x(x)$ is studied, superposition (i.e. mathematical multiplication) with a linear, orthogonal transmission function $\tau_y(y)$ yields a separation of the examined diffraction pattern from the undiffracted light wave.

4.4 Diffraction at spatially periodic objects

Spatially periodic objects, in optics often referred to as gratings; show a discrete far-field diffraction pattern, in contrast to the spatially continuous diffraction patterns of spatially aperiodic objects. This is due to spatial frequency spectrum of periodic objects that consists of discrete frequencies only.

4.4.1 Diffraction orders in the Fraunhofer diffraction pattern

Each discrete spatial frequency of a one-dimensional periodical object with spatial periodicity g is a multiple of the fundamental frequency $1/g$ and produces by illumination with monochromatic light a maximum in the far-field, a so-called *diffraction order*.

For periodic diffracting objects, the Fourier integral of the transmission function of a Fourier series can be simplified. For a 2-dimensional object with a spatially dependent complex-valued transmission function $\tau(x,y)$ and spatial periodicities g_x and g_y, the Fourier coefficients $A_{l,m}$, describing the complex-valued amplitudes of the diffracted waves are given by

$$A_{l,m} = \frac{A_{\text{in}}}{g_x g_y} \int_0^{g_x} \int_0^{g_y} \tau(x,y) \exp\left(-2\pi \mathrm{i} \left(\frac{l}{g_x} x + \frac{m}{g_y} y \right)\right) dx dy \,. \tag{60}$$

The complex transmission function $\tau(x,y)=\rho(x,y)\exp(i\varphi(x,y))$ summarizes changes of amplitude and phase of the wave transmitted through the diffracting object. For a one-dimensional periodic object the amplitude simplifies to

$$A_l = \frac{A_{\text{in}}}{g} \int_0^{g} \tau(x) \exp\left(-2\pi \mathrm{i} \frac{l}{g} x\right) dx \,. \tag{61}$$

In this equation, the diffracting object is described by a spatially resolved complex-valued transmission function $\tau(x)$ as a function of the position x. The given integral does not take the second spatial coordinate into account, so that it is only valid for objects with a constant transmission function with respect to the y direction (*linear gratings*).

Such transmission function $\tau(x)$ can be sinusoidal, as in the case of a grating obtained by holographic recording of a two-wave-interference (see section 4.1). The transmission function may in this example take any value within a certain range.

4.4.2 Fraunhofer diffraction at linear binary gratings

The values of the transmission function obtained when addressing a LCD are limited to 256 values due to the addressing of the transmission function value as a single 8-bit colour channel of the VGA signal. The most simple example of a discretization of the transmission function is of course a signal that consists of only *two* different transmission values (binary elements, see section 4.3). For linear gratings it is possible to describe the grating with the transition points between the areas with the two transmission values τ_1 and τ_2 (see Figure 7).

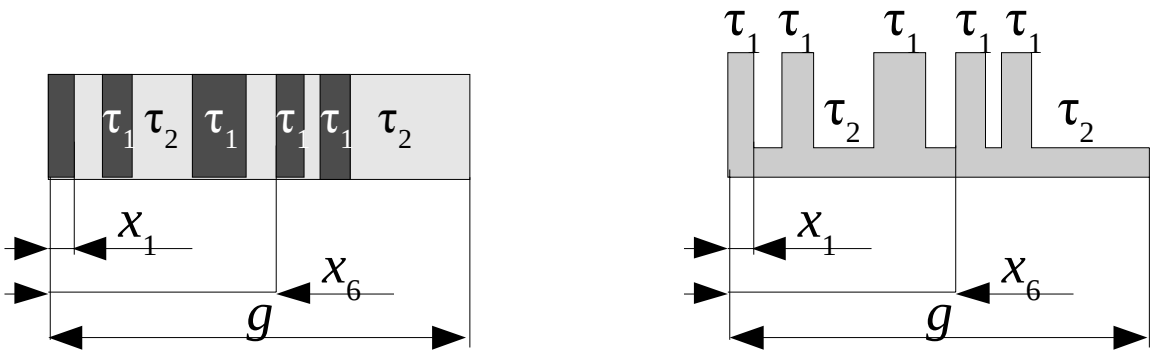

Figure 7: A linear binary grating with the transmission values τ_1 and τ_2, grating period g and 10 transition points $x_1 \ldots x_{10}$ (x_1 and x_6 are shown). Left a top view of a grating is shown; right a profile of a relief grating is shown as an example

We will now analyse a simple linear binary grating with only two transition points. For a grating period g there is only one free transition point called x_1, the second is located at 0 or (totally equivalent) at g. There is a general transmission function

(62) $$\tau(x) = \begin{cases} \tau_1 \ldots 0 \le x \le x_1 \\ \tau_2 \ldots x_1 \le x \le g \end{cases}.$$

Thus the amplitude of the zero order is

(63) $$A_0 = A_{\text{in}} \cdot \left[\tau_2 - \frac{x_1}{g} \cdot (\tau_2 - \tau_1) \right]$$

and that of the higher orders is given by

(64) $$A_l = \frac{\mathrm{i} \cdot A_{\text{in}}}{2 \cdot \pi \cdot l} \cdot (\tau_2 - \tau_1) \cdot \left(1 - \exp\left(-\mathrm{i} 2\pi \frac{l}{g} x_1 \right) \right).$$

Energy-related quantities as for example light intensity and light power are proportional to the valued square $A \cdot A^*$ of the complex-valued amplitude A. The diffraction efficiency, as the ratio between energy quantities, therefore is given by

(65) $$\eta_l = \frac{A_l \cdot A_l^*}{A_{\text{in}} \cdot A_{\text{in}}^*}.$$

The diffraction efficiencies depending to x_1 are then

(66) $$\eta_0 = \frac{x_1^2}{g^2} \cdot \left| \tau_2 - \tau_1 \right|^2 + \left| \tau_2 \right|^2 \cdot \left(1 - 2 \frac{x_1}{g} \right) + \frac{x_1}{g} \cdot \left(\tau_1 \tau_2^* + \tau_1^* \tau_2 \right)$$

for the zero order and

(67) $$\eta_l = \frac{\left| \tau_2 - \tau_1 \right|^2}{\pi^2 \cdot l^2} \cdot \sin^2 \left(\pi l \frac{x_1}{g} \right) \quad \text{for} \quad l \neq 0.$$

The diffraction efficiencies of the individual orders therefore have a characteristic envelope of the form $\mathrm{sinc}^2(\pi l x_1 / g)$, which is not dependent on the individual transmission

values τ_1 and τ_2. This means, for example, that with a transition point $x_1=g/k$ (with an integer number k) all diffraction orders $l=nk$ disappear with the exception of the zero order.

For this reason a grating with a ratio of the structure widths of 1:1 (i.e. $x_1=g/2$), produces only odd diffraction orders. Depending on the amplitudes ρ_1, ρ_2 and the phases φ_1, φ_2 of the two transmittance values τ_1 and τ_2, the transmission function of such a grating can be written as

(68)
$$\tau(x)=\begin{cases}\rho_1\cdot e^{i\cdot\Phi_1}\ldots 0\le x\le\dfrac{g}{2}\\ \rho_2\cdot e^{i\cdot\Phi_2}\ldots\dfrac{g}{2}\le x\le g\end{cases}$$

By evaluation of the integral in equation (61), the amplitude of the zero diffraction order A_0 is obtained as

(69)
$$A_0=\frac{A_{in}}{2}\cdot\left(\rho_1\cdot\exp(i\cdot\Phi_1)+\rho_2\cdot\exp(i\cdot\Phi_2)\right)$$

and for $m=2k+1$ the amplitude in the l^{th} diffraction order A_l is

(70)
$$A_l=\frac{i\cdot A_{in}}{\pi\cdot l}\cdot\left(\rho_2\cdot\exp(i\cdot\Phi_2)-\rho_1\cdot\exp(i\cdot\Phi_1)\right).$$

With the phase difference $\Delta\Phi=\Phi_1-\Phi_2$, the diffraction efficiency in the diffraction orders is obtained as

(71)
$$\eta_0=\frac{1}{4}\left[\rho_1^2+\rho_2^2+2\rho_1\rho_2\cos(\Delta\Phi)\right]$$
$$\eta_l=\frac{1}{\pi^2 l^2}\left[\rho_1^2+\rho_2^2-2\rho_1\rho_2\cos(\Delta\Phi)\right]\quad\text{for }(l\neq 0)$$

The diffraction efficiencies in the diffraction orders are independent of the grating period g. Using the setting of the greyscale values of the addressed binary grating the amplitudes ρ_1, ρ_2 and the relative phases φ_1, φ_2 will be adjusted.

For complex binary linear gratings with more than two transition points x_k the discussion shall be restricted to pure phase gratings with phase values φ_1 and φ_2. For gratings whose transmittance values also have an amplitude component, the characteristics are very similar, as discussed in section 4.3.

The amplitudes of the diffraction orders, which are created by such a grating with $2K$ transition points, can be written for all diffraction orders $l\neq 0$ as

(72)
$$A_l=\frac{\sin(\Delta\Phi/2)}{\pi l}\sum_{k=1}^{2K}(-1)^k\exp(-2\pi i\frac{lx_k}{g}).$$

The diffraction efficiencies of the orders are calculated best with the additional quantities

(73)
$$S_l = \sum_{i=1}^{2K} (-1)^i \sin(2\pi l x_i)$$
$$C_l = \sum_{i=1}^{2K} (-1)^i \cos(2\pi l x_i)$$

and

(74)
$$Q = \sum_{i=1}^{2K} (-1)^i x_i \,.$$

The diffraction efficiencies of the orders are then

(75)
$$\eta_0 = 1 - 4Q(1-Q)\sin^2(\Delta\Phi/2)$$

for the zero order and

(76)
$$\eta_l = \frac{\sin^2(\Delta\Phi/2)}{\pi^2 l^2}\left(C_l^2 + S_l^2\right)$$

for higher orders.

4.4.3 Diffraction at dynamically addressed pixelated grating

When generating gratings with the help of a dynamic addressable spatial light modulator the transition points can no longer be chosen completely freely. Instead, the grating period consists of N pixels of the size p, the grating period is therefore given by Np. All transition points $x_k = X_k p$ are multiples of the pixel size p. This pixelation already has an influence on the amplitude of certain diffraction orders. Using equation (72) it is easy to prove that

(77)
$$A_N = 0$$

and

(78)
$$A_{m+N} = \frac{m}{m+N} A_m \,.$$

Both equations indicate that in a grating consisting of N individual spatial pixels only N diffraction orders can have independently selectable amplitudes. The equations have been derived for binary phase gratings, but remain also valid for other binary gratings with any transmittance values τ_1 and τ_2 because of the considerations of section 4.3.2.

The addressable dynamic linear gratings have not only restrictions on the choice of the transition points. Additional effects are caused by the edges of each liquid crystal cells. These cell boundaries act as a separate, additional diffraction grating and can be described in different directions as binary linear amplitude gratings with the transmittance values $\rho_1=0$ and $\rho_2<1$ and two transition points w_b and g (see equations (66) and (67)).

When a dynamic grating is addressed, effects of diffraction appear at both gratings simultaneously. There are now a few different approaches to a mathematical description.

(1) The first and simplest description is the direct calculation of the amplitudes of the orders for a grating period. This is, for example, possible for an addressed Ronchi grating

with the transmittance values τ_1 and τ_2. Involving grating ridges, the resulting grating consists of four transition points: $x_1=w_b$, $x_2=p$, $x_3=p+w_b$ and $x_4=2p=g$. From the amplitudes of the diffraction orders the diffraction efficiencies are obtained as

$$\eta_l = \begin{cases} |\tau_1+\tau_2|^2 (p-w_b)^2 & \text{for } l=0 \\ |\tau_1+\tau_2|^2 \sin^2(\pi l w_b/(2p))/(\pi l)^2 & \text{for even } l \text{ with } l\neq 0 \\ |\tau_2-\tau_1|^2 \cos^2(\pi l w_b/(2p))/(\pi l)^2 & \text{otherwise} \end{cases} \tag{79}$$

It is obvious that the diffraction efficiencies are dependent on the cell boundary width. For the special case of an ideal binary phase grating with $\tau_1+\tau_2=0$ all even diffraction orders disappear again, so that the diffraction pattern is quite similar to the one obtained without cell boundaries.

(2) The second description is derived from the fact that the combined grating of addressed pixels and the intermediate cell boundaries can be written as a product of both transmission functions, because we describe the cell boundaries with the transmittance 0 and the cells with a non-zero amplitude transmittance value.

The frequency spectrum (and thus the Fraunhofer diffraction pattern in the far-field) is obtained by the Fourier transform of a product of two functions, which are, following the convolution theorem, calculated by a convolution of the two individual Fourier spectra. Since both transmission functions are periodic, both spectra are discrete so that the convolution of the two spectra is discrete, too.

According to equation (78) the discrete spectrum can be written as

$$\tilde{A}_m = A_m \left(\left(1-\frac{w_b}{p}\right) + \sum_{\substack{k=-\infty \\ k\neq 0}}^{+\infty} \frac{m}{m-kN} \frac{i}{2\pi k} (1-\exp(2\pi i k \frac{w_b}{p})) \right). \tag{80}$$

The diffraction pattern is similar to the one we would obtain without the cell boundaries (i.e. $w_b=0$). The amplitudes are simply multiplied with a factor that independent from the addressed grating. The first term is usually much greater than remaining terms in the equation shown above, and can be interpreted as a loss factor by the non-transparent cell boundaries. The exact calculation of the summation received from equation (79) is quite complicated, so yet another description is interesting.

(3) The third description and computation possibility is based on the *sampling theory*. The N discrete pixels of an SLM can be interpreted as a representation of N sampling values from a local continuous function, taken at distances corresponding to the pixel spacing,.

Of course, according to the *Whittaker-Shannon theorem* the sampled function is limited by an upper frequency: the original function between two sampling values should be in good agreement with the approximation of an interpolation function between these two values. If the function has greater changes between two sampling points, information is lost inevitably. In this case, the sampled function has a *spatial frequency bandwidth* which is too high. In other words, in this case the sampling distances are too large.

This means that a function obtained by the interpolation of sampling points is limited in its spatial frequencies, and the amplitudes of higher spatial frequencies are recurrences of the limited fundamental spectrum; with an envelope given by the interpolation. It is interesting that to some degree this was already deduced directly at the beginning of this section for binary linear pixelated gratings, without any sampling theory.

However, the sampling theory is more flexible and allows the description of diffraction effects of any even two-dimensional pixelated diffracting objects, as it can be created

with an SLM Therefore a brief introduction will be given here for the one-dimensional case.

A sampling $f_s(x)$ of a function $f(x)$ at N points with a distance p is given by

(81) $$f_S = f \cdot \mathrm{comb}\left(\frac{x}{p}\right).$$

The pixelated function f_I interpolated for a contiguous interval is given by the convolution

(82) $$f_I = f_S \otimes \mathrm{rect}(p).$$

Then the Fourier transformation of the function f can be numerically calculated by the discrete Fourier Transformation (DFT) of the sampled function $f_s(x)$. This is useful for the calculation of diffraction effects, especially when using the FFT(‚fast Fourier transform')-implementation.

In summary the spatial frequency spectrum and therefore the diffraction far-field is obtained as

(83) $$[\mathcal{F}(f_I)](\nu_x) = \left(\mathrm{comb}(\nu_x p) \otimes \mathcal{F}(f)\right) \cdot \mathrm{sinc}(\nu_x p).$$

The central N frequencies are given by the DFT of the sampled transmittance function of the diffracting element. Higher frequencies occur as a repetition of the fundamental frequencies with an enveloping curve, which in turn is described by the Fourier-transformation of the pixel shape function (or interpolation function). In the analytical form shown here, these correlations are of considerable importance for the numerical simulation of the propagation of light after diffraction at pixelated structures and hence for the design of diffractive optical elements.

4.4.4 Diffraction angles of the orders

With the spatial periodicity g, often referred to as *grating period*, the diffraction angles α_l are determined by the grating equation

(84) $$g(\sin(\theta + \alpha_l) - \sin\theta) = l \cdot \lambda,$$

where θ denotes the angle of incidence of the light. For perpendicularly incident light we have $\theta = 0$, and the equation is simplified to

(85) $$g \sin\alpha_l = l \cdot \lambda.$$

It can be seen that this equation can be written equivalently in terms of the x components of the wave vectors $\mathbf{k}$ for the incident wave and $\mathbf{k'}$ for the diffracted wave, yielding

(86) $$k_x' = k_x + l \cdot \frac{2\pi}{g} = k_x + l \cdot k_g,$$

where k_g denotes the absolute value of the wave vector of the grating. Introducing the spatial grating frequency ν_g, a similar correlation for the spatial frequencies of the diffracted waves is obtained:

(87) $$\nu_x' = \nu_x + l \cdot \frac{1}{g} = \nu_x + l \cdot \nu_g.$$

The notation with grating frequencies or wave vectors is be preferable when calculating the directions of light propagation (or the diffraction angle) for gratings with a two-dimensional periodicity. For example, the wave vector of the diffracted wave satisfies equation (86) in the two directions perpendicular to the direction light propagation. The missing vector component of the propagation direction can then be calculated from the absolute value of the wave vector, which is determined by the wavelength.

4.5 Influence of linear and quadratic phase functions

With an adequate distance from the diffracting object the Fraunhofer far-field diffraction can be observed. When a lens is put into the optical path, the far-field diffraction pattern can be observed in its rear focal plane (see section 4.5.1). However, A lens can be represented by a phase function and a diffracting object itself can contain such a 'lens phase', resulting in a position change of the plane of far-field diffraction. The same holds for the use of a refractive prism and the presence of a linear phase function in the diffracting object itself.

4.5.1 Quadratic phase functions – Fourier transformation with a lens

The far-field diffraction pattern can be observed at finite distance making use of a lens. The transmittance of the field through the lens leads to a position-dependent phase shift and can be described by multiplication with the lens transmittance function

$$\tau_{\text{lens}} = e^{-\mathrm{i}\frac{k}{2f}\left(x^2+y^2\right)}. \tag{88}$$

Because of the limited distance the diffraction has to be computed with the Fresnel approximation of the Kirchhoff integral. Denoting the distance behind the lens, at which the Fourier transformation of the light field can be observed as Δz, we get

$$E(x,y,\Delta z) = \frac{e^{\mathrm{i}kz}}{\mathrm{i}\lambda\Delta z}\int_{-\infty}^{\infty}\int_{-\infty}^{\infty} E(x',y',0)\, e^{-\mathrm{i}\frac{k}{2f}\left(x'^2+y'^2\right)} e^{\frac{\mathrm{i}k}{2\Delta z}\left((x'-x)^2+(y'-y)^2\right)} dx'\,dy'. \tag{89}$$

The exponents of both exponential functions are quite similar. By using $\Delta z = f$ (shifting the observation point into the focal plane of the lens) they can be combined to

$$\begin{aligned} E(x,y,f) &= \frac{e^{\mathrm{i}kf}}{\mathrm{i}\lambda f} e^{\mathrm{i}\frac{k}{2f}\left(x^2+y^2\right)} \int_{-\infty}^{\infty}\int_{-\infty}^{\infty} E(x',y',0) e^{\frac{\mathrm{i}k}{f}((x'x)+(y'y))} dx'\,dy' \\ &= \frac{e^{\mathrm{i}kf}}{\mathrm{i}\lambda f} e^{\mathrm{i}\frac{k}{2f}\left(x^2+y^2\right)} \mathcal{F}[E]\left(\frac{x}{\lambda f}, \frac{y}{\lambda f}\right). \end{aligned} \tag{90}$$

In the focal plane of a lens a field distribution is formed that equals the Fourier transformation of the field distribution before the lens multiplied with a phase factor. Therefore an intensity distribution is observed which is proportional to the intensity distribution of the Fourier transformation of the input field which describes its far-field diffraction pattern.

Exactly the same characteristics *without a lens* can be observed with a diffracting object which incorporates a phase function τ_{lens}. The focal length satisfying the phase term in the light field behind the diffracting object or the (last) lens, respectively, is decisive, rather than the origin of the phase term. Possible origins of lens phase terms are diffracting objects, actual lenses and also the incident wave, which can be convergent or divergent and in this case contributes to the quadratic part of the phase of the light field. The coefficient of the resulting spherical phase function determines the plane in which the Fraunhofer diffraction pattern can be observed.

4.5.2 Linear phase functions and the shifting theorem

From a property of the Fourier transformation it can be derived that the far-field diffraction does not change significantly when the diffracting object is translated. The original diffraction pattern is superimposed with a linear phase function:

$$\begin{aligned}\mathcal{F}[f(x-x_0)](\nu_x) &= \mathcal{F}[f(x)](\nu_x)\cdot\exp(2\pi \mathrm{i}\,\nu_x x_0)\\ &= \mathcal{F}[f(x)](\nu_x)\cdot\exp(\mathrm{i}k_x x_0)\end{aligned}. \tag{91}$$

Vice versa, a linear phase function in the light field behind the diffracting object introduces an offset to the spatial frequency spectrum and correspondingly the Fraunhofer diffraction pattern is spatially shifted. Like for a 'lens phase', it is not important if the linear phase term is actually introduced by a prism in front of the diffracting object, or if a linear phase term is added to the transmission function of diffracting object, or if the illuminating wave is incident at an angle (with wave vector element k_x). The effect to the diffraction pattern is the same.

4.5.3 Spatial separation of diffracted and undiffracted light waves

It is known from the conventional holography that the reference wave illuminating the hologram contributes a bright spot to the diffraction pattern at the reconstruction plane of a Fraunhofer hologram. This spot is created by the light which is not diffracted by the hologram since the diffraction efficiency of the hologram is limited.

When recording a conventional hologram the field of light waves diffuse scattered by an object interferes with an adequate reference field and the formed interference pattern is saved in a recording material, usually a photo emulsion. When originating from an spatially extended, irregular-shaped object, this interference pattern has the structure of a complex diffraction grating.

The creation of this so called hologram requires the coherence of the object and reference wave fields (see section 4.1.2). The illuminated hologram appears as an diffraction grating. Illuminated with the reference wave, wave fields which resemble the structure of the object wave are formed in a diffraction order. Thus images of the object are reconstructed in three dimensions.

The reconstruction plane of the reference wave and the reconstruction of the holographically recorded object can be separated along the propagation axis of the light. Therefore a spherical wave is used as the reference wave at the recording and as a result a Fresnel hologram is generated. Exactly the same characteristics can be achieved by multiplicative superposition of a Fraunhofer hologram calculated for the far-field and a lens phase.

Superpositions of numerically calculated phases for Fraunhofer far-field diffraction of two-dimensional objects with analytical phase functions, e.g. the quadratic phase functions representing a lens, will be denoted below as *computer generated holograms* (CGH).

This term was introduced when it became possible to calculate the interference pattern of object and reference wave for simple objects and generating an optical element without the interference based recording of a (conventional) hologram.

An alternative for the spatial separation of the reconstruction of the illumination wave from the reconstruction of the holographic recorded object is the use of an off-axis reference wave.

4.6 Applications of Fourier optics

So there are many applications of the Fourier optic thinkable, only two selected examples shall be presented here. First an introduction to iterative numerical calculation of diffractive optical elements will be given. The last paragraph of this theoretical

introduction presents the concept of the spatial frequency filtering, which quite clearly illustrates the concept of 'spatial frequencies'.

4.6.1 Design of diffractive elements

By solving the inverse diffraction problem for a desired diffraction pattern the required diffracting structure can be calculated and produced with suitable micro-fabrication methods. The result is a so called *diffractive optical element* (DOE) which reconstructs the desired image (by diffraction and interference) in the far-field when illuminated with a coherent light source. With some restrictions DOEs can replace classical optical elements like lenses, beam splitter, prisms and even beam forming elements. Furthermore, even more complex elements like multi-focusing lenses can be created.

For many applications, the suppression of the zero diffraction order and of undesired higher diffraction orders is the challenge. DOEs have considerable chromatic aberrations and the diffraction efficiency is limited. Nevertheless DOEs are already used in many applications, especially when the available space is limited or the optical function could not be realized with other optical elements.

A brief schematically description of the calculating algorithm also used in the included 'OptiXplorer' software is presented below. It is an iterative Fourier transformation algorithm (IFTA). The basic principle of the algorithm is shown in Figure 8.

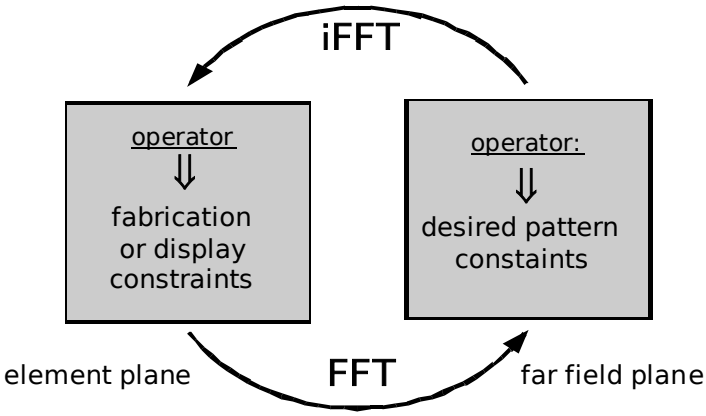

Figure 8: Schema of an iterative Fourier transformation algorithm (IFTA)

The calculating steps referred to 'FFT' and 'iFFT' in the figure represent the numerical simulation of the propagation of the light between the plane of the diffracting object and the plane of the far-field diffraction. In the plane of the far-field the present diffraction pattern generated by the diffracting object will be approximated to the desired diffraction pattern. In turn in the plane of the object (or element) the required diffracting object, numerical calculated from the diffraction pattern, is adjusted according to the technical facilities (pixel size, available values of the transmittance function, etc.).

After a sufficient number of calculating steps usually the operator of the object plane will be defined increasingly restrictive. In general, a quantization to a number of realizable transmittance values (normally phase steps) is necessary. After the last calculating step the object achieves the production conditions. The quality of the desired diffraction pattern by the calculated object differs from case to case and investigation of such design problems is an important part of the field of *Diffractive Optics*.

4.6.2 Spatial frequency filtering

For an object placed in front of a lens having a distance d to it, the light propagation in front of the lens can be simulated using the Fresnel approximation of the Kirchhoff diffraction integral. The result shows that the light in the focal plane is only changed by a phase factor dependent on d, and for the special case $d = f$ the field in the focus plane is

equivalent to the Fourier transformation of the field in the object plane (apart from a factor, which does not depend on x and y). The calculation yields

(92) $$E(x, y, f) = \frac{e^{ik2f}}{i\lambda f} e^{i\frac{k}{2f}\left(x^2+y^2\right)} \mathcal{F}[E]\left(\frac{x}{\lambda f}, \frac{y}{\lambda f}\right).$$

The spatial frequency spectrum can be manipulated in the focus plane. The transformation and inverse transformation of the light field can be conveniently done in a so-called 4f setup which utilizes two lenses of equal focal length. In this setup the object, the first lens, the filter plane, the second lens, and the output plane of the system are all separated by the focal length of the lenses.

By using all kinds of filter objects the meaning of the different spatial frequencies can be easily demonstrated. Mechanical blocking of parts where higher spatial frequencies would transmit leads to blurring in the image. Blocking lower spatial frequencies modifies the total brightness.

Based on these concepts, it is possible to understand and discuss the concepts of dark-field imaging or phase-contrast microscopy, which are also based on specific manipulation of the spatial frequencies.

5 References for further reading

Optics in general

1. Eugene Hecht, *Optics,* Addison Wesley Publishing Company; 4th edition (2001)
2. Dieter Meschede, *Optics, Light and Lasers*, Wiley-VCH, Weinheim (2003)
3. Stephen G. Lipson, Henry S. Lipson, David S. Tannhauser, *Optical Physics,* Cambridge University Press, Cambridge (1995)

Polarisation and physics of LC cells

4. Edward Collett, *Polarised Light* (Optical Engineering, Vol. 36), Dekker (1992)
5. Amnon Yariv, Pochi Yeh, *Optical Waves in Crystals,* John Wiley & Sons, New York (1984)
6. Pochi Yeh, *Optical Waves in Layered Media,* John Wiley & Sons, New York (1988)
7. H. Kim and Y. H. Lee, *Unique measurement of the parameters of a twisted-nematic liquid-crystal display,* Appl. Opt. 44(9), pp. 1642-1649 (2005)

Fourier Optics and Diffractive Optics

8. Joseph W. Goodman, *Introduction to Fourier Optics*, Third Edition, Roberts and Company Publishers (2004)
9. Frank Wyrowski and Jari Turunen (ed.), *Diffractive Optics for Industrial and Commercial Applications,* Wiley-VCH (1998)
10. Bernhard Kress and Patrick Meyrueis, *Digital Diffractive Optics*, John Wiley & Sons (2000)
11. R. L. Morrison, Symmetries *that simplify the design of spot array phase gratings*, J. Opt. Soc. Am. A 9(3), pp. 464–471 (1992)

12. L. L. Doskolovich, V. A. Soifer, G. Alessandretti, P. Perlo, and P. Repetto., *Analytical inital approximation for multiorder binary grating design*, Pure Appl. Opt. (3) pp.921–930 (1994)
13. F. Wyrowski and O. Bryngdahl, *Iterative Fourier-transform algorithm applied to computer holography*, J. Opt. Soc. Am. A 5, pp. -1065 (1988)
14. Wolfgang Stößel, *Fourieroptik: Eine Einführung*, Springer-Verlag (1993)

II EXPERIMENTAL TUTORIAL

The tutorial comprises six modules, each of which dealing with a different topic. Module AMP contains fundamental experiments on the polarisation of the light sources and the polarisation modifying characteristics of the LC display, which forms the basis for amplitude modulation. Furthermore, an optical projector setup is assembled using the light modulator as the image source. Module JON investigates the fundamental parameters of the liquid crystal display using Jones matrices. Module LIN deals with separable diffraction gratings. Both the display addressed with no signal as well as the display addressed with binary diffraction gratings will be analysed. Module RON determines the phase shift from measurements of the power in the diffraction orders of Ronchi gratings. Module CGH deals with computer generated holograms (CGHs) and Fresnel zone lenses as well as with the application of dynamic optics. Finally, module INT determines the maximum phase range of the light modulator using a two-beam interferometer.

During the tutorial, horizontal and vertical gratings will often be referred to. To avoid misunderstandings we would like to make clear which direction is which. The light modulator stands upright when the connections are on top. An addressed image appears upright. Horizontal gratings form diffraction orders in a vertical direction and vertical gratings form diffraction orders in a horizontal direction.

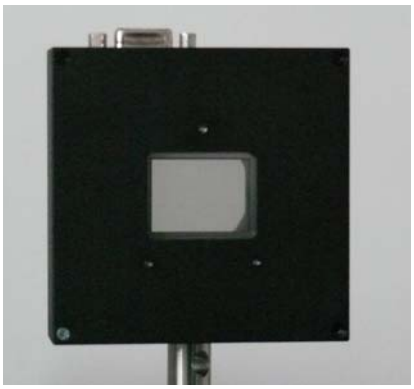

Figure 9: The upright LC2002-light modulator with the connections on top

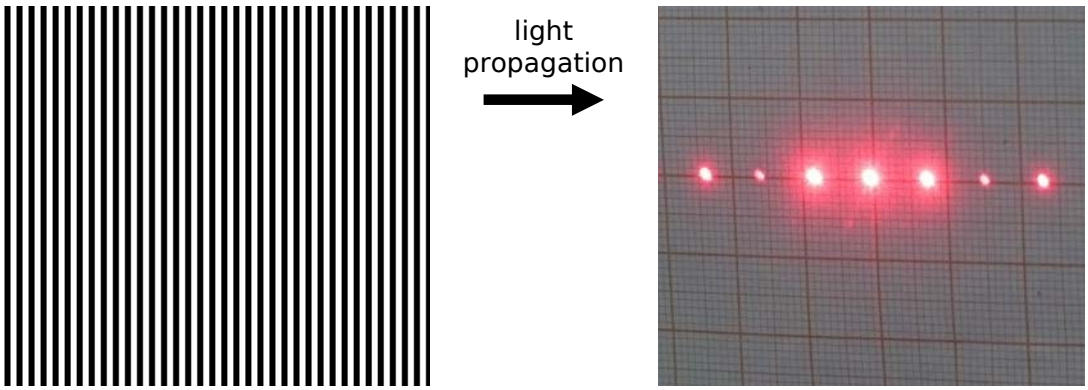

Figure 10: Vertical grating, left: addressed image on the light modulator, right: diffraction pattern with horizontal diffraction orders

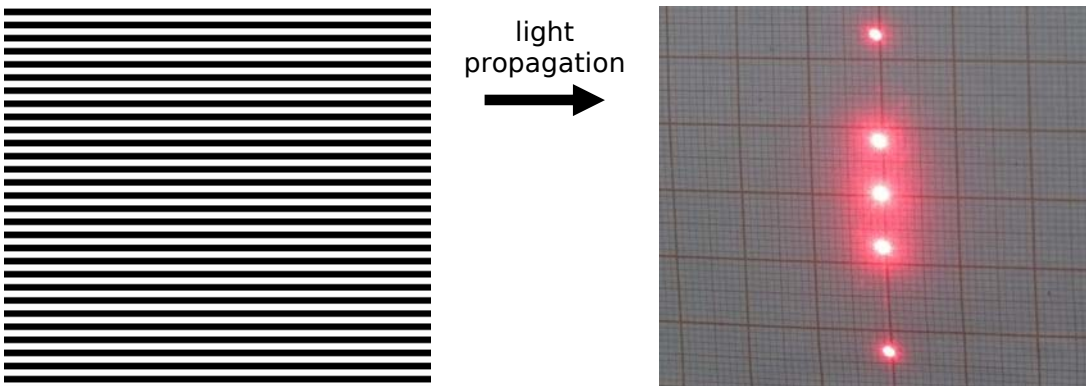

Figure 11: Horizontal grating, left: addressed image on the light modulator, right: diffraction pattern with vertical diffraction orders

6 Module AMP: Amplitude modulation and projection

6.1 Objectives

To understand the following experiments and the functionality of the LC display, the polarisation of light plays a crucial role. Therefore the polarisation characteristics of the light sources will be determined first. Then a projector setup will be assembled using the light modulator as the image source. During the experiment contrast and pixel size will be determined.

6.2 Required components

- **Light modulator:** LC2002
- **Light sources** (at least one of the following)**:** laser module, LED lights
- **Optics:** 2 rotatable polarisers, lens, projection screen
- **Instruments** (at least one of the following)**:** powermeter, photodiode, LDR-photo resistor and ohmmeter

6.3 Suggested tasks and course of experiments

AMP1 Polarisation characteristics of light sources

The polarisation characteristics of different light sources shall be determined. In order to do so, the light transmitted by a rotatable polariser will be measured with a detector.

Experimental setup used:

Light source, polariser, focusing lens, and detector

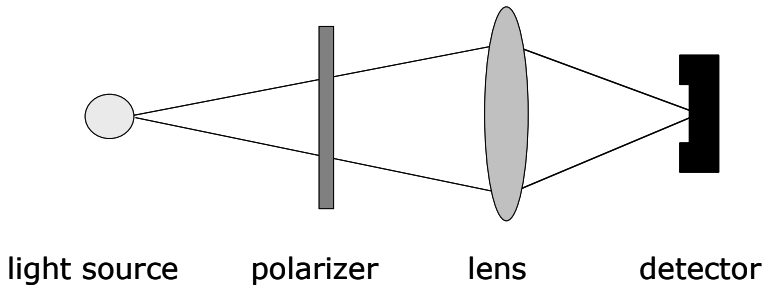

Figure 12: Measurement of the polarisation characteristics of a light source

The polariser is rotated by 10°-15° for each data point. For an unpolarised light source (e.g. an LED), single data points should vary by no more than 3%, whereas for linearly polarised light sources a sinusoidal angular dependence should be observed. Typically, the transmitted power of the provided laser module can be reduced to 1% of the maximum value.

AMP2 Angular distribution of linearly polarised light

A polariser is used to create linearly polarised light. Using a second polariser as an analyser, the angular distribution of the intensity will be measured. This experiment verifies Malus' law. Additionally, from the measured data the contrast can be determined.

Experimental setup used:

Linearly polarised light source, analyser, focusing lens, detector

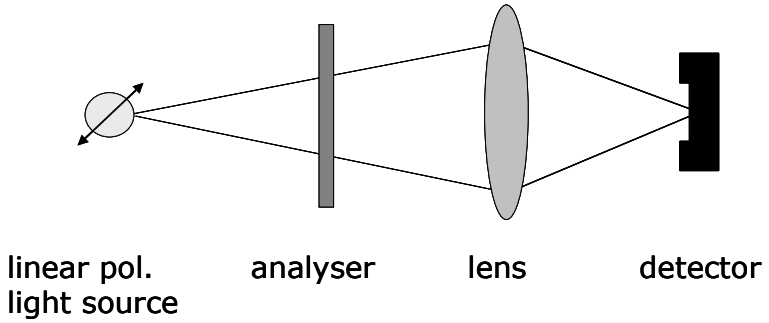

Figure 13: Measurement of the polarisation characteristic of a linearly polarised light source

If the used light source is not linearly polarised, a fixed polariser provides linearly polarised light. The second polariser (the analyser) will be rotated by 10°-15° for each data point. Using LEDs as light sources, the transmitted power can be reduced to 0.3% of the maximum value, so that the contrast ratio is greater than 2500:1. The graph shows the $\cos^2$ dependence and the agreement with the theory. When using light sources with significant infrared emission one has to be aware that polarisers are wavelength dependent, and the infrared part is transmitted through the setup without being polarised.

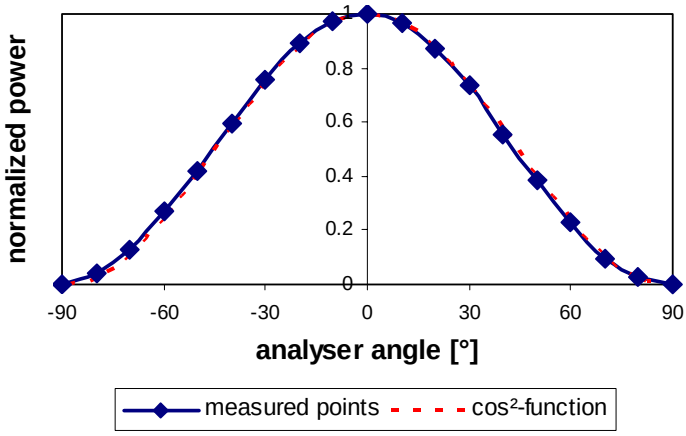

Figure 14: Power of the linearly polarised light versus analyser position

AMP3 Polarising properties of the light modulator

In this experiment, the polarising properties of the light modulator will be determined. The LC display is placed between two polarisers, or alternatively a linearly polarised light source and a polariser, and experiment AMP2 will be repeated, i.e. the angular distribution of the intensity will be measured again.

Experimental setup used:

Linearly polarised light source, light modulator, analyser, focusing lens, and detector

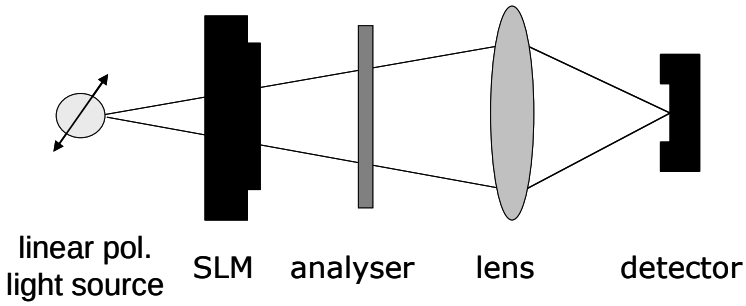

Figure 15: Measurement of the polarisation characteristics of the light modulator

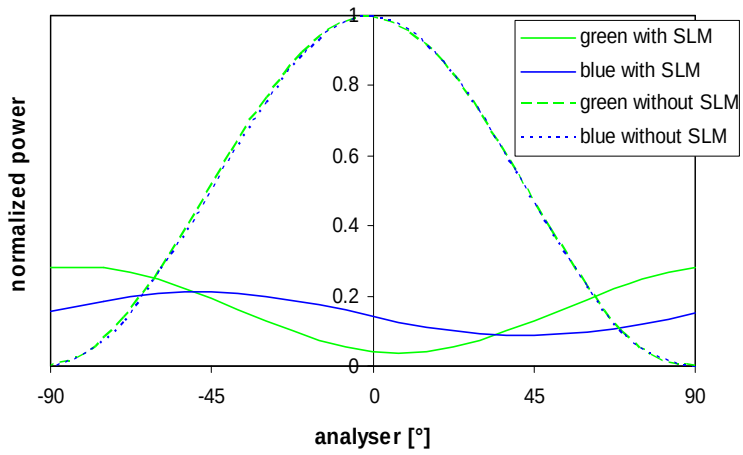

Figure 16: Comparison of the intensities with and without the light modulator (SLM) for two different light sources (blue and green LED) against the analyser position

The measured power is significantly lower compared to experiment AMP2. A shift can be seen in Figure 16. The maximum is shifted by 90° for a green light source, but only 45° for a blue light source. For both light sources the measured power never drops to zero; therefore it is evident that the light is not linearly polarised anymore.

AMP4 Projector setup

First, the setup is assembled with a static slide. As soon as a focused image is observed on the projection screen, the slide is replaced by the combination of polariser/light modulator/analyser. The light modulator is placed in the plane of the slide.

Experimental setup used:

Light source, collimating lens ($f = 75\ \mathrm{mm}$), slide (later replaced by polariser/light modulator/analyser), object lens ($f = 100\ \mathrm{mm}$), projection screen

Optical path for illumination: The object lens should be placed at a plane conjugate to the light source. The aim is to get as much light through the objective aperture as possible. Because the LEDs used are large, the image size of the light source is reduced in order to get more light through the aperture. Ideally, the light source is located in the

front focus plane of the collimating lens. The LC display of the SLM is positioned as close to the collimating lens as possible, so that the aperture of the display is fully illuminated.

Optical path for projection: The object lens images the addressed content of the display, focused and enlarged, onto the projection screen. At the same time, the image plane of the light source should be at an infinite distance.

As a result, both optical paths are linked. Ideally, the rear focal plane of the collimating lens is identical to the front focal plane of the object lens.

AMP5 Optimising the projector setup

The arranged setup with the LCD shall be optimised. The goal is to achieve a high light intensity for white areas while maintaining a high contrast. This can be achieved through parallel rotation of the polarisers. To understand the properties of an LC display it is also interesting to investigate the light transmission when only the analyser is rotated.

Experimental setup used:

Light source, collimating lens, polariser, SLM, analyser, object lens, and projection screen

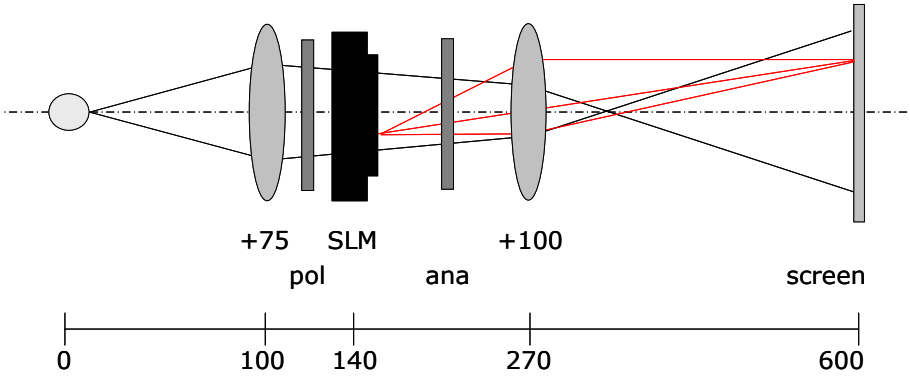

Figure 17: An example for a projector setup with the optical path for illumination (black) and the optical path for imaging (red)

The display is addressed both half black and half white using the software function ‘Horizontally Divided Screen’. Then both intensities for the calculation of the contrast can be measured directly with a detector mounted on a translation stage. Alternatively, an addressing of a white screen is possible and by pressing the inverting button in the right function bar the screen can be switched to black. This makes it possible to measure both intensities consecutively with a fixed detector. The polarisers are rotated perpendicularly to one another. Upon parallel rotation of the polarisers with adequate step sizes, the change in contrast is measured.

A green LED shows a maximum contrast for a polariser/analyser rotation of -45°/-135°. The contrast is 0.96 and the contrast ratio 55:1. Using a laser as the light source, a maximum contrast of 0.99 and a contrast ratio of 140:1 can be measured. Keeping the first polariser fixed at the optimised position and rotating only the second one will produce a low-contrast image at an angle of 45°, a black-white-inverted image at 90° and an optimum image at 180°.

AMP6 Pixel size of the LC display

The pixel size of the display can be calculated with the equations of classical optics. The display will be addressed with a rectangular object of known dimension. It will be imaged by a (thin) lens, whose focal distance is also known.

Experimental setup used:

Light source, collimating lens, polariser, SLM, analyser, object lens, and projection screen

A white image with a black square with the size of 200x200 pixels in its centre will be addressed on the display. The object size of the black square on the display can be calculated from the image size, the image distance and the focal length of the lens.

(93) $$G = \frac{B}{b/f - 1}.$$

Using graph paper as the projection screen, the accuracy of the image size should be ± 0.5 mm. The error is given by

(94) $$\Delta G = \frac{\Delta B}{b/f - 1} + \frac{\Delta b \cdot B}{f(b/f - 1)^2}.$$

The pixel size can be determined to 32 µm ± 2-3 µm.

AMP7 Relation between pixel voltage and modification of the polarisation state

Every grey level corresponds to a specific voltage a single LCD element is addressed with. The different voltage leads to a different tilt of the liquid crystal molecules and therefore a different polarisation state. For different positions of the analyser, the intensity will be measured for a number of uniform grey level images addressed to the display.

Experimental setup used:

Light source, collimating lens, polariser, SLM, analyser, object lens, and detector

For six grey levels (250, 200, ..., 0) the rotation angle of the analyser for the smallest and largest measured power values is determined. The graphical representation of the result yields a different ellipse for each grey level.

In parametric form, the semimajor axis a corresponds to maximum power, and accordingly the semiminor axis b corresponds to minimum power (measured with the analyser rotated by 90° to the maximum). The angle of the analyser for the maximum measured power corresponds to the angle Δ, which denotes the rotation of the semimajor axis to the x-axis.

(95) $$\vec{x}(\varphi) = \begin{pmatrix} \cos\Delta & -\sin\Delta \\ \sin\Delta & \cos\Delta \end{pmatrix} \begin{pmatrix} a \cdot \cos\varphi \\ b \cdot \sin\varphi \end{pmatrix}.$$

Figure 18 shows polarisation ellipses for three different grey levels with the following rotation angles:

grey level	angle Δ [°]
250	45
150	0
50	-45

Table 1: Rotation of the polarisation ellipse

As can be seen in Figure 18, the orientation of the ellipse is rotated as a function of the grey level.

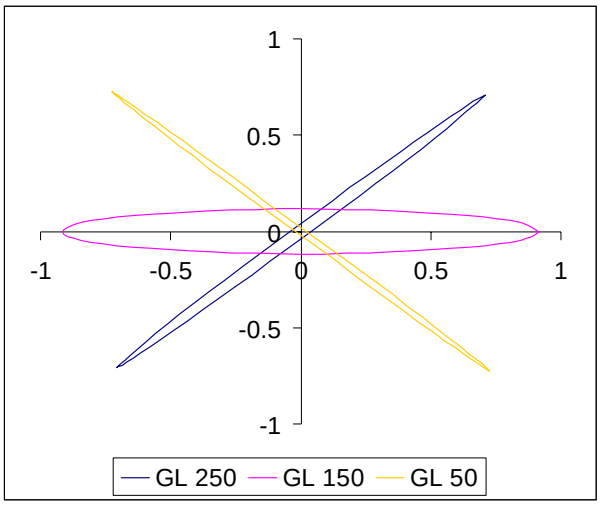

Figure 18: Rotated polarisation ellipses for different grey levels (GLs)

6.4 Keywords for preparation

Polarisation of light, generating polarised light, optical elements to change the polarisation state, contrast, liquid crystals, functionality of a LCD, amplitude modulation, pixel size, classical optics.

6.5 References

Dennis Goldstein

Polarized Light, Second Edition, Revised and Expanded

Marcel Dekker Ltd, 2 Rev Exp (2003)

Bergmann; Schäfer

Lehrbuch der Experimentalphysik, Band 3, Optik

Gruyter, Berlin (2004)

Eugene Hecht

Optik (3.Auflage)

Oldenbourg Verlag, München Wien (2001)

7 Module JON: Determination of Jones matrix representation and TN-LC cell parameters

7.1 Objectives

To predict the transmission characteristics of an LC display, one needs to know the Jones matrix W. The Jones matrix components depend, as described in section 3.3, on the mostly unknown display parameters α, β and ψ. Using simple transmission measurements, one can determine the Jones matrix components.

For the determination of the Jones matrices for different birefringence β one can use light sources with different wavelengths; or one can address different grey values on the LC display while using a single wavelength.

The derivation of the display parameters is only unambiguous in the case of an unaddressed display; see section JON4. For this measurement at least three different wavelengths are required.

7.2 Required components

- **Light modulator:** LC2002
- **Light sources** (at least one of the following)**:** laser module(s), LED lights
- **Optics:** 2 rotatable polarisers, lens, $\lambda/4$-waveplate if polarised light source is used
- **Instruments** (at least one of the following)**:** powermeter, photodiode, LDR-photo resistor and ohmmeter

7.3 Suggested tasks and course of experiments

JON1 Determination of the polarisation characteristics and check of the setup

To determine the Jones matrix, angle-dependent transmission measurements are taken for a system comprising polariser, LC display and analyser. To avoid very small transmissions, due to specific polariser angle combinations, one needs to have a nearly constant transmission for all angles behind the first polariser. In the case of a linearly polarised light source this can be accomplished by using a $\lambda/4$-waveplate.

As part of this experiment, it is beneficial to examine the effect of a $\lambda/4$-waveplate on linearly polarised light. With a $\lambda/4$-waveplate for the used wavelength and a 45° angle of the main axis to the linearly polarised light, circularly polarised light will be created, in other cases elliptically polarised light. For the experiments, a detector will be used to determine the transmitted light through a rotatable polariser. Eventually a lens must be used to focus the collimated light on the detector.

Experimental setup used:

Light source, $\lambda/4$-waveplate, polarisers, LC display, detector, and lens (optional).

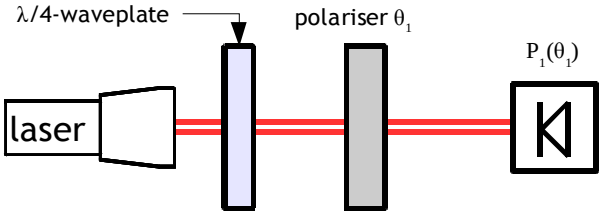

Figure 19: Polarisation characteristics measurement of the light source and check of the setup

Single values are taken while the polariser is rotated in increments of 10° - 15°. The sum of the powers

(96) $$P_{1\Sigma} = P_1(\theta_1) + P_1(\theta_1 + 90°)$$

should be constant. Variations of ±2 % can be tolerated. For bigger variations the setup must be checked for beam displacements or beam steering, potentially caused by the polariser which might move the light beam relative to the detector area. For an example of the measurement see Figure 20.

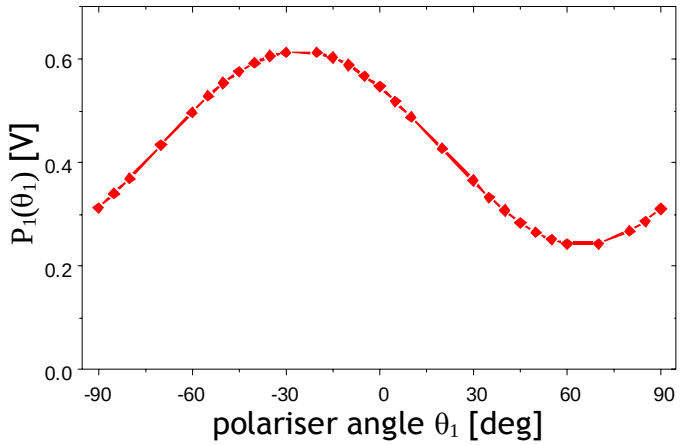

Figure 20: Polarisation characteristic of a laser diode (λ=650 nm) as light source with λ/4-waveplate

If the LC display and the analyser are added to the experimental setup, see Figure 21, the power sum

(97) $$P_{2\Sigma}(\theta_1) = P_2(\theta_1, \theta_2) + P_2(\theta_1, \theta_2 + 90°)$$

must be a constant for one fixed polariser angle θ_1 and a variation of θ_2.

The sum $P_{2\Sigma}(\theta_1)$ is a function of the polariser angle θ_1. Depending on the stability of the light source it is recommended to take several values for one polariser setting and to use the mean value.

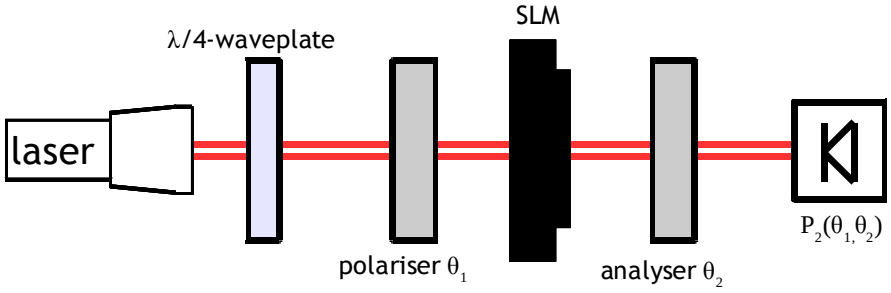

Figure 21: Transmission measurement through the LC display for determination of the Jones matrix components

JON2 Transmission curve for different polariser angle combinations

In section I3.5, the Jones matrix of the SLM was introduced as a function of the parameters f, g, h und j:

$$W_{\text{TN-LC}}^{\text{fghj}} = e^{-i\cdot\beta}\cdot\begin{pmatrix} f - i\cdot g & h - i\cdot j \\ -h - i\cdot j & f + i\cdot g \end{pmatrix}.$$

These Jones matrix components include the twist angle α, the 'director' angle ψ and the birefringence β. Only β is a function of the wavelength and of the applied voltage V: $\beta(\lambda,V)$ to the LC display. The display parameters α and ψ are constant for all wavelengths and applied voltages. If one wishes to examine various states of the LC display, this can be achieved by addressing different grey values on the display or by using a different wavelength. In this section, the Jones matrix components for one single state are determined.

Two polariser angle combinations are most suitable for the determination of the Jones matrix components. First, both polarisers are rotated clockwise ($\theta_1 = \theta_2$, same direction rotation) and second, one polariser is rotated clockwise and the other anticlockwise ($\theta_1 = -\theta_2$, opposite direction rotation).

The transmission $T(\theta_1,\theta_2)$ for both cases follows from the general form:

(98)
$$\begin{aligned} T^{+}(\theta_1) &= T(\theta_1,+\theta_1) = f^2 + (g\cdot\cos(2\theta_1) + j\cdot\sin(2\theta_1))^2 \\ T^{-}(\theta_1) &= T(\theta_1,-\theta_1) = g^2 + (f\cdot\cos(2\theta_1) + h\cdot\sin(2\theta_1))^2 \end{aligned}.$$

Experimental setup used (see Figure 21):

Light source, λ/4-waveplate, polarisers, LC display, detector, and lens (optional).

Software used:

A computer programme is required to determine the coefficients of sinusoidal functions with offset x_0, amplitude a and phase φ

$$f(x) = x_0 \pm a\cdot\sin(x+\varphi)$$

from the measured data by a numerical fit.

Again, polariser angles are varied in increments of $10°$ maximum. The smaller the chosen angle intervals are, the more accurately the development of the measurement curves can

be evaluated. The angular range, which is covered during the measurement, should be chosen large enough, for example 180°.

For the normalisation of the measurement curves it is necessary to measure the power of the polariser combination $P_2(\theta_1,\theta_2)$ and the crossed combination $P_2(\theta_1,\theta_2 + 90°)$. The transmission $T_2(\theta_1,\theta_2)$ can be obtained from the measurement data via

(99) $$T(\theta_1,\theta_2) = \frac{P_2(\theta_1,\theta_2)}{P_{2\Sigma}(\theta_1)}.$$

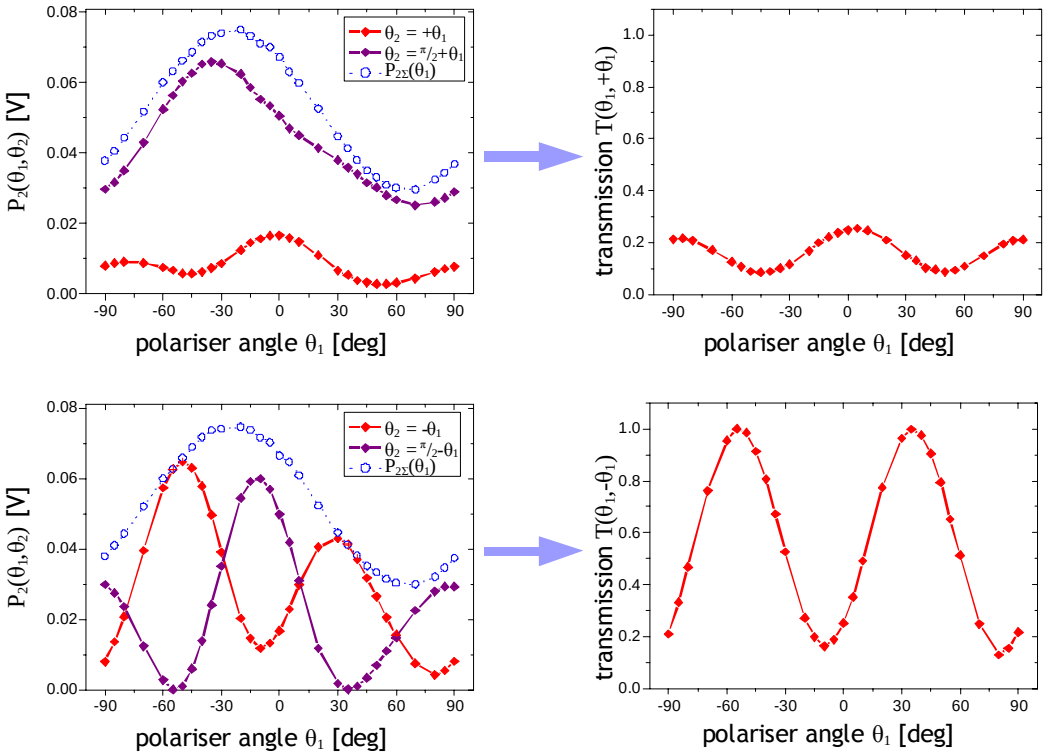

Figure 22: Example for the normalisation of curves of the 'LC2002' in a state with no applied voltage at λ = 650 nm; left curves are $P_2(\theta_1,\theta_2)$, $P_{2\Sigma}(\theta_1)$ and right curves corresponding $T(\theta_1,\theta_2)$

For an example of such a measurement and the normalised transmission curves see Figure 22. The equations for same and opposite direction rotations from equation (98) can be condensed to

(100) $$T^{\pm}(\theta_1) = C_1^{\pm} + C_2^{\pm} \cdot \cos(4\theta_1 + \Phi^{\pm}).$$

The Jones matrix components can be obtained from the constants $C_1^{\pm}$, $C_2^{\pm}$ and $\Phi^{\pm}$ by fitting the transmission curves of one single state.

The absolute values of the Jones matrix components can be derived from:

same direction rotation

$$f^{+} = \pm\sqrt{C_1^{+} - C_2^{+}}$$
$$g^{+} = \pm\sqrt{2C_2^{+}} \cdot \sin\left(\Phi^{+}\right)$$
$$j^{+} = \pm\sqrt{2C_2^{+}} \cdot \cos\left(\Phi^{+}\right)$$
$$h^{+} = \pm\sqrt{1-\left(f^{+2} + g^{+2} + j^{+2}\right)}$$

opposite direction rotation

$$g^{-} = \pm\sqrt{C_1^{-} - C_2^{-}}$$
$$f^{-} = \pm\sqrt{2C_2^{-}} \cdot \sin\left(\Phi^{-}\right)$$
$$h^{-} = \pm\sqrt{2C_2^{-}} \cdot \cos\left(\Phi^{-}\right)$$
$$j^{-} = \pm\sqrt{1-\left(g^{-2} + f^{-2} + h^{-2}\right)}$$

λ[nm]	state	$\|f\|$	$\|h\|$	$\|g\|$	$\|j\|$	sgn(gj)	sgn(fh)
650	V=0	0.287 ± 0.004	0.872 ± 0.003	0.389 ± 0.005	0.04 ± 0.01	+1	+1

Table 2: Absolute values and signs two products of Jones matrix components at λ = 650nm

Additionally one obtains the signs for two different products of matrix components, sgn(g·j) and sgn(f·h), from sinus and cosinus of $\Phi^{\pm}$. The Jones matrix components determined from the same and opposite direction rotations must be identical within the accuracy of the measurements. The obtained Jones matrix components at λ=650 nm are listed in Table 2.

In general it is impossible to determine *all* signs of the Jones matrix components. For some cases this can be done after the determination of the display parameters from the Jones matrix components.

JON3 Determination of display parameters from Jones matrix components

As a result of the trigonometric form of the equations f, g, h and j, which describe the Jones matrix components as a function of the display parameters, there are many mathematically equivalent solutions for the parameters α, β and ψ. The solution set includes the physical solution.

Single solutions can be obtained by using customary search algorithms of a computer algebra system. These solutions depend on the chosen solution parameters and intervals. The combination of numeric and graphic solution search, as shown here, ensures that all possible solutions are found. Because of the diversity of the potential solutions, it is impossible to determine the display parameters from the Jones matrix components of one single state.

Software used:

A computer programme for searching the null of an equation is required.

If one writes the twist angle α as a function of the parameter γ

(101)
$$|\alpha| = \gamma \cdot \sqrt{\frac{f^2 + h^2 - \cos^2\gamma}{\sin^2\gamma}},$$

one can also write the Jones component f as a function of the parameter γ, defining

$$z(\gamma)=\sqrt{\frac{f^2+h^2-\cos^2\gamma}{\sin^2\gamma}}\sin\gamma\sin\left(\gamma\sqrt{\frac{f^2+h^2-\cos^2\gamma}{\sin^2\gamma}}\right)+\cos\gamma\cos\left(\gamma\sqrt{\frac{f^2+h^2-\cos^2\gamma}{\sin^2\gamma}}\right) \quad (102)$$

Displaying this function with the determined Jones components f and h in an interval, one can see the points of intersection of the function $z(\gamma)$ with $\pm|f|$ which are equivalent to the nulls of $z(\gamma)\pm|f|$; see Figure 23. The nulls of the function $h(\gamma)$ with $\pm|h|$ can be determined an equivalent manner. These nulls, each of which represents one possible solution, can now be determined with a selective numerical null search.

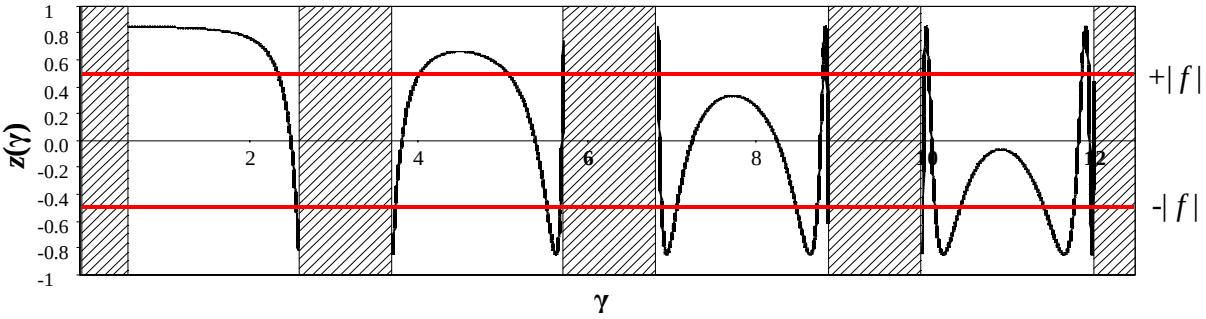

Figure 23: Example of the graphic-numerical analysis at λ = 780 nm — every intersection point of $z(\gamma)$ with $\pm|f|$ yields one possible solution of the display parameters α and β

The outlined solution schema in Figure 24 shows the determination of the display parameters from the obtained numerical solutions.

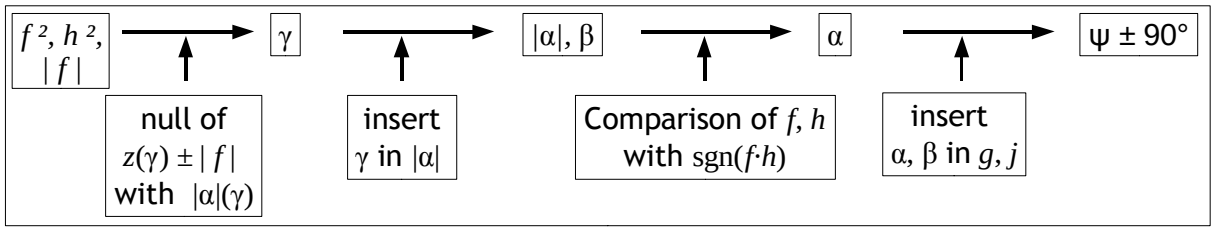

Figure 24: Solution schema for the calculation of the display parameters from the absolute values and signs of products of the Jones matrix components

Every null gives a set of possible display parameters. In Table 3 all display parameters α and β obtained from the nulls are listed for the angular range of -180° ≤ α ≤ 180°.

α [deg]	-127.50	-116.08	-113.30	-103.16	-100.43	-89.55	61.06	66.76	68.47	75.11	76.85	82.72
β[deg]	2.91	6.40	9.64	8.83	5.59	2.11	2.48	5.75	8.93	9.75	6.56	3.29

Table 3: Set of display parameters α and β obtained from nulls for the wavelength λ=650 nm

Without additional measurements one cannot conclude the real display parameters from this solution set obtained from a single Jones matrix.

Only the display parameter α and ψ are determined by the mechanical configuration of the LC-cell and are therefore constants. The, on the other hand, is a function of the wavelength of the light and of the applied voltage to the LC cell. Measurements with different wavelengths or cell voltages deliver more solution sets for α, β and ψ. By comparing these solution sets, one should be able to find solutions in which α and ψ are identical – which is the condition for the *real* solution and helps to eliminate the ambiguity of the multiple potential solution.

In the following, measurements with variable birefringence β will be described; first, for at least three different wavelengths without applied voltage and second, for one fixed wavelength and a numbers of different applied voltages.

JON4 Measurement of Jones matrix components with different wavelengths

Transmission curves for six different wavelengths are shown in Figure 25. The Jones matrix components obtained from these curves are listed in Table 4.

Now it is possible to compare the solutions of the twist angle α, which is a constant for all birefringence values β(λ,*V*), for every measured wavelength.

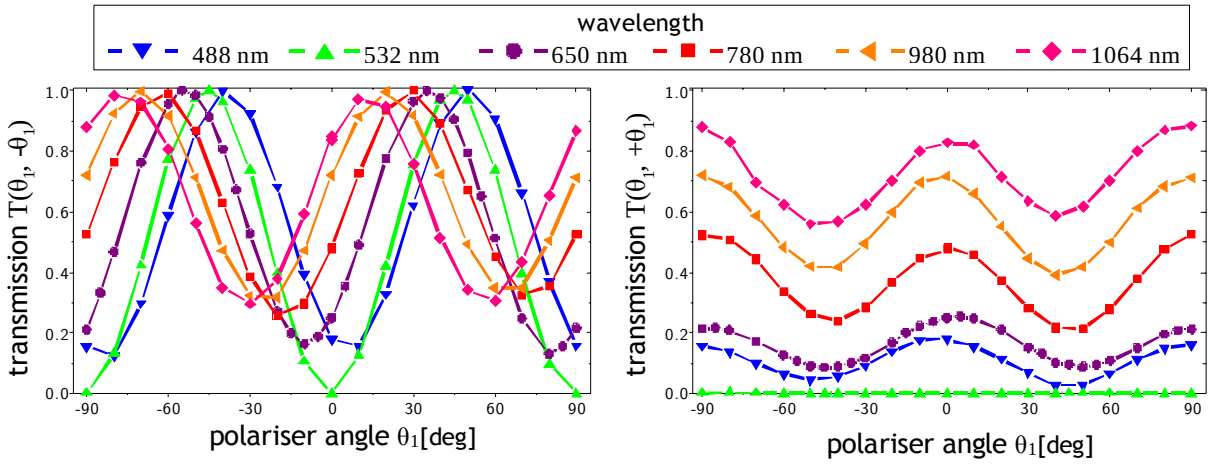

Figure 25: Transmission curves $T^{-}(\theta_1) = T(\theta_1, -\theta_1)$ and $T^{+}(\theta_1) = T(\theta_1, +\theta_1)$ for six different wavelengths

In the solution sets, which are plotted in Figure 26, only one solution can be found for all six wavelengths: α = - 90°.

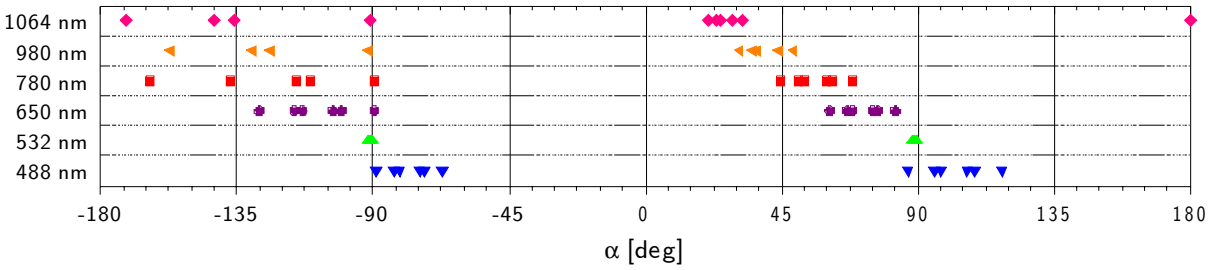

Figure 26: Solution sets obtained using the graphic-numerical analysis in the range (-180°, +180°) for the twist angle α with no applied voltage at six different wavelengths

λ [nm]	state	|f|	|h|	|g|	|j|	sgn (gj)	sgn (fh)
488	V=0	0.195 ± 0.009	0.911 ± 0.003	0.362 ± 0.006	0.0 ± 0.1	-1	-1
532	V=0	0.015 ± 0.001	0.9996 ± 0.0002	0.015 ± 0.003	0.009 ± 0.004	-1	+1
650	V=0	0.287 ± 0.004	0.872 ± 0.003	0.389 ± 0.005	0.04 ± 0.01	+1	+1
780	V=0	0.473 ± 0.009	0.703 ± 0.007	0.530 ± 0.009	0.05 ± 0.08	+1	+1
980	V=0	0.635 ± 0.004	0.532 ± 0.003	0.560 ± 0.004	0.031 ± 0.007	-1	+1
1064	V=0	0.752 ± 0.007	0.372 ± 0.008	0.541 ± 0.009	0.04 ± 0.02	-1	+1

Table 4: $|f|$, $|h|$, $|g|$ and $|j|$ as well as the signs of the products for six different wavelengths

To obtain an unambiguous result for the twist angle α, the use of three wavelengths should be sufficient, since the trend of the birefringence β can be used as an exclusion criterion; the birefringence β is inversely proportional to the used wavelength λ.

Hence, the twist angle α, the birefringence β and the 'director' angle ψ or $\psi \pm 90°$, are determined for the case of no applied voltage to the LC display.

While determining the 'director' angle ψ, no difference is made between the ordinary and the extraordinary axis. Therefore the angle is only determined to $\pm\pi/2$.

λ[nm]	α [deg]	β [rad]	ψ [deg]
488	-88.80	3.20	-43.61
532	-90.03	2.69	N/A
650	-89.55	2.11	-41.91
780	-89.76	1.75	-42.19
980	-91.52	1.44	-44.17
1064	-90.97	1.16	-43.37

Table 5: Solutions of the display parameters obtained from transmission curves with no applied voltage to the LCD

JON5 Measurement of Jones matrix components with different cell voltages

Now the second possibility to vary the birefringence is introduced. The transmission curves of nine different grey values at $\lambda = 650$ nm are shown in Figure 27. The obtained Jones matrix components are listed in Table 6. The nine grey values can be addressed to the LC display using the software 'OptiXplorer'.

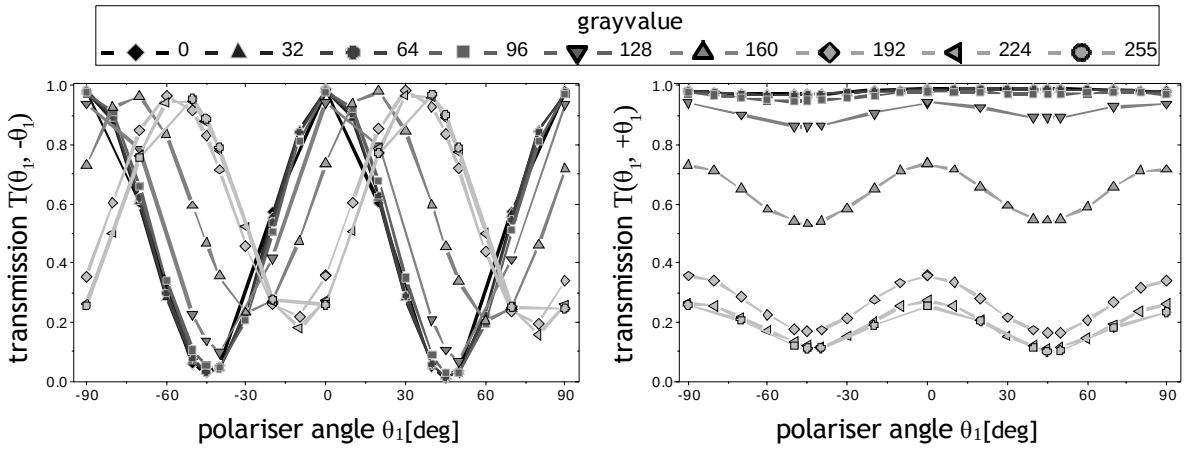

Figure 27: Transmission curves $T^{-}(\theta_1) = T(\theta_1, -\theta_1)$ and $T^{+}(\theta_1) = T(\theta_1, +\theta_1)$ for nine different grey values at $\lambda = 650$ nm

λ [nm]	state	$\|f\|$	$\|h\|$	$\|g\|$	$\|j\|$	sgn (gj)	sgn (fh)
650	G = 255	0.307 ± 0.005	0.859 ± 0.007	0.404 ± 0.01	0.04 ± 0.07	+1	+1
650	G = 224	0.325 ± 0.006	0.845 ± 0.004	0.412 ± 0.006	0.021 ± 0.03	+1	+1
650	G = 192	0.397 ± 0.006	0.794 ± 0.004	0.450 ± 0.006	0.016 ± 0.03	+1	+1
650	G = 160	0.728 ± 0.004	0.501 ± 0.004	0.459 ± 0.006	0.002 ± 0.02	+1	+1
650	G = 128	0.920 ± 0.002	0.235 ± 0.007	0.310 ± 0.01	0.05 ± 0.07	+1	+1
650	G = 96	0.976 ± 0.004	0.085 ± 0.005	0.177 ± 0.01	0.02 ± 0.04	-1	+1
650	G = 64	0.985 ± 0.003	0.042 ± 0.004	0.136 ± 0.02	0.03 ± 0.05	-1	+1
650	G = 32	0.985 ± 0.003	0.028 ± 0.004	0.141 ± 0.02	0.02 ± 0.04	-1	+1
650	G = 0	0.9998 ± 0.0002	0.003 ± 0.003	0.028 ± 0.01	0.04 ± 0.03	+1	+1

Table 6: $|f|$, $|h|$, $|g|$ and $|j|$ as well as the signs of the products for nine grey values at λ=650 nm

Using the solution schema as presented above, inconsistencies arise regarding the Jones matrix components in the case of applied voltages, that is to say for different addressed grey values.

A comparison of the results from calculating the matrix components obtained with $|\alpha|$ and β and the measurement results gives divergent results for the Jones matrix component h. The deviation of the calculation is greater than in the case without applied voltages. Using the graphic-numerical analysis on the Jones matrix component in the case of grey value G=128, one finds a null at $\gamma = 1.69437$ from $z(\gamma)\pm|f|$ and an inverse calculation gives the measured Jones matrix component $f = \pm 0.920$ but it also gives $h = \pm 0.123 \neq 0.235$. If one determines the null with $h(\gamma) \pm |h|$ one finds the null $\gamma = 1.80801$, and an inverse calculation

gives the measured Jones matrix component $h = \pm 0.235$, but now it also gives $f = \pm 0.844 \neq 0.920$.

Also, using a mixed analysis with a combined null gives a result which differs greatly from the measurement: With the null $\gamma = 1.69437$ one finds $h = \pm 0.190$ and $f = \pm 0.875$. Even if one assumes the twist angle to be $\alpha = -90°$, the numerical analysis is inconsistent with the results of the measurements.

The theoretical model, which is the basis of these Jones matrices, does not sufficiently describe the case with applied voltage. According to Kim and Lee (see reference in section 7.5), the symmetry of the Jones matrix remains in the case of applied voltage. Therefore in this case, it is possible to measure the Jones matrix components as described. However, in cases with applied voltages statements about the display parameters require a more complex theoretical examination.

7.4 Keywords for preparation

Polarisation of light, conversion of polarisation states using waveplates, liquid crystals, alignment of the molecules in an LC display, Jones formalism, numerical fitting of measurement curves, numerical analysis of measurement data, searching for nulls with a computer algebra system

7.5 References

C. Soutar and K. Lu, *Determination of the physical properties of an arbitrary twisted-nematic liquid crystal cell,* Opt. Eng. 24(9), pp. 608-610, 1994

J. A. Davis, D. B. Allison, K. G. D'Nelly, M. L. Wilson and I. Moreno, *Ambiguities in measuring the physical parameters for twisted-nematic liquid crystal spatial light modulators,* Opt. Eng. **38**(4), pp. 705-709, 1999

M. Yamauchi, *Origin and characteristics of ambiguous properties in measuring physical parameters of twisted nematic liquid crystal spatial light modulator,* Opt. Eng. **41**(5), pp. 1134-1141, 2002

A. Hermerschmidt, S. Quiram, F. Kallmeyer and H. J. Eichler, *Determination of the Jones matrix of a LC cell and derivation of the physical parameters of the LC molecules* ,Liquid Crystals and Applications in Optics, M. Glogarova, P. Palffy-Muhoray, and M. Copic, eds., Proc. SPIE **6587**, 2007. (doi: 10.1117/12.722895)

H. Kim and Y. H. Lee, *Unique measurement of the parameters of a twisted-nematic liquid-crystal display,* Appl. Opt. **44**(9), pp. 1642-1649, 2005

8 Module LIN: Linear and separable binary beam splitter gratings

8.1 Objectives

Illuminating a spatial light modulator with a coherent light source generates diffraction patterns behind the display similar to those that appear behind a conventional optical grating. One can consider the non-addressed display as an optical grating. This diffraction pattern generates a diffraction pattern in the far-field when illuminated by a collimated light source. With a so-called 'Fourier lens' the diffraction far-field pattern can be created in the rear focal plane of the lens. This diffraction pattern allows conclusions to be drawn about the characteristics of the display. For example, the pixel size can be determined.

Using a refractive diverging lens in order to increase the diffraction angle, the patterns created by addressed linear gratings can be observed and quantitatively measured. These diffraction effects caused by the phase modulation of transmitted light can be manipulated by modifying the diffracting structure.

The distribution of the diffraction intensities and the diffraction efficiency will be determined. Using the 'OptiXplorer' software, binary gratings with up to six transition points in horizontal as well as in vertical direction can be easily generated. The width of the ridges and grooves can be chosen freely. The experimental results can be compared to the theoretical considerations. The powers in the diffraction orders can be measured with a power detector and documented by a digital camera.

8.2 Required components

- **Light modulator:** LC2002
- **Light source:** laser module
- **Optics:** converging lens (e. g., f = 250 mm), diverging lens (e. g., f = -30 mm), projection screen
- **Instruments** (at least one of the following)**:** power meter, photo diode, LDR photo resistor and ohmmeter
- **Optional:** digital camera

8.3 Suggested tasks and course of experiments

LIN1 Diffraction pattern with light modulator placed in front of Fourier lens

The collimated laser beam is transmitted through the light modulator. A converging lens generates the far-field diffraction pattern in its rear focal plane. The light modulator is placed in the front focal plane.

Experimental setup used:

Laser module, light modulator, lens (f = 250 mm), and projection screen

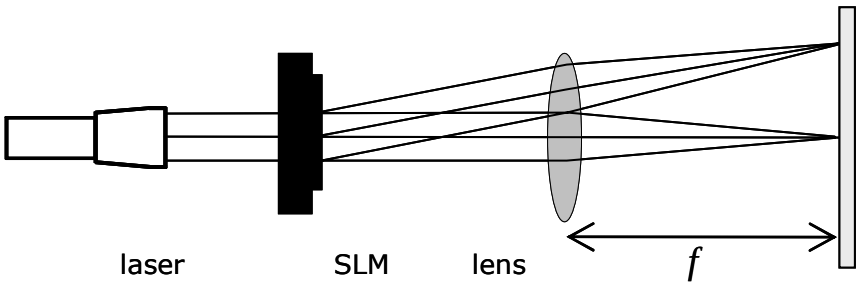

Figure 28: A Fourier lens generates the far-field diffraction pattern in its rear focal plane

Upon transmission through a lens and subsequent propagation to its rear focal plane, a Fourier transformation of the light distribution, which is a two-dimensional input signal, is obtained. In other words, by using a collimated laser beam the Fourier plane coincides with the rear focal plane of the lens. Shifting the modulator in front of the lens does not change the image in the Fourier plane.

Due to the aperture of the lens, the light that can contribute to the diffraction pattern is restricted. That means for a particular diffraction order, only partial waves from a certain part of the illuminated area on the modulator can contribute. This effect can be minimized by placing the modulator directly in front of the lens. If the screen is not positioned in the rear focal plane of the lens, the size of the diffraction pattern depends on the position of the light modulator.

LIN2 Diffraction pattern with light modulator behind Fourier lens

The position of the Fourier plane does not change when the light modulator is positioned behind the lens. But the size of the transformation decreases when the distance between the modulator and the rear focal plane decreases.

Experimental setup used:

Laser module, lens (f = 250 mm), light modulator, and projection screen

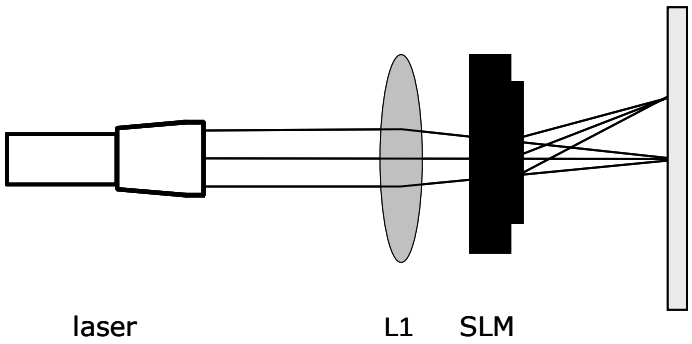

Figure 29: Fourier lens in front of the light modulator

LIN3 Intensity distribution in diffraction orders of non-addressed display

The intensity of the single diffraction orders in horizontal and vertical direction shall be measured. From the results one can calculate the filling factor of the LCD cells.

Experimental setup used:

Laser module, light modulator, projection screen, and light detector

To keep the setup simple, the expanding optic of the laser module will be used to focus the beam. When placing the laser right in front of the light modulator, the diffraction orders will be separated enough for measurements of individual orders to be made in a distance of about 70-90 cm.

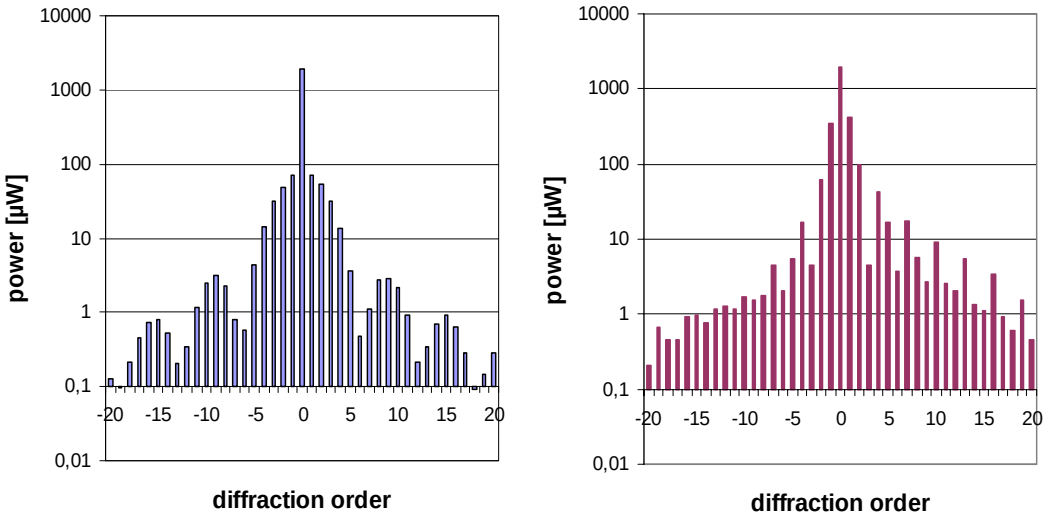

Figure 30: Measured power in horizontal (left) and vertical (right) diffraction orders at a non-addressed display

Comparing the two figures one can see the different distribution in horizontal and vertical direction. In horizontal direction a diffraction pattern which is symmetrical to the zero order can be seen. Periodical minima occur approximately in every sixth order. The vertical diffraction orders show an asymmetric distribution of the intensity in the diffraction pattern. Periodical minima can be observed, too. But these are less clear and have a period of approximately three orders.

The reason for this lies in the structure of a single pixel. It consists of the transparent part of the liquid crystal cell and the non-transparent part of the control electronics. Assuming a transmission of $\tau_0 = 0$ for this part of the cell, the display can, simply put, be seen as a two-dimensional separable grating with a structure as shown in Figure 31. The reciprocal value of the period of the minima corresponds to the position of the transition points for each direction. See also section 4.4.2, in particular equation (67). For a one-dimensional grating with any two transmission values τ_1 and τ_2 we obtain

$$\eta_l = \frac{|\tau_2 - \tau_1|^2}{\pi^2 \cdot l^2} \cdot \sin^2\left(\pi l \frac{x_1}{g}\right).$$

This means that for $x_1=g/k$ every diffraction order that satisfies $l=nk$ disappears. Separable gratings fulfil this condition separately in x and y direction. Therefore $l=6n$ and $x_1=g/6$ for horizontal diffraction orders and $l=3n$ and $x_1=g/3$ for vertical diffraction orders. The transition points are therefore located at $1/6$ and $1/3$ of the pixel width, respectively.

With a width of $5/6$ in horizontal direction and approximately $2/3$ in vertical direction a fill factor of about $55\,\%$ can be approximated for the transparent part of the display cell.

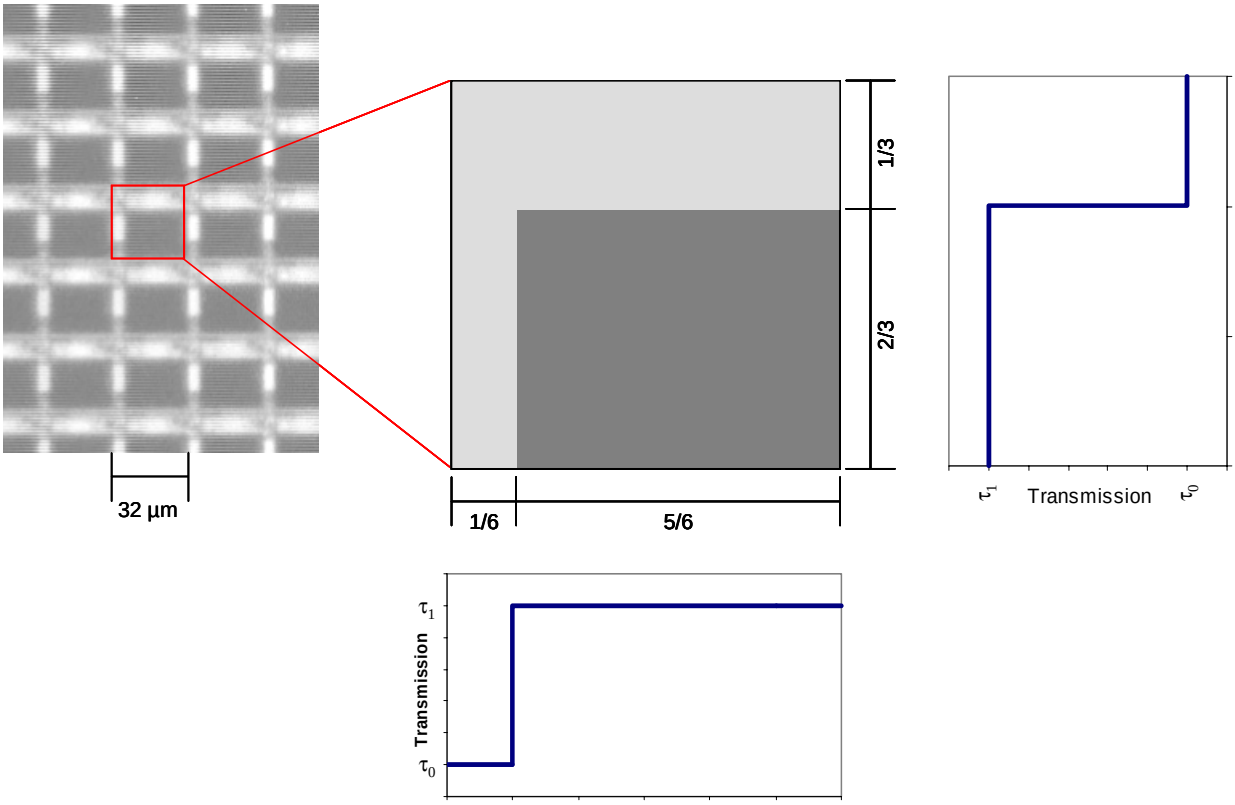

Figure 31: Left: microscopic image of the micro-display of the LC2002; Right: simplified model of a pixel with its transmission

LIN4 Determination of the pixel size

The diffracting properties of the LC display are based on the pixelated layout. It acts as a grating with a period g given by the pixel size, and the created diffraction orders are observed at angles α satisfying

$$g \cdot \sin\alpha = m \cdot \lambda \quad \text{with m = (1, 2, 3,...).}$$

Experimental setup used:

Laser module, lens ($f = 250$ mm), light modulator, and projection screen

The Fourier plane coincides with the rear focal plane. The distance between the second orders on the screen is 20 mm. Therefore g is given by:

$$g = \frac{2 \cdot 650\text{nm}}{\sin(10/250)} = 32.5\mu\text{m}\,.$$

LIN5 Increasing diffraction angle with divergent lens

By placing a divergent lens behind the light modulator, the convergent beams will be expanded and the Fourier plane will be shifted parallel to the beam direction. At the same time the angle as well as the size of the diffraction pattern increases.

Experimental setup used:

Laser module, lens ($f = 250$ mm), light modulator, lens ($f = -30$ mm), and projection screen

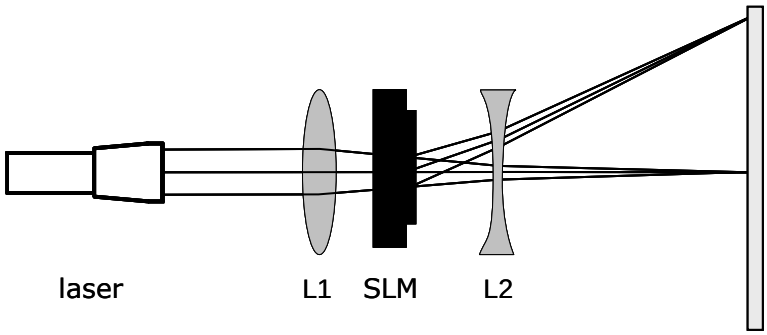

Figure 32: Setup with Fourier lens (L1) and diverging lens (L2) to increase the diffraction angle

The diverging lens is placed behind the light modulator and is responsible for the increased angle of the diffracted light beams. The angle will be calculated in the following paragraphs.

First, the light passes a distance d behind the light modulator before it transmits through the diverging lens with the focal length f. Using the ABCD matrix analysis and replacing the focal length f with the refraction power $p = 1/f$ we obtain

(103)
$$\begin{bmatrix} 1 & 0 \\ -p & 1 \end{bmatrix} \cdot \begin{bmatrix} 1 & d \\ 0 & 1 \end{bmatrix} \cdot \begin{pmatrix} r_1 \\ \alpha_1 \end{pmatrix} = \begin{bmatrix} 1 & d \\ -p & (-d \cdot p)+1 \end{bmatrix} \cdot \begin{pmatrix} r_1 \\ \alpha_1 \end{pmatrix} = \begin{pmatrix} r_2 \\ \alpha_2 \end{pmatrix}.$$

The magnified angle α_2 is given by

(104)
$$\alpha_2 = -r_1 \cdot p + \alpha_1 (1 - d \cdot p).$$

For the beam passing the light modulator along the optical axis we have r_1=0, so that

(105)
$$\alpha_2 = \alpha_1 (1 - d \cdot p).$$

That means that the diverging lens has to be placed at a certain distance to the light modulator. For $d = 0$ there is no magnification of the diffraction angle.

To calculate the pixel size of the display, the distances x_1 and x_2 between the two first diffraction orders on the screen for two different distances z_1 and z_2 need to be measured. The angle between beam and optical axis can be approximated by

$$\alpha' = \Delta x / \Delta z \, .$$

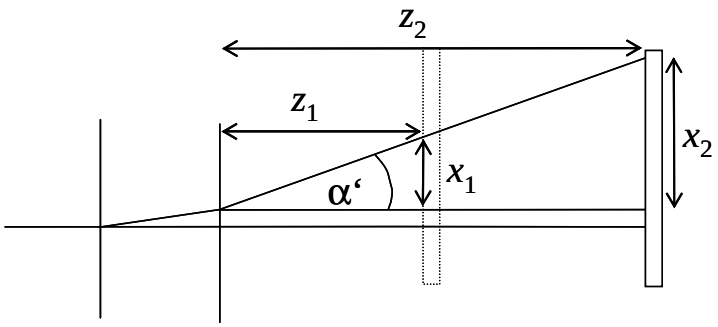

Figure 33: Determination of the diffraction angle

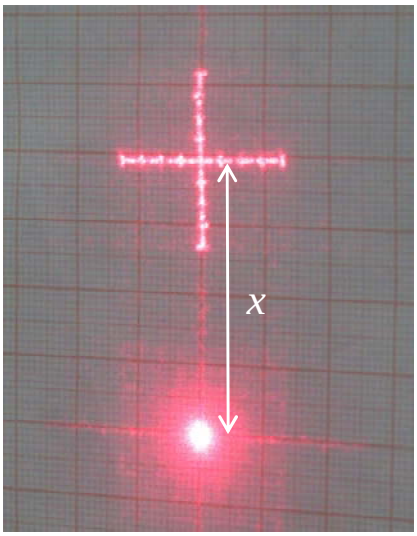

Figure 34: Distance measurement using graph paper

The diffraction angle α directly behind the display is given by

$$\alpha = \frac{\alpha'}{1 - d \cdot p}.$$

The grating period and therefore the pixel size is given by

$$g = \lambda / \sin(\alpha).$$

With the setup described above the following results were obtained: d = 175 mm, Δx = 131 mm, Δz = 450 mm; with p = -1/30 mm and λ = 650 nm one can determine that g = 30.5 µm.

LIN6 Operation of the display in the ‘phase-mostly’-mode

After studying the non-addressed display, it will now be addressed with gratings created by the ‘OptiXplorer’ software. The instructions for the software can be found in section 16.

First, a beam-splitting grating with a period of 18 pixels and 6 transition points will be examined. The ridge/groove sequence is 4/1/4/4/1/4 pixel and creates a 1:4 beam splitter.

The setup used works in the 'phase-mostly'-mode, meaning that the influence of the amplitude modulation is minimized. Therefore the polariser and analyser will be added to the setup. The intention is to minimize the zero order by choosing suitable polariser/analyser positions and adequate grey levels for addressing the grating. The chosen angles for the polariser and analyser derive from the calculations based on the Jones matrices determined in chapter JON5. The phase shift $\Delta\Phi$ between the two grey levels has to be $\Delta\Phi = \pi$. The choice of grey levels is based on the measurements from section RON1 and RON3.

Experimental setup used:

Laser module, polariser, lens ($f = 250$ mm), light modulator, lens ($f = -75$ mm), analyser, projection screen and detector

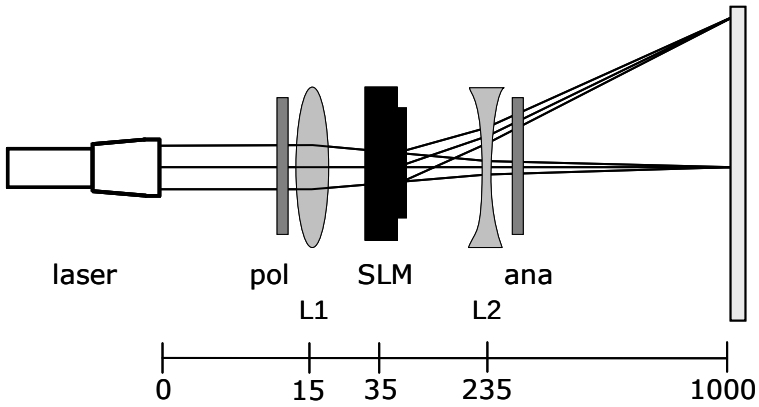

Figure 35: Setup for 'phase-mostly'-mode

The polariser is set at 59° and the analyser at 110° with respect to p-polarisation. The phase shift is $\Delta\Phi \approx \pi$ for grey levels 111 and 203 (see Figure 42). The results of the measurements are listed in Table 7.

By choosing adequate values for the rotation of the polariser/analyser and the grey levels, one can decrease the power in the zero order to less than 1/1000 of the power in the zero order of a homogeneous grey level image. The result of the measurements is in agreement with the theoretically expected values (for the theoretical calculations see section 4.4.2 and experiment LIN9). The settings used in this description should be used as starting points to obtain optimum results for your particular SLM.

measured value	power [µW]	diffraction efficiency	theor. diffraction efficiency
'Blank Screen' GL111	199		
'Blank Screen' GL203	204		
4/1/4/4/1/4-grating: -3rd order	35.9	17.77	18.01
4/1/4/4/1/4- grating: -1st order	33.9	16.78	17.27
4/1/4/4/1/4- grating: 0 order	0.3	0.15	0
4/1/4/4/1/4- grating: +1st order	33.7	16.68	17.27
4/1/4/4/1/4- grating: +3rd order	36.0	17.82	18.01

Table 7: Diffraction efficiency in the 'phase-mostly' mode

LIN7 Addressed linear gratings

The setup from experiment LIN6 can be operated without polarisers. It is recommended to use the grey levels 0 and 255. Since each polariser transmits only 30% of the incident power, the measured power in the diffraction orders increases by up to ten times, but the zero order will have significantly more power, too.

Experimental setup used:

Laser module, lens ($f = 250$ mm), light modulator, lens ($f = -75$ mm), projection screen and detector

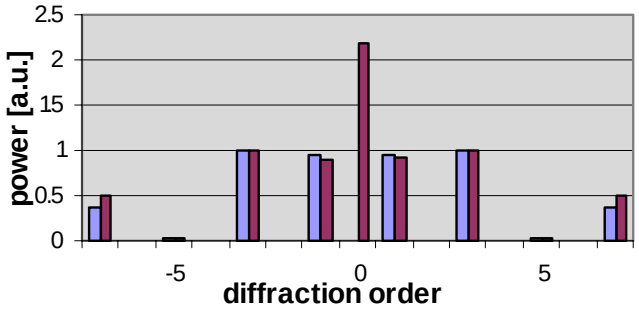

Figure 36: Comparison of the theoretical (blue) and measured (red) power of the diffraction orders. (ridge/groove-sequence: 4/1/4/4/1/4)

diffraction order	-5	-4	-3	-2	-1	0	1	2	3	4	5
power [µW]	6.7	0.3	234.6	0.77	213	516	218	0.72	237	0.3	6.82

Table 8: Measured results 4/1/4/4/1/4-grating

As seen in Figure 36, no power will be expected in the zero order for an ideal grating. But the measured results show a significant zero order. The power included in this order ($I = 500$ µW) is around 30 % of the power measured in the zero order of a homogeneous grey level image (or of a non-addressed display, respectively) ($I_0 = 1{,}77$ mW). For comparison, in the 'phase-mostly' mode (LIN6) the measured power in the zero order was nearly zero.

To separate the diffracted orders from the undiffracted order, in the following an additional perpendicular 2/2-grating will be superimposed over the described gratings. The result is a separable binary grating (see section 4.3.3). With this setup the single diffraction orders can be easily measured with a powermeter.

A 4/1/4/4/1/4 grating structure will be addressed vertically and then horizontally to the display. According to theory, the diffraction orders will be distributed symmetrically around the zero order, but as one can see in Figure 37, the distribution depends on the direction of the grating on the display.

The reason for this is a crosstalk of the electrical fields of the single pixels in vertical direction (see also Figure 31). The phase shift is influenced by the resulting fringe effects and so the grating is not truly a binary grating anymore. Therefore for the following experiments horizontal gratings will be used.

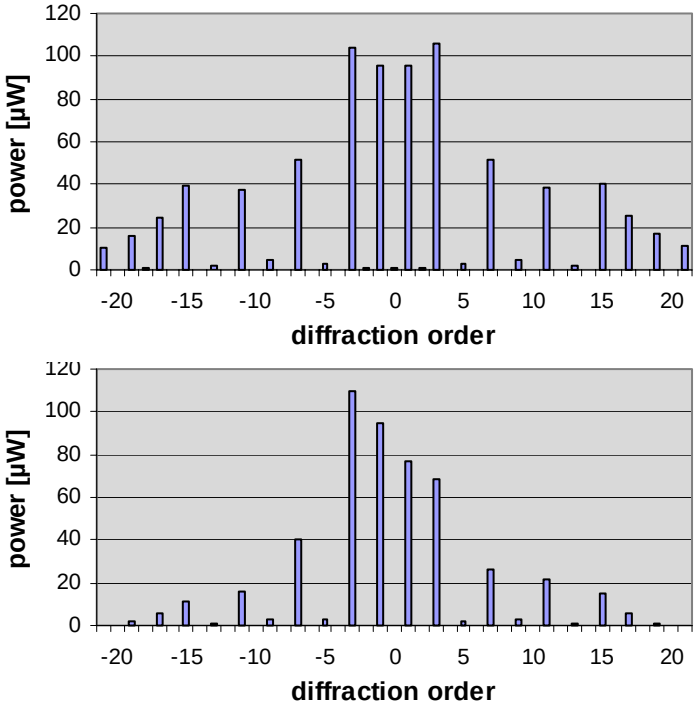

Figure 37: Power distribution of the diffraction orders for horizontal (top) and vertical (bottom) 4/1/4/4/1/4 grating

diffraction order (2/2)	Diffraction order (4/1/4/4/1/4 grating)										
	-5	-4	-3	-2	-1	0	1	2	3	4	5
+1(ver)	3.16	0.45	109.4	0.53	94.8	0.58	77.2	0.56	68.8	0.36	2.04
0	0.2	10.8	0.45	2.05	0.58	443	0.56	2.3	0.3	10.7	0.36
+1(hor)	3	0.36	104.3	0.56	95.9	0.58	95.8	0.53	105.6	0.45	3.04

Table 9: Power [µW] of the diffraction orders for vertical and horizontal 4/1/4/4/1/4 binary diffraction gratings

It is left to the experimenter to conduct the suggested experiments using the light modulator in the 'phase-mostly' mode or to add a second perpendicular grating to separate the diffracted orders from the zero order. For symmetrical reasons one should use horizontal gratings in any case.

LIN8 Comparison of different binary gratings with the same period

A 4/1/4/4/1/4 grating separates the incidence beam into four beams. Now a grating structure is chosen, which separates the incidence beam into two. The first one has a 1/7/1/1/7/1 ridge/groove sequence, the second one a 3/3/3/3/3/3 sequence.

Experimental setup used:

Laser module, lens ($f = 250$ mm), light modulator, lens ($f = -75$ mm), projection screen, and detector

An additional perpendicular 2/2 grating is chosen to separate the diffraction orders from the zero order.

Both the 1/7/1/1/7/1 grating as well as the 3/3/3/3/3/3 grating cover 18 pixels. This is also the grating period g for the first grating; in contrast, the second one in fact has a period of only 6 pixels. Therefore only each third diffraction order is observed for the 3/3/3/3/3/3 grating compared to the 1/7/1/1/7/1 grating. Both gratings mainly divide the incident beam into two beams; but the diffraction angle α is higher by a factor of 3 for the second one.

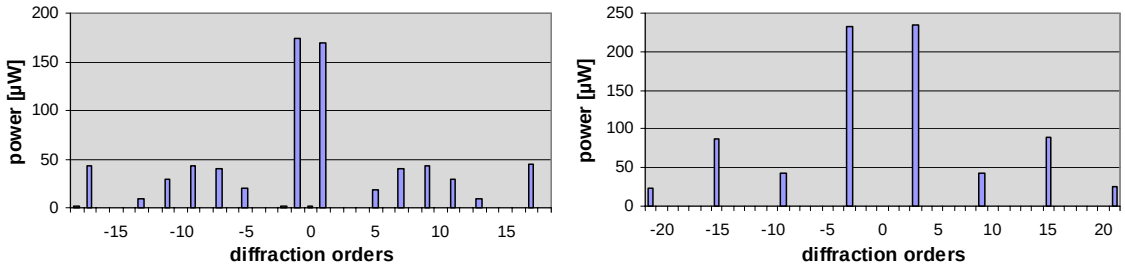

Figure 38: Comparison of two 1:2 beam splitter (left: 1/7/1/1/7/1; right: 3/3/3/3/3/3). The numbering of the diffraction orders refers to a grating period of 18 pixels for both gratings

LIN9 Comparison of calculated and measured diffraction efficiencies

Leaving the undiffracted (zero) order aside for a display not working in 'phase-mostly' mode, one can see the measured distribution is in accordance with the calculated one. As an example, this is presented here for four different gratings. Two 1:5 beam splitters (1/7/6/7 and 1/9/7/9), the 1:2 beam splitter from experiment LIN8 (1/7/1/1/7/1) and a 1:7 beam splitter (2/10/5/4) are investigated.

Experimental setup used:

> Laser module, lens ($f = 250$ mm), light modulator, lens ($f = -75$ mm), projection screen and detector

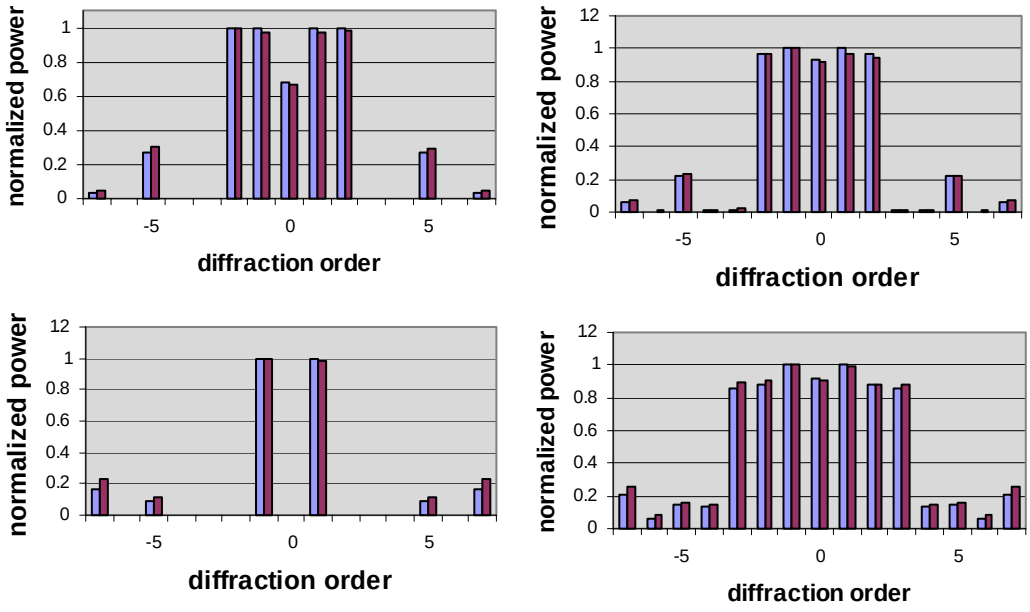

Figure 39: Comparison of calculated (blue) and measured power (red) of the single diffraction orders. (top left to bottom right: 1/7/6/7, 1/9/7/9, 1/7/1/1/7/1, 2/10/5/4)

With the theory introduced in section 4.4.2 the single diffraction orders can be calculated. The diffraction efficiencies are given by

$$\eta_0 = 1 - 4Q(1-Q)\sin^2(\Delta\varphi/2)$$

for the zero order and by

$$\eta_l = \frac{\sin^2(\Delta\varphi/2)}{\pi^2 l^2}\left(C_l^2 + S_l^2\right)$$

for higher orders with

$$S_l = \sum_{i=1}^{2K}(-1)^i \sin(2\pi l x_i)\ ,$$

$$C_l = \sum_{i=1}^{2K}(-1)^i \cos(2\pi l x_i)$$

and

$$Q = \sum_{i=1}^{2K}(-1)^i x_i\ .$$

For a better comparison with the measured values in Figure 39, the calculated values are normalised to the maximum. Table 10 shows the calculated values as an example.

	Diffraction order												
Grating structure	**-6**	**-5**	**-4**	**-3**	**-2**	**-1**	**0**	**1**	**2**	**3**	**4**	**5**	**6**
1/7/6/7	0,00	4,44	0,04	0,00	16,33	16,23	11,11	16,23	16,33	0,00	0,04	4,44	0,00
1/9/7/9	0,08	3,43	0,13	0,21	15,38	15,98	14,79	15,98	15,38	0,21	0,13	3,43	0,08
1/7/1/1/7/1	0,00	2,94	0,00	0,00	0,00	31,34	0,00	31,34	0,00	0,00	0,00	2,94	0,00
2/10/5/4	0,81	1,72	1,62	10,47	10,76	12,14	11,11	12,14	10,76	10,47	1,62	1,72	0,81
3/12/6/5	1,13	1,20	1,47	11,98	12,83	10,28	9,47	10,28	12,83	11,98	1,47	1,20	1,13

Table 10: Theoretical diffraction efficiency [%] for different grating structures

LIN10 Comparison of different gratings with same beam partition

Three grating structures will be examined, each with a 1:3 beam partition. The single gratings differ in their periods and in their ridge/groove sequences, while the number of transition points remains the same. The gratings used are: 1/2/9/2 (period = 14), 2/3/12/3 (period = 20) and 1/3/12/2 (period = 18).

Experimental setup used:

Laser module, lens (f = 250 mm), light modulator, lens (f = -75 mm), projection screen and detector

The same beam partition can also be achieved with different gratings. One can see differences, for example, for higher diffraction orders. The grating with the 2/3/12/3 sequence (Figure 40, top right) suppresses the second orders but has high powers in the third and fourth orders, thereby decreasing the diffraction efficiency. In comparison, the 1/3/12/2 grating has a higher diffraction efficiency but also has higher powers in its second diffraction orders. Generally speaking, it is possible to fit the diffraction pattern to a particular application.

Table 11 shows the diffraction efficiency as the ratio of the power in the desired diffraction order to the power of the zero order of a homogenous grey level image (software: 'Blank Screen').

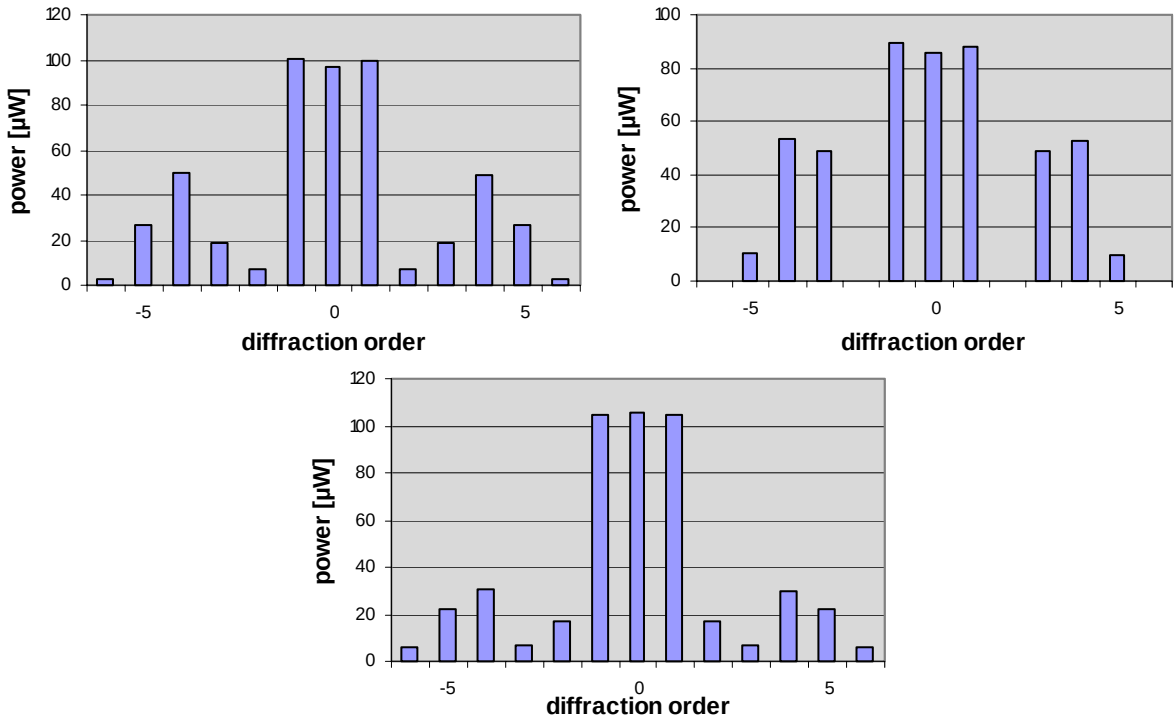

Figure 40: Comparison of three 1:3 beam splitters
(top left: 1/2/9/2 grating, top right: 2/3/12/3 grating, bottom 1/3/12/2 grating)

Grating structure	Diffraction efficiency
1/2/9/2	34.5 %
2/3/12/3	30.8 %
1/3/12/2	36.6 %

Table 11: Diffraction efficiency of different gratings

LIN11 Comparison of separable and non-separable arrays

The 'OptiXplorer' software contains two 5x5 beam splitter designs which will serve as examples for a comparison between separable and non-separable binary gratings.

Experimental setup used:

Laser module, lens ($f = 250$ mm), light modulator, lens ($f = -75$ mm), projection screen, and detector

A separable beam-splitting grating has separable linear gratings in x and y direction. The transmission function can be denoted as a product $\tau(x,y) = \tau_1(x)\,\tau_2(y)$ (see section 4.3.3).

Observing the diffraction patterns of the two gratings, one can see that the signal and noise orders follow the symmetry of the separable grating whereas the noise orders of the non-separable grating are distributed with only hermitian symmetry.

8.4 Keywords for preparation

Optical gratings, functionality of a liquid crystal display, pixel size, filling factor, classical optics, ABCD-matrices, plane waves, coherence, diffraction, interference, theory of the far-field, grating functions, Fraunhofer and Fresnel diffraction, Fourier transformation

8.5 References

Eugene Hecht

Optik (3.Auflage)

Oldenbourg Verlag, München Wien (2001)

Dieter Meschede

Optik, Licht und Laser (2.Auflage)

Teubner (2005)

J. L. McClain et al.

Spatial light modulator phase depth determination from optical diffraction information

Optical Engineering, Vol. 35 No. 4, pp. 951-954 (1996)

9 Module RON: Diffraction at dynamically addressed Ronchi gratings

9.1 Objectives

Using the distribution of the easily determined diffraction efficiencies of the diffraction orders of Ronchi gratings, one can determine the voltage dependent phase shift of the grating. Ronchi gratings, necessary for the measurements, can be produced and addressed to the LC display of the SLM by using the software 'OptiXplorer'.

One can use the angles of the polarisers to create different configurations of the LC display (see section I3.5), for example an 'amplitude-mostly' or a 'phase-mostly' configuration. The polariser angle settings can be determined or estimated by the use of Jones matrix components in simulations of the transmission characteristics of the LC display or simply by trying.

According to section 4.4 one can derive the phase shift from the diffraction efficiency, obtained by simple transmission measurements. One can examine effects, like a spatial frequency dependency of the phase shift, at the same time.

9.2 Required components

- **Light modulator:** LC2002
- **Light source:** Laser module
- **Optics:** 2 rotatable polarisation filters
- **Instruments:** Power instrument

9.3 Suggested tasks and course of experiments

RON1 Determination of the power transmission of the grey values

To calculate the phase shift according to equation (71) one needs to know the power transmission $T_i = \rho_i^2$ of the LC display. The grey value images can be produced by using the software 'OptiXplorer'.

Experimental setup used (see Figure 41):

Light source, polarisers, LC display, detector and diaphragm.

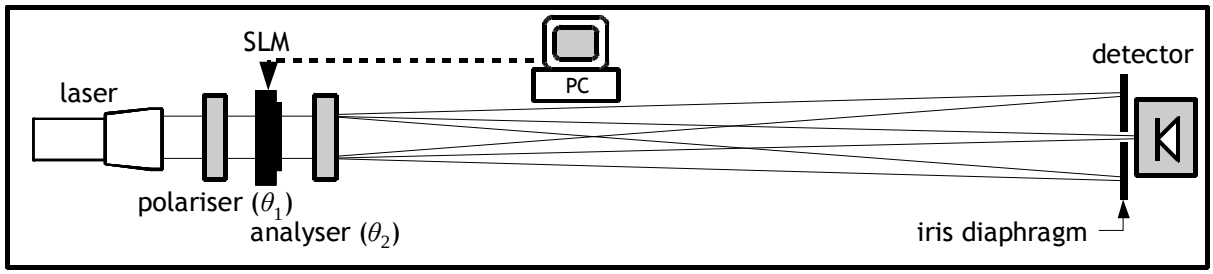

Figure 41: Experimental setup to measure the power transmission and the light power in diffraction orders

In order to block higher diffraction orders, an iris diaphragm is used, particularly for gratings with large grating constants, which produce orders with small diffraction angles.

One should measure the light power, which is proportional to the diffraction efficiency, for at least every tenth grey level in the zero diffraction order of the pixel grating. For this measurement all LC pixels are addressed with the same voltage, meaning addressing a uniform image consisting of one grey value. The measured powers P_i are proportional to the power transmissions T_i. By examination of the measurement curves, one can determine the LC display configuration for the polariser angles in use.

The measured light powers P_i should be normalised to

(106)
$$T = \frac{P_i}{P_{\theta_2} + P_{\theta_2 \pm 90°}} \quad .$$

For this purpose one measures the light transmission of a configuration with a $\pm 90°$ rotated analyser angle θ_2. For the description of the amplitude properties of a LC display two terms are used, on the one hand the contrast ratio

$$1 : x = P_{\min} : P_{\max} ,$$

which is used for the description of 'amplitude-mostly'-configurations, and on the other hand the contrast

$$\Delta\rho = \frac{P_{\max} - P_{\min}}{P_{\max} + P_{\min}} ,$$

which is used for 'phase-mostly'-configurations.

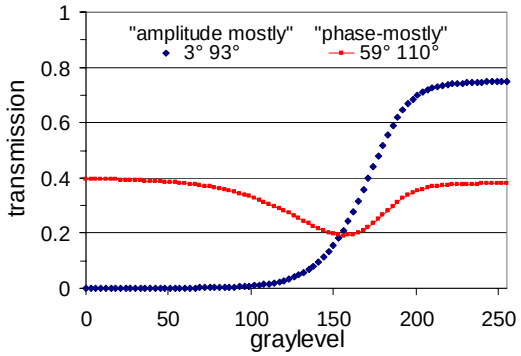

Figure 42: Power transmission T_i of the LC display for an 'amplitude-mostly'-configuration ($\theta_1 = 3°$, $\theta_2 = 93°$) and a 'phase-mostly'-configuration ($\theta_1 = 59°$, $\theta_2 = 110°$) at $\lambda = 650$ nm

The blue curve ($\theta_1 = 3°$, $\theta_2 = 93°$) represents an 'amplitude-mostly'-configuration with a contrast ratio of 1:1750, while the red curve ($\theta_1 = 59°$, $\theta_2 = 110°$) represents a 'phase-mostly'-configuration with a contrast of $\Delta\rho = 0.348$.

RON2 Transmission measurements in diffraction orders of Ronchi gratings

The light power in the diffraction orders can be obtained for various grating constants as a function of the addressed grey level. The Ronchi gratings can be produced with the 'OptiXplorer' software.

Experimental setup used (see Figure 41):

Light source, polarisers, LC display, detector, and diaphragm.

One grey value (e.g. G_1) of the Ronchi grating is fixed, as a reference value. The other grey value (G_2) of the Ronchi grating should be varied in increments of a maximum of 10 grey levels ranging from 0 to 255.

For sufficiently large grating constants, the zero and ±1st diffraction orders of horizontal and vertical Ronchi gratings show the same development. The light power measurement has to be as accurate as possible, since the phase shift will be calculated from these measurement values.

One possibility to check the setup and the detection accuracy is a comparison of the measured powers at equal grey levels. For instance, the zero diffraction order in the case of (G_1=G_2) has to be the same as the power transmission T_i determined earlier for the same grey level.

Using the iris diaphragm one can make sure, in the case of large grating constants, that only one diffraction order at a time is detected. Basically the measurement of one diffraction order should be sufficient for the calculation of $\Delta\Phi$, however multiple orders (+1st, 0, -1st) should be measured to minimize possible errors. With a coupled analysis the impact of measurement imprecision and edge effects can be minimized and systematic measurement errors can be detected more easily.

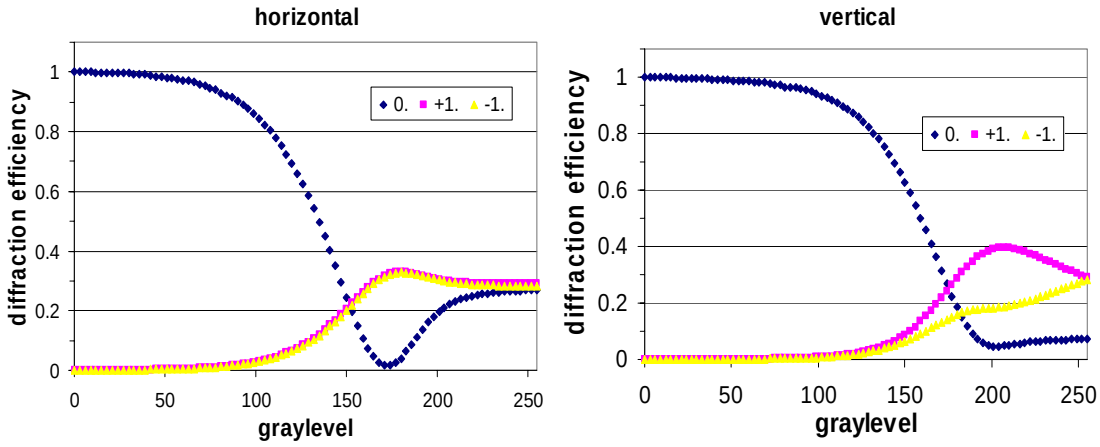

Figure 43: Diffraction efficiencies in a 'phase-mostly'-configuration (θ_1 = 59°, θ_2 = 110°) in the 0 and ±1st diffraction orders of horizontal and vertical Ronchi gratings with a grating constant of g =384 µm and a fixed grey level 'black' at λ = 650 nm

The LC cells have addressing bars (i.e. the non-transparent part of the control electronics, see also section LIN2), with a different horizontal and vertical width. The effect of these bars can be observed.

In Figure 44 one can see a grating constant dependent, and therefore a spatial frequency dependent development of the diffraction efficiency of vertical Ronchi gratings.

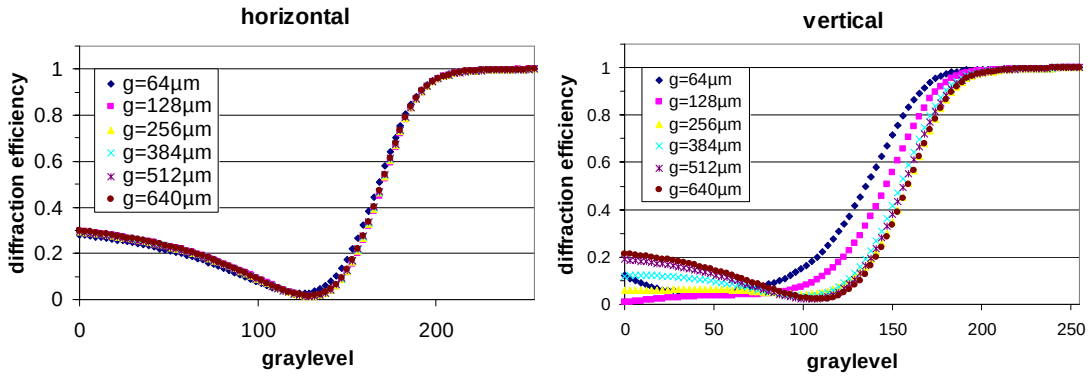

Figure 44: Diffraction efficiencies in a 'phase-mostly'-configuration ($\theta_1 = 59°$, $\theta_2 = 110°$) in the zero diffraction order of horizontal and vertical Ronchi gratings with different grating constants and a fixed grey level 'white' at $\lambda = 650$ nm

One can assume that the smaller bar width in the vertical direction of the LC display causes more crosstalk of the electrical fields between neighbouring pixels. The magnitude of this crosstalk depends on the grating constant. For small grating constants the transition values draw nearer. As a result, the phase modulation is a function of the grating constant and therefore of the spatial frequency.

RON3 Calculation of the phase shift from transmission measurements

From the transmission in the different diffraction orders and the knowledge of the amplitude transmission T_i one can calculate the phase shift as a function of the grey level. The transmissions of horizontal and vertical Ronchi gratings measured earlier as a function of the grey level G_2 and the power transmissions T_i of the respective grey levels are needed for the analysis.

In reference to equation (71) from section 4.4, the relative phase shift $\Delta\Phi$ can be calculated by solving the equation for $\Delta\Phi$ using the measurement values. The transmission $T_1 = \rho_1^2$ of the reference grey level G_1 is constant. However, usually a coupled analysis of the zero and first diffraction orders provides better results:

(107) $$\Delta\Phi = \arccos\left(\frac{(\rho_1^2 + \rho_2^2)\cdot(4\cdot\eta_0 - \pi^2\cdot\eta_{\pm1})}{\rho_1\cdot\rho_2\cdot(8\cdot\eta_0 + 2\pi^2\cdot\eta_{\pm1})}\right).$$

The range of the arccos function is (-π, + π). Hence, the calculation of the relative phase shift $\Delta\Phi$ must be adapted in case it draws near multiples of ±π. For example, if one chooses the reference grey level G_1='black', the $\cos(\Delta\Phi)$ varies from $\cos(\Delta\Phi = 0) = 1$ to the reversal point $\cos(\Delta\Phi = \pi) = -1$ and again back to +1.

Hence, the relative phase shift after $\Delta\Phi = \pi$ is

$$\Delta\Phi = 2\pi - \arccos\left(\frac{(\rho_1^2 + \rho_2^2)\cdot(4\cdot\eta_0 - \pi^2\cdot\eta_{\pm1})}{\rho_1\cdot\rho_2\cdot(8\cdot\eta_0 + 2\pi^2\cdot\eta_{\pm1})}\right).$$

After the point $\Delta\Phi = 2\pi$ the phase shift is again determined by the earlier equation, after $\Delta\Phi = 3\pi$ again by the latter and so forth. It was also observed that the reversal point is not always equal |1|.

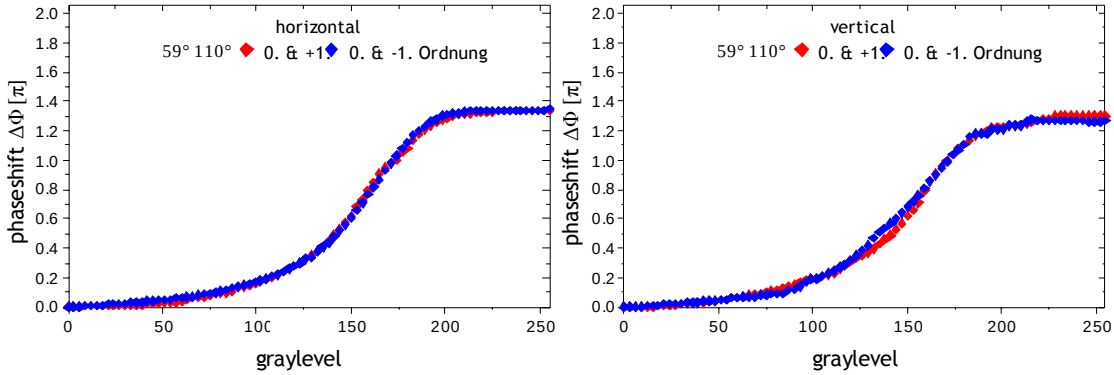

Figure 45: Calculated phase shift from transmission measurements in the 0 and ±1st diffraction orders in a 'phase-mostly'-configuration ($\theta_1 = 59°$, $\theta_2 = 110°$) with reference grey level 'black' at λ=650 nm

RON4 Automated measurement with LabView programme ‚DynRon'

With the LabView programme ‚DynRon' measurements can be automated. The ‚DynRon' software creates bitmaps representing Ronchi gratings with one fixed and one variable gray level. The bitmaps are displayed on the LCD of the SLM and the software reads in the signal voltage provided by a detector which is placed in the zero or first diffraction order. Thus is is possible to store the diffraction efficiency as a function of the graylevel contrast in a table. Details about the software can be found in section IV18.

The features of the ‚DynRon' programme make it possible to analyse the amplitude and phase modulation of a polariser-SLM-analyser combination in a fast an convenient way. Therefore it is possible to determine the best polariser orientations for ‚phase-mostly' and ‚amplitude-mostly' configurations, for example for a new wavelength for which not all parameters (like the Jones matrix componenets) are known.

9.4 Keywords for preparation

Diffraction of light, contrast, symmetric diffracting objects, liquid crystals, spatial frequencies and grating constants

9.5 References

J. Remenyi, P. Varhegyi, L. Domjan, P. Koppa, and E. Lorincz, *Amplitude, phase, and hybrid ternary modulation modes of a twisted-nematic liquid-crystal display at 400 nm,* Appl. Opt. 42(17), pp. 3428–3434, 2003.

Joseph W. Goodman, *Introduction to Fourier Optics,* Roberts & Co; Auflage: 3 (2004)

10 Module CGH: Computer generated holograms and adaptive lenses

10.1 Objectives

Computer generated holograms can be calculated with the 'OptiXplorer' software. The advantages of such dynamic structures are one of the topics of this module. The holograms will be modified with lens and prism functions included in the software. The optical parameters of these diffractive elements will be determined. To keep this setup compact some experiments will use a diverging lens to increase the diffraction angle as described in section LIN5.

Note 1: It is recommended to be familiar with the setup of section LIN5 to increase the diffraction angle with a diverging lens.

Note 2: Since the examined structures are phase DOEs, no polarisers are needed. One has to keep in mind that the laser light is linearly polarised. Since the display rotates the polarisation plane of the light, it is necessary to fit the rotation of the laser to have a far-field pattern with optimal intensity and quality.

Note3: The addressed images should be full-screen images since window edges, taskbars and buttons are also diffracting structures and degrade the image.

10.2 Required components

- **Light modulator:** LC2002
- **Light source:** laser module
- **Optics:** lenses (f = -250 mm, f = -30 mm, f = +150 mm, f = +250 mm), projection screen
- **Instruments:** power instrument

10.3 Suggested tasks and course of experiments

CGH1 Determination of pixel size using an addressed Fresnel zone lens (FZL)

The pixel size will be determined by using a binary zone lens generated with the 'OptiXplorer' software.

Experimental setup used:

Laser module, light modulator and projection screen

The innermost radius r of a binary zone lens is given by

(108) $$r = \sqrt{n \cdot \lambda \cdot f}\ .$$

The distance between the lens plane and the nth focus is f, where n = 1 for the focus furthest away. The distance to this focus will be measured. Using a zone lens with an

inner radius of 35 pixels a focal distance of $f = 1870$ mm can be measured. The laser emits with a wavelength of 650 nm. Therefore a pixel size of 31.5 µm can be calculated.

The error is given by

(109) $$\Delta r = \frac{\partial r}{\partial f} \cdot \Delta f = \frac{1}{2} \cdot \frac{\lambda}{\sqrt{\lambda \cdot f}} \cdot \Delta f \quad .$$

With an accuracy of ± 3 cm for the distance the error is 0.9 µm. Additionally, it could be examined if any more foci can be observed and if their positions correspond to the calculated ones.

CGH2 Design diffractive optical elements with an IFTA algorithm

The 'OptiXplorer' software can generate diffractive optical elements from any image. It is possible to modify the number of quantization iteration steps and the number of phase quantization levels. Depending on the chosen parameters the quality of the reconstruction can be very different. A phase DOE with 256 grey levels needs only a few iteration steps for a good reconstruction, whereas a binary DOE needs at least the tenfold number of steps for a similar quality.

The upper limit for the size ofthe bitmap file, which can be loaded to represent the desired diffraction pattern, is 200x200 pixels. In the software, the bitmap is automatically converted to a two-dimensional array of data and embedded to a larger field with 2^nx2^n Pixes (n = 2, 3, ..., 8). For different array sizes the same bitmap will deliver diffracting structures with different diffraction angles, simpy because the resulting grating periods are larger.

The ‚OptiXplorer' software opens for each calculated DOE an additional window showing the simulated diffraction pattern, in a gray scale representation 0..255 ranging from zero to the maximum of the field. For a simple diffraction pattern of 3x3 spots (represented by a white square area of 3x3 pixels) binary DOEs can be computed for different size of the embedding and different numbers of quantisation steps of the IFTA.

The relative powers of the diffraction orders should be determined by a measuerement and be compared with the simulation. The experimental setup introduced in section LIN6 es beneficial for these measurements as it offers „phase-mostly" modulation and for binary DOEs even true phase-only modulation with phase shift π. In this way, the disturbing zero order can be minimized.

Experimental setup used:

> Laser module, lens ($f = 250$ mm), light modulator, lens (f = -30mm), projection screen or light detector (see Figure 35)

The bitmap files ‚whiteSquare32.png' and ‚whiteSquare64.png' contain a square area of 3x3 white pixels embedded into data arrays of sizes 32x32 and 64x64. With the ‚Optixplorer' software binary DOEs (i.e. ‚phase quantization levels' = 2) can be computed using 1, 10 and 100 quantisation iteration steps. When the obtained DOEs are displays on the LCD of the SLM, the diffraction orders can be measured at a sufficiently distance to separate them. The iris diaphram should be used in order to block adjacent diffraction orders. The polariser is oriented at 59°, the analyser at 110° with respect to the direction of p polarisation. For the gray levels 111 and 203 the phase shift corresponds to $\Delta\Phi \approx \pi$ (see Figure 42).

The obtained results can be compared with the simulated diffraction patterns, in which the brightest diffraction order is represented with a grayscale of 255. To make a comparison easy, the measured values are nomalised with respect to the strongest off-axis order.

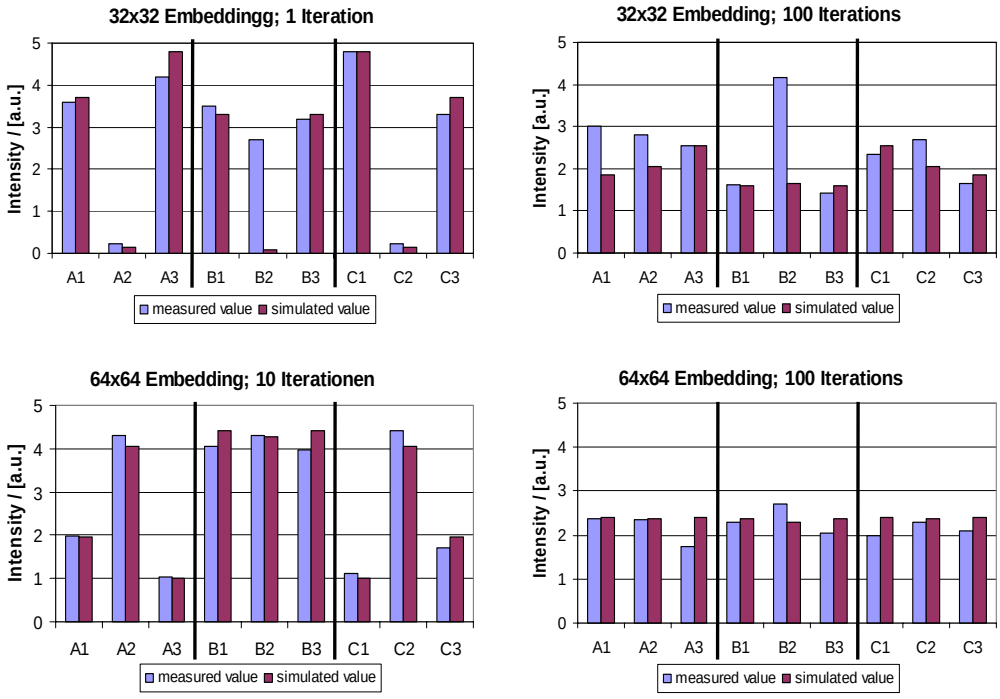

Figure 46: Normalized intensity of the diffraction orders of a 3x3 spot arrays obtained from a binary DOE.. A1, A2, A3 are the top row from left to right; B1, B2, B3 the center row and C1, C2, C3 the lowest row.

From Figure 46 it is obvious that the uniformity of the power distribution increases with the number of computational steps in the iterative quantisation. With 10 steps the uniformity is rather low compared to the one obtains with 100 steps. It can be seen that a larger data array size is also beneficial.

For a DOE with four quantisation levels, the setup does not provide phase-only modulation. Moreover, the software automatically uses equidistant graylevels to represent the phase levels. The diffrence between the simulated and the real modulation created by the SLM leads (among other effects) to a significant increas of the zero order.

However, by changing the values of the grayscale palette with a image processing software to optimised values (for a 650nm wavlength 0, 142, 172 und 255 are the best choice, representing phase modulations of 0, $\pi/2$, π and $3/2\,\pi$, see Figure 45), the zero order can be decreased significantly, as is shown in Figure 47. For other wavelengths, suitable grey levels can be be determined from measurements described int the modules RON (see section 9) or INT (see section 11).

In Figure 47 it can again be seen that the uniformity of the spot-to-spot power distributions is dependent on the number of quantisation iteration steps in the IFTA design computations.

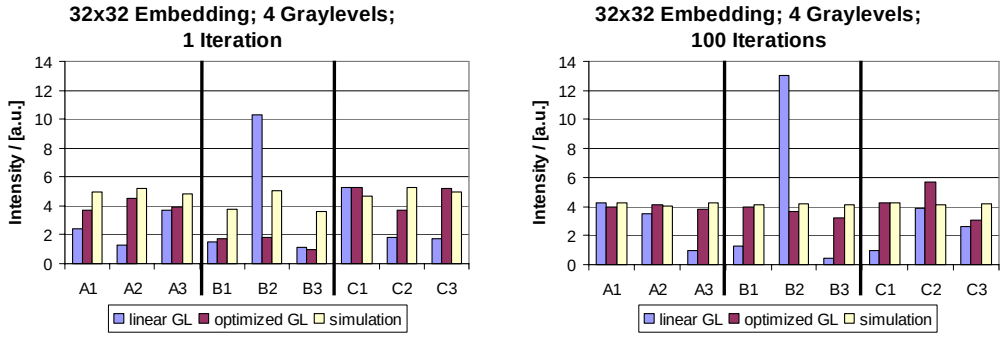

Figure 47: Normalized intensity of the diffraction orders of a 3x3 spot arrays for 4-Level DOEs. Expermental values are shown for linear and for optimised grayscale palettes of the phase-modulating DOE.

CGH3 Focal length of the diffractive lens

A DOE is created with the 'OptiXplorer' software. In the simplest case it is a blank screen. With the toolbar at the right window edge a lens phase will be added. The focus created by this diffractive lens should be found and the corresponding focal length be determined.

Experimental setup used:

Laser module, light modulator, and projection screen

If the focus cannot be clearly determined, adding the lens phase to a different DOE may be helpful (for example 'grid.bmp' or 'coords.bmp').

One can expect a focal length of about 800 mm with an added lens phase of 100.

lens phase	focal length f [mm]	1/f [1/m]
100	800	1.250
75	1040	0.962
50	1540	0.649
25	3000	0.333

Table 12: Focal length and optical power as a function of the lens phase

CGH4 Separation of diffraction orders by addressing a lens phase

Usually, when reconstructing a CGH there is a disturbing bright point in the middle — the zero order. Using a diverging refractive lens and a diffractive converging lens added to the DOE one can spatially separate the reconstruction planes of the zero and the first order (see section 4.5.3 and Figure 52).

The working distance can be decreased using the setup known from module 2 with a converging and a diverging lens. During this experiment, the distance between the focus and the reconstruction plane will be measured using the diverging lens to focus the image.

Experimental setup used:

Laser module, lens ($f = 150$ mm), light modulator, lens ($f = -30$ mm), and projection screen

For different lens phases, the focus plane and the Fourier plane is focused on the screen by moving the diverging lens. The translation Δz will be noted down; $\Delta z = 0$ is chosen for a diffractive lens with an optical power of $p_2 = 0$ (i.e. no lens addressed). Furthermore, the following parameters are given for this experiment (see also Figure 48 and Figure 49):

p_1 = 1/(150mm)	optical power of lens L1
p_3 = 1/(-30mm)	optical power of lens L3
p_2	optical power of diffractive lens L2 of SLM
d = 542 mm	distance L1 – screen
d_1 = 10 mm	distance L1 – SLM
d_2	distance SLM – L2
d_3	distance L2 - screen

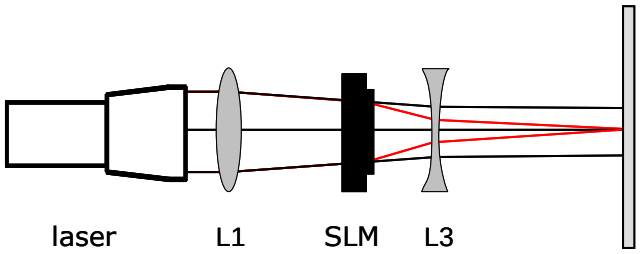

Figure 48: An added lens phase causes a focusing of the diffracted light (red). The undiffracted light is focused behind the screen (black).

diffractive lens	shift/mm
-100	29
-75	20
-50	13
-25	6
0	0
25	-6
50	-11
75	-16
100	-20

Table 13: Separation of the zero and first orders by a diffractive lens

In Table 13 one can see the measured data points for different diffractive lenses.

In the following the measured results are compared to calculated results obtained using ABCD matrices. In the following, a collimated beam which propagates parallel to the

optical axis with the radius r is analysed. The propagation of the beam after the first lens L1 is given by

(110) $$\begin{bmatrix} 1 & d_3 \\ 0 & 1 \end{bmatrix} \cdot \begin{bmatrix} 1 & 0 \\ -p_3 & 1 \end{bmatrix} \cdot \begin{bmatrix} 1 & d_2 \\ 0 & 1 \end{bmatrix} \cdot \begin{bmatrix} 1 & 0 \\ -p_2 & 1 \end{bmatrix} \cdot \begin{bmatrix} 1 & d_1 \\ 0 & 1 \end{bmatrix} \cdot \begin{bmatrix} 1 & 0 \\ -p_1 & 1 \end{bmatrix} \cdot \begin{bmatrix} r \\ 0 \end{bmatrix} = \begin{bmatrix} r_S \\ \alpha_S \end{bmatrix}$$

For the next steps a computer algebra system is recommended. Since a complete list of the single steps exceeds the scope of this document, only a few intermediate results will be presented.

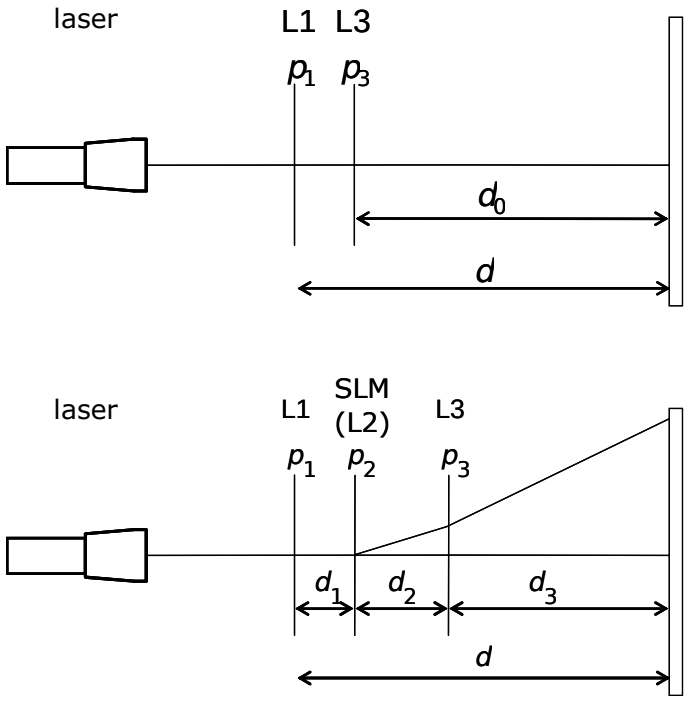

Figure 49: Setup for the determination of the optical power of the diffractive lens; without and with the SLM

First we will examine the setup without the diffractive lens, meaning $p_2 = 0$ and $d_2 = 0$ (see top of Figure 49). Furthermore, for the focused image in the plane of the screen $r_s = 0$.

Substituting $d_1 = d - d_0$ we obtain

(111) $$d_0 = \frac{1}{2} \cdot (d - 1/p_1) \cdot \left(1 \pm \sqrt{1 - \frac{4 \cdot 1/p_3}{d - 1/p_1}} \right).$$

Since $p_3 < 0$ and $(d\text{-}1/p_1) > 0$, the argument of the root is greater than 1. Therefore only an addition of the square root results in a positive value for d_0. Inserting the parameters given above we get $d_0 = 420\ \text{mm}$.

Now the SLM will be addressed with an additional diffractive lens ($p_2 \neq 0$). To focus the Fourier plane on the screen, lens L3 will be shifted. This distance is Δz and therefore $d_3 = d_0 + \Delta z$. For $r_s = 0$ we get

(112) $$\begin{aligned}&\left(\left(d_2\cdot d_3-d_1\cdot d_2\cdot d_3\cdot p_1\right)p_2+\left(d_2+d_1\right)d_3\cdot p_1-d_3\right)p_3+\\&\left(\left(d_1\cdot d_3+d_1\cdot d_2\right)p_1-d_3-d_2\right)p_2+\left(-d_3-d_2-d_1\right)p_1+1=0\end{aligned}.$$

By substituting $d_2 = d - d_1 - (d_0 + \Delta z)$ and $d_0 = 420\,\text{mm}$ and by using the other known values, the optical power p_2 [1/m] is given by

(113) $$p_2=-\frac{50\cdot\Delta z\cdot\left(448+\Delta z\right)}{7\cdot\left(-63000+308\cdot\Delta z+\Delta z^2\right)}.$$

For the Taylor expansion around $\Delta z = 0$ the first derivative is required, which is obtained as

(114) $$f'(dz)=-\frac{50}{7}\cdot\left(\frac{448+2\cdot\Delta z}{-63000+308\cdot\Delta z+\Delta z^2}-\frac{\Delta z\cdot\left(448+\Delta z\right)\cdot\left(308+2\cdot\Delta z\right)}{\left(-63000+308\Delta z+\Delta z^2\right)^2}\right).$$

Inserting $\Delta z = 0$, it is found that $f'(0) = 16/315 = 5.08 \times 10^{-2}$. For the second derivative we get $f''(0) = 7.2 \times 10^{-4}$. Therefore the first three terms of the Taylor expansion are

(115) $$T_f\left(dz\right)=0+5.08\cdot10^{-2}\times\Delta z+\frac{1}{2}\times7.2\times10^{-4}\Delta z^2.$$

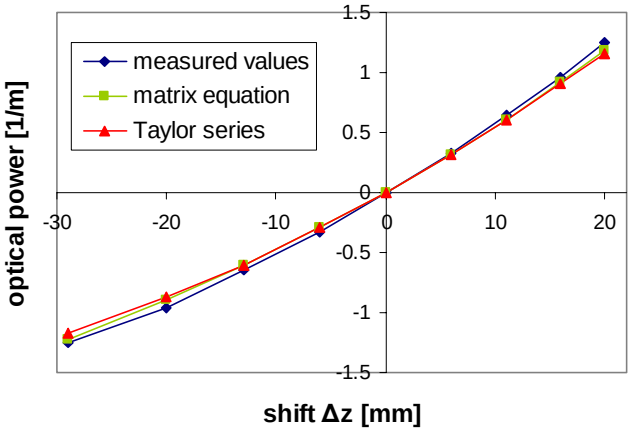

Figure 50: Comparison of the measured values with the results from ABCD matrices and the Taylor expansion

CGH5 Separation of diffraction orders by addressing a prism phase

By adding a prism phase to the addressed DOE it is also possible to separate the orders. The diffraction pattern will be shifted in x and y direction (see Figure 52). The shift of the image is determined for different prism phase functions and conclusions about the spatial frequency of the prism phase are made.

Experimental setup used:

Laser module, light modulator, lens (f = -250 mm) and projection screen

If the reconstructed hologram does not have to be positioned on the beam axis, a prism phase can be used to diffract it away from this axis. The result is a spatial separation from the zero order. In this experiment, the dependence of the diffraction angle on the addressed prism phase will be investigated.

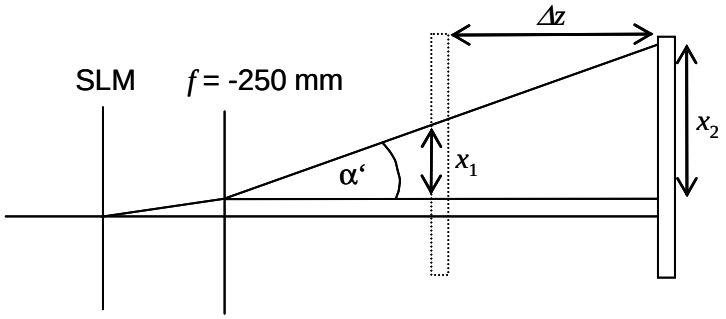

Figure 51: Determination of the angle α’

To experimentally determine the angle caused by the addressed prism phase, the reconstructed image is focused on the screen. The shift x_1 is measured for different prism phase functions. Then the screen is shifted by the distance Δz in z direction and the image is focused with the telescope lens of the laser module. This does not affect the diffraction angle. Again the shift x_2 will be measured. Now the angle α’ between the beam behind the diverging lens and the optical axis is given by

$$\alpha' = \Delta x / \Delta z \qquad \text{with} \quad \Delta x = x_2 - x_1 \ .$$

The angle α in front of the diverging lens (f = -250 mm) is given by

$$\alpha = \frac{\alpha'}{(1 - d/f)}$$

where d denotes the distance between the SLM and the lens.

prism phase	shift Δx [mm]	$\alpha'=\Delta x/\Delta z$ [rad]	$\alpha=\alpha'(1-d/f)$ [rad]	$g=\lambda/\sin(\alpha)$ [1/mm]	spatial frequency [1/mm]	pixel per period	pixel size [µm]
-100	-39.3	-0.025192	-0.009400	-0.0691	-14.46	2	34.57
-75	-29.25	-0.018750	-0.006996	-0.0929	-10.76	2.67	34.84
-50	-20	-0.012821	-0.004784	-0.1359	-7.36	4	33.97
-25	-9.5	-0.006090	-0.002272	-0.2861	-3.50	8	35.76
0	0	0.000000	0.000000				
25	9.5	0.006090	0.002272	0.2861	3.50	8	35.76
50	20	0.012821	0.004784	0.1359	7.36	4	33.97
75	29.5	0.018910	0.007056	0.0921	10.86	2.67	34.55
100	39.3	0.025192	0.009400	0.0691	14.46	2	34.57

Table 14: Measured data and calculated parameters for different prism phase functions (Δz = 1560; d = 420 mm; f =-250 mm; λ = 650 nm)

The grating period g can be determined from $g = \lambda/\sin(\alpha)$ and therefore the spatial frequency is given by $f_x = 1/g = \sin(\alpha)/\lambda$. Knowing the number of pixels of a single period of the prism phase function, one can determine the pixel size. For example by creating a blank screen with the ‘OptiXplorer’ software and adding a prism phase with the button on

the right-hand toolbar, one can count the number of periods. Dividing this number by the screen resolution one can determine the number of pixels for a single period.

In Table 14 the measured data and the calculated values are listed. Thereby the screen was shifted by Δz = 1560 mm.

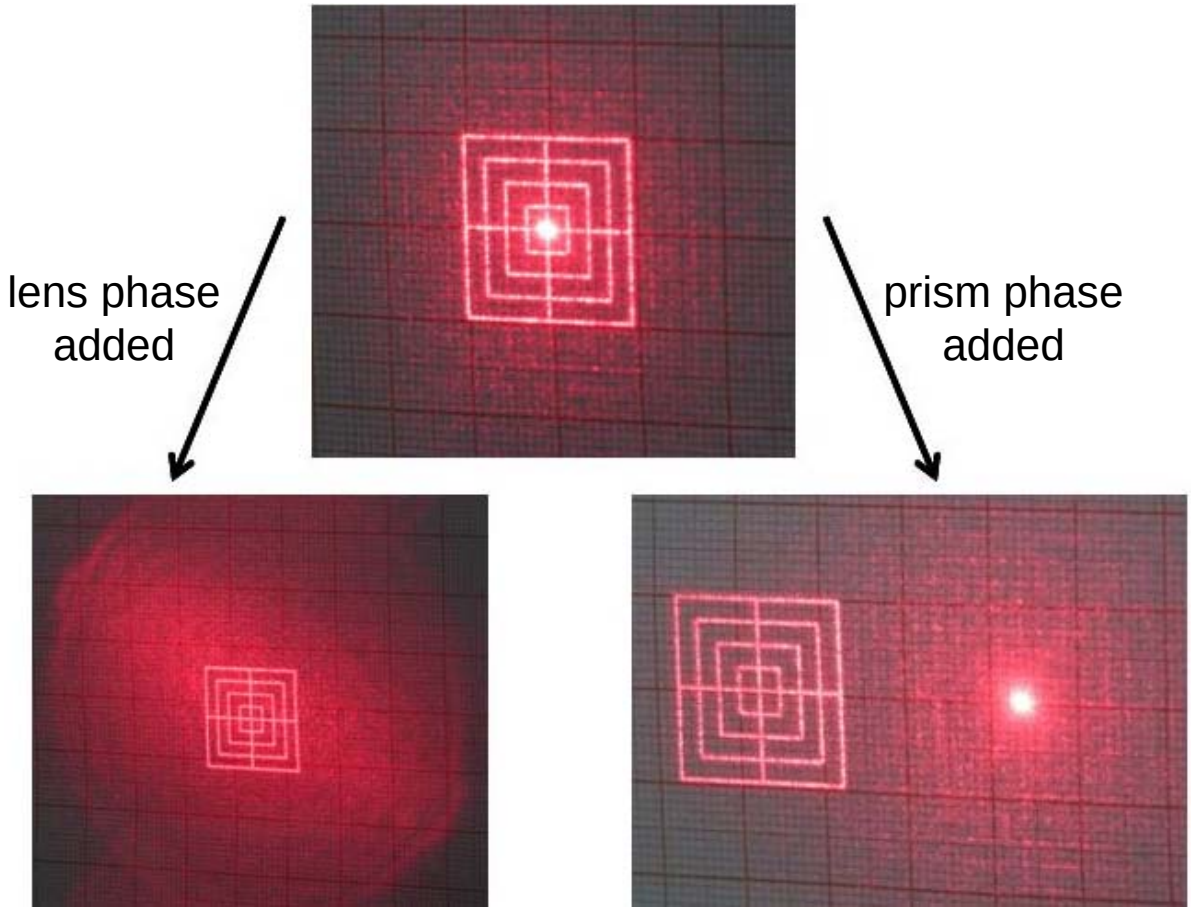

Figure 52:
Top: focused zero order
Left: zero order defocused
Right: diffraction pattern shifted

CGH6 Demonstration of two DOEs addressed on one display

Finally a short experiment with a qualitative description. Two different DOEs will be addressed side by side on the screen. For example the width of two full screen windows will be halved. The resulting diffraction pattern contains both images generated by the two DOEs but each will only have half the intensity.

10.4 Keywords for preparation

Fraunhofer and Fresnel diffraction, Fresnel zone plate, diffraction, interference, Fourier transformation, diffractive optical elements, far-field theory, lens systems, ABCD matrices, functionality of an LCD

10.5 References

Eugene Hecht
Optik (3.Auflage)
Oldenbourg Verlag, München Wien (2001)

Dieter Meschede
Optik, Licht und Laser (2.Auflage)
Teubner (2005)

11 Module INT: Interferometric measurement of the phase modulation

11.1 Objectives

The phase modulation that can be achieved with a spatial light modulator for a coherent light source can be measured with a two beam interference setup. The method which will be shown here can be used for transmission as well as for reflective displays. No beam-splitting elements need to be used which could potentially disturb the measurement.

It is recommended to install the 'PhaseCam' software which is a part of the 'OptiXplorer' kit. The description of the software can be found in section 17.

11.2 Required components

- **Light modulator:** LC2002
- **Light source:** Laser module
- **Optics:** 2 polarisers, lens ($f = 220$ mm) and microscope objective (20x/0.4), aperture mask
- **Instruments:** CCD camera, photodiode

11.3 Suggested tasks and course of experiments

The display is illuminated by two coherent and collimated laser beams created by a double-hole mask. Both beams are separately guided to an appropriate half of the LCD. The left one will be addressed with a constant grey level whereas the other half will be addressed with grey levels varying from 0 to 255. A lens behind the display lets both beams interfere with one another and a microscope objective images the expanded interference pattern onto a detector (CCD camera, array-detector, photodiode). A phase shift as a function of the addressed grey level will appear as a shift in the interference pattern perpendicular to the optical axis (see Figure 53).

The phase shift $\Delta\Phi$ between two grey levels is given by the shift of the minima Δy and the length of the period g.

(116)
$$\Delta\Phi = \frac{2\pi}{g} \cdot \Delta y$$

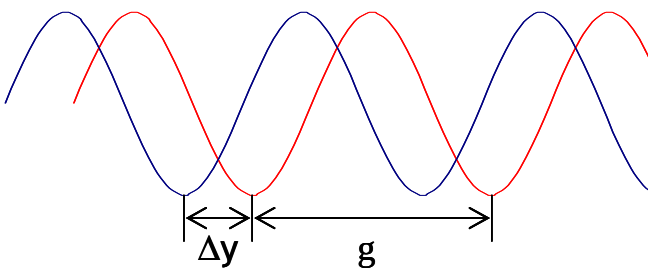

Figure 53: Shift of the interference minima

This shift can be detected by a CCD camera and analysed by the 'PhaseCam' software. If one does not want to use the software the horizontally divided screen with dynamic grey levels can be created with the 'OptiXplorer' software.

Figure 54: Example for addressed grey levels

Instead of the CCD camera, a different sensor could also be used. In any case, care has to be taken that the length of the grating period g (meaning the distance between two minima at a constant grey level) and the shift of the minima Δy depending on the addressed grey levels can be measured with sufficient accuracy.

A very simple setup, making use of a prism, is shown in Figure 55. However, it can be shown easily that such a setup needs a length of several metres to obtain an analysable image. Reasonable is a period of about 100 pixels on the CCD camera. With a pixel size of about 10 µm one gets a minimum distance of g = 1 mm. Therefore

$$\sin(2\theta) = 2\lambda/g = 2 \cdot 0.65\mu m/1000\mu m \Rightarrow \theta \approx 0.04° .$$

That means the angle between the two beams should be 0.04°. The distance between the two beams is 7 mm meaning that they will only intersect at a distance of 10 m.

Increasing the angle will decrease the size of the interference pattern so that it gets too small for the resolution of the camera. Therefore a magnification optic is necessary.

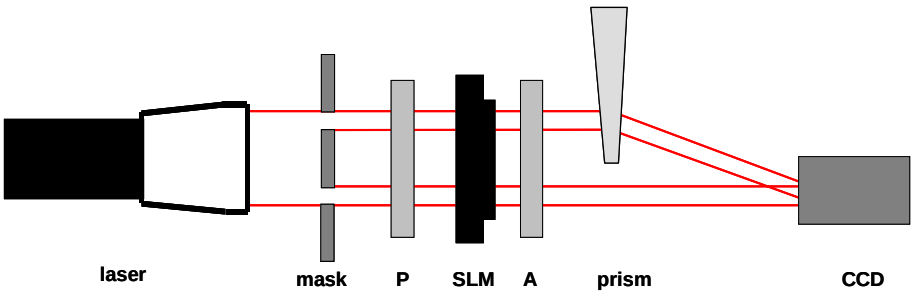

Figure 55: Setup for interferometric measurement of the phase shift

Instead of a prism a lens could also be used to make the beams intersect. The interference pattern is generated in the focus of the lens and will be imaged by a microscope objective on the CCD sensor. The length of such a setup will be around 1 m. Figure 56 shows such a setup.

Often it is also important to know the amplitude modulation for a certain phase modulation. This can be determined by a slightly modified setup. One beam has to be blocked and the CCD camera has to be replaced by a photo detector. Here the whole display is addressed with a homogeneous grey level.

INT1 Setting up the experiment

The optical setup is shown in Figure 56. The laser module emits a collimated beam. A double-hole mask (hole diameter ~3mm, distance ~7mm) creates two beams (one for each half of the LCD). A linear polariser in front of the SLM sets the incoming polarisation state. Since the laser emits elliptically polarised light, it is possible that the polariser blocks too much light. In this case the laser should be rotated until enough light is transmitted through the polariser.

The two beams will be guided through the analyser behind the SLM and combined by a lens. The interference pattern of the two beams will then be imaged onto the CCD chip by a microscope objective.

Here we want to estimate the focal length of the lens. Above, it was mentioned that the angle between the two beams should be around 0.04°. The used microscope objective has a magnification of 20. Therefore, in the focus of the lens the angle between the two beams is $\theta \approx 20 \times 0.04° = 0.8°$. The focal length is given by

$$\tan\theta = \frac{\Delta x}{2 \cdot f} \Rightarrow f = \frac{\Delta x}{2 \cdot \tan\theta}. \tag{117}$$

With a distance of $\Delta x = 7$ mm between the two beams at the double-hole mask, the focal length is $f \approx 250$ mm.

If the 'PhaseCam' software is used, the shift of the interference pattern will be detected and saved for later analysis. To start with, the user chooses an interference minimum which is used as a starting point for the measurement. The shift of this minimum during the measurement directly represents the phase shift for the addressed grey level.

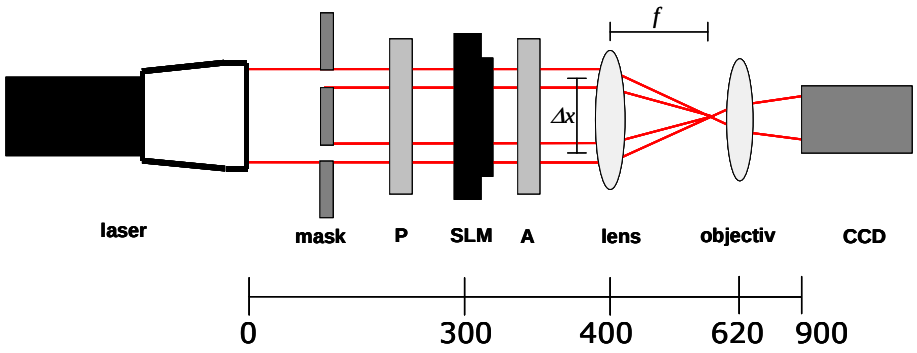

Figure 56: Two-beam interferometer to detect the phase shift

INT2 Measurement using the 'OptiXplorer' software

With the 'OptiXplorer' software the display will be addressed with a horizontally divided screen with two different grey levels, generating a clearly visible interference pattern in the detector plane. It is important to take care that the image has a good contrast and that the detector is not saturated. For this grey level the period will be determined and a minimum for the relative shift is chosen. The corresponding half of the display will then be addressed with a second grey level. Using the scroll bar in the right-hand toolbar one can modify the addressed grey level continuously and in this way the shift of the minimum can be followed easily.

According to equation (116) the relative phase shift between the two grey levels can be determined. Since it takes a lot of time to determine the phase shift for all grey levels this is

only an example measurement to compare with the automated measurements using the 'PhaseCam' software.

INT3 Adjustment and automated measurement with 'PhaseCam' software

The 'PhaseCam' software offers an automation of the measurements described in INT2. It is recommended to have a look at the 'Preview' before starting the measurement to make sure that everything is correctly adjusted, that the interference pattern has sufficient contrast. Figure 57 shows an example camera image. It could be necessary to insert a neutral density filter in order to make sure that the camera is not saturated.

After proper adjustment, push the 'test image' button. A stable image will be recorded and displayed. A particular line will be selected for measurement by clicking the right mouse button inside of that image. This line should have a sinusoidal intensity profile. Afterwards, select 'readout lines' in order to determine the intensity profile of the measurement line. The minima and maxima as well as the period of the interference pattern will appear in the lower right-hand corner of the software window. Until now the value of 'x-Start' (which is 20 by default) should not be changed so that the programme can determine the period with as many minima as possible.

After selecting the measurement line, open the grey level window using the corresponding button and make sure that it occupies the full screen of the LCD. It is convenient to open that window before the adjustment in order to create an interference pattern similar to the one that is seen at the start of the measurement.

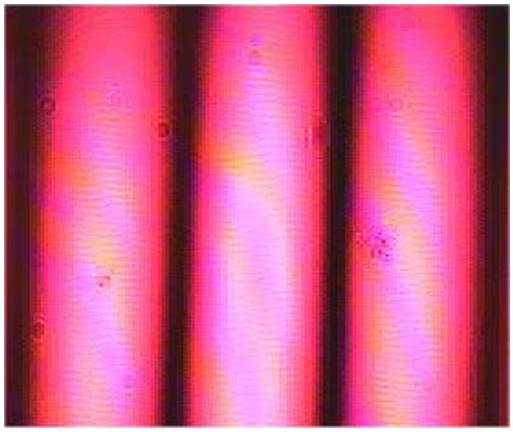

Figure 57: Interference pattern detected by a camera

Before starting the measurement, the increments have to be chosen. This option changes the time and the resolution of one measurement. This is always a compromise since fast measurements have a low resolution and slow measurements have a high resolution.

The 'Start' button starts the measurement and grey levels varying from 0 to 255 are addressed onto the active half of the grey level window in succession.

INT4 Evaluation of the automated measurement

If one selects the 'Show Image' button after the measurement is finished, the live image will be replaced by an image in which the selected measurement line for each addressed grey level is drawn one below the other. This image gives the first impression of the measurement and clearly shows if and how the interference pattern has been shifted.

A convenient function for the first rough determination of the total phase shift is implemented. If the user moves the cursor onto the image shown and clicks and holds the right mouse button, a bar will appear at the position of the cursor. If the user holds

the button and moves the cursor, a second bar appears and the distance in pixels will be displayed just above the image (see Figure 58). If the start and the end value are chosen for both bars, one can see how far the interference pattern was shifted during the measurements. By taking the period of the interference pattern into account, the phase shift can easily be calculated.

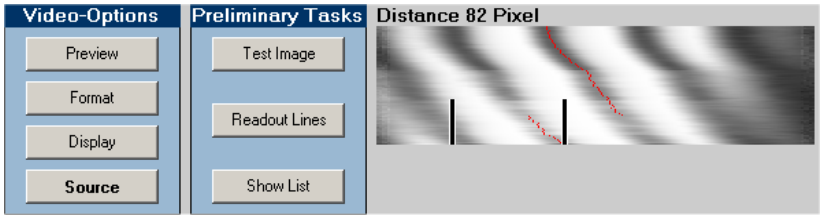

Figure 58: Metering bars

By pushing the 'Show Measurement Points' button after the image described above is shown, the measurement points (values with minimum intensity) will appear as red dots. If the distribution of these dots has no big jumps or irregularities (which can be a result of vibrations or air flow), the measurement will be evaluable. It is possible that the measurement points 'jump' to the next minimum [mod 2π]. This can be corrected afterwards in a spreadsheet program like 'Microsoft Excel' by adding or subtracting one period. Now one can save the measurement as a '.txt' file that includes the period and position values for each addressed grey level.

By pushing the 'Save Image' button the image of the shifted interference pattern can be saved for the sake of documentation.

The phase modulation as a function of the addressed grey level can be calculated by using a spreadsheet program. Therefore the first value has to be subtracted from each measurement value (Δy) in order to set the starting point to zero (grey level 0). With the period g the phase shift can be found according to equation (116).

INT5 Testing different configurations

The 'PhaseCam' software allows an automated and fast measurement of the phase shift for any polariser/analyser configurations. Therefore it is comparatively easy to optimize the setup for a particular kind of modulation (i.e. amplitude or phase modulation). To give an example, the measurements for finding a maximum of the phase shift are shown.

For the measurements the following polariser/analyser configurations are used: 310°/10°; 355°/55°; 40°/280°

The results obtained from evaluation with a spreadsheet program are shown in Figure 59. In Figure 60 the saved images from the 'PhaseCam' software are shown. The maximum occurring phase shift of more than 1.4π was measured with a polariser/analyser configuration of 310°/10°.

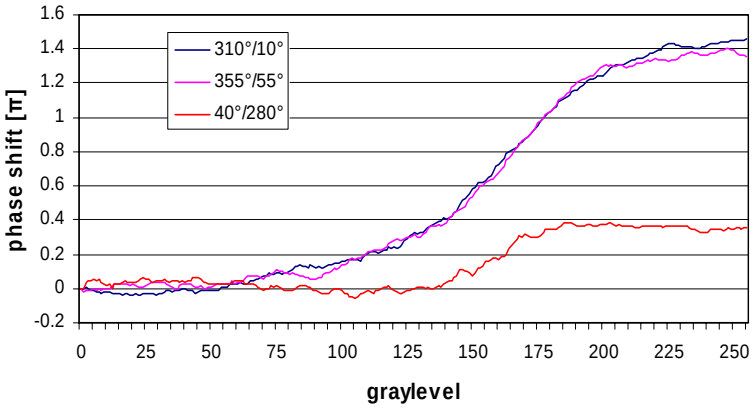

Figure 59: Phase shift of the display with different polariser/analyser configurations

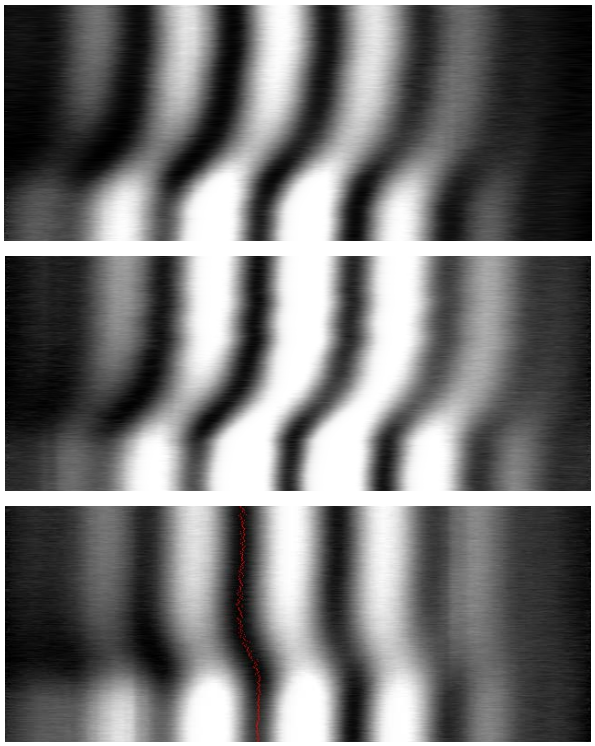

Figure 60: Measurement images of the 'PhaseCam' software (top to bottom: polariser/analyser 310°/10°; 355°/55°; 40°/280°)

11.4 Keywords for preparation

Interference, interferometric methods, amplitude and phase modulation

11.5 References

Eugene Hecht

Optik (3.Auflage)

Oldenbourg Verlag, München Wien (2001)

Stephen G. Lipson, Henry S. Lipson, David S. Tannhauser
Optik
Springer, Berlin (1997)

C. Souter et al.
Measurement of the complex transmittance of the Epson liquid crystal television
Optical Engineering 33(4), 1061-1068 (1994)

D. A. Gregory and J. L. McClain
Wavefront Splitting Interferometer for Measurement of Phase Modulation
Microwave Opt. Technol. Lett. 86, 292-294 (1995)

III OPERATING INSTRUCTIONS

12 Spatial Light Modulator LC2002

12.1 Cautions

12.1.1 Avoid humidity and dust

Do not use the LC2002 outside buildings and in humid or dusty places.

12.1.2 Keep heat away

Keep the LC2002 away from extreme heat as it may cause damage. When using the LC2002 its display case and power pack become warm. Take care for sufficient ventilation, and keep the devices away from heat such as heating radiators, strong sun light, etc.

If you plan to apply the LC2002 with powerful light sources, heat-protection filters must be introduced between light source and LCD matrix. We strongly recommend you to consult HOLOEYE in this case.

12.1.3 Keep water away

If water or some other liquid is spilled into the LC2002 device serious damage can occur. Please, consult HOLOEYE services in such a case.

12.1.4 Avoid touching the LCD

Avoid touching the LCD because this might cause damage to it or reduce its optical quality.

12.1.5 Cleaning the LCD

Wipe the LCD very carefully with a soft, dry and clean cloth or with compressed air. If you are not sure if and how to clean the LCD, consult HOLOEYE services.

12.1.6 Electrical Connections

Connect the LC2002 only to other components if the power supplies of all components are switched off. For power supply of the LC2002 use **only** the power pack plug which is delivered with the LC2002.

12.1.7 Maintenance

Do **not** open and touch the LC2002 device as this is dangerous and may seriously damage it. Do not attempt to disassemble the LC2002. There are no user serviceable or adjustable parts inside.

Attention:

If the stated cautions are disregarded, the warranty claim expires.

12.2 Technical Data

Display

Type:	SONY LCX016AL-6
Colours:	Grey-level image playback
Active Area:	26.6 mm x 20.0 mm (1.3")
Number of image pixels:	832 x 624
Pixel pitch:	32 µm
Image frame rate:	max. 60 Hz
Contrast ratio:	typically 200:1

Device

Dimensions (L x W x D):	82 mm x 82 mm x 23 mm
Weight:	0.15 kg
Operating voltage of power pack plug:	100-230 V AC ± 10% 50-60 Hz
Power input of power pack plug:	max. 150 mA
Operating voltage of LC2002:	15 V DC ± 5% Positive terminal at inner pin
Power input of LC2002:	ca. 250 mA

12.3 Connectors

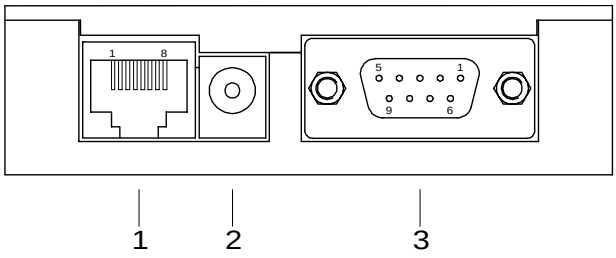

Figure 61: Connectors of the LC2002

The device provides three female connectors. As depicted in Figure 61, these connectors are:

1 - the serial port connector for configuration of the device

2 - the power supply connector

3 - the VGA video input connector

12.3.1 Serial Port

Configuration of serial port connector (1):

Pin 1	+5V Gs	Pin 5	RXD
Pin 2	+5V Gs	Pin 6	CTS
Pin 3	TXD	Pin 7	GND
Pin 4	RTR	Pin 8	GND

Connection parameters:

Transfer rate	19200 Bit/s
Data bits	8
Parity	none
Stop bits	1
Data flow control	Hardware handshake RTR / CTS

12.3.2 Power Supply

The direct current (DC) connector (2) is used for power supply of the device. The power pack cable (15 V) has to be plugged to this connector. The positive terminal is the inner connector pin.

12.3.3 Video input

The video input (3) must be connected to the graphics board of a personal computer using the VGA adapter cable delivered with the LC2002. The computer is used as the source of image and video data. The connector configuration is specified as follows:

Pin	Function
1	Red colour signal
2	Green colour signal
3	Blue colour signal
4	HSYNC (line synchronisation signal)
5	VSYNC (image synchronisation signal)
6	GND red colour signal
7	GND green colour signal
8	GND blue colour signal
9	GND

12.4 Connecting the LC2002 for Usage

For using the LC2002 at least one computer with a VGA graphics board is required. The computer is required for controlling the LC2002 and providing images or videos to be displayed on the LCD. Instead of the PC, a VGA camera can be used as image-signal source.

First, the LC2002 driver software must be correctly installed on the computer. Then, the computer can be connected to the LC2002 as shown in Figure 62.

Attention: Plug the serial port and VGA connector first and the power supply connector always at last.

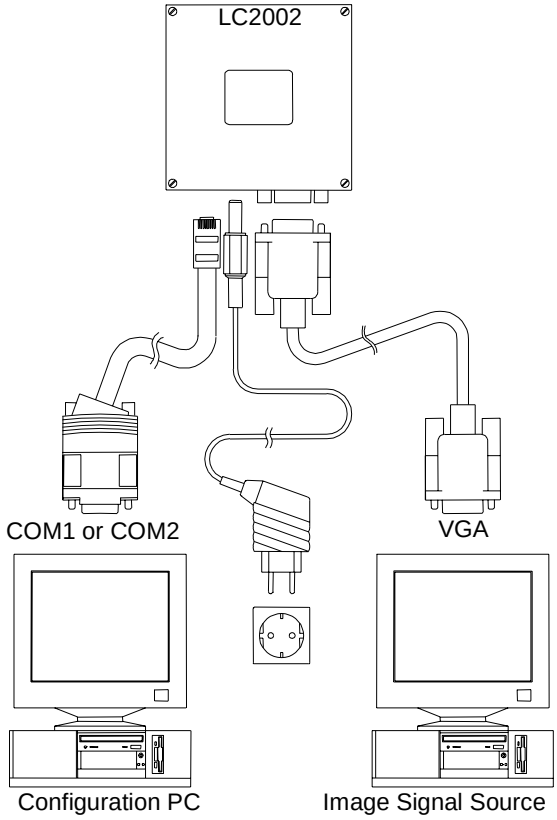

Figure 62: Connecting the LC2002 for usage.

12.5 RS-232 Commands

12.5.1 Command structure

The RS-232 commands are strings of ASCII symbols that have to end with an end symbol. An end symbol is used to separate a command from its subsequent one and trigger the LC2002 to decode and execute the command.

Specified end symbols are **Carriage Return** (0Dh), **Line Feed** (0Ah) and **semicolon** (3Bh).

For the commands there is no distinction between capital and small letters. Generally, blanks are not allowed in a command unless they are directly in front of an end symbol.

The LC2002 device has an ‘echo’ function that confirms each correctly decoded command. After successful decoding the string ‘**OK**’ is sent by the LC2002 to its RS-232 interface. In case of a false command or an unsuccessful execution the LC2002 send an error code, e.g., ‘**ERR 3**’. The list and meaning of all error codes is given in section 12.6.

The echo function can be switched on and off. When the device is switched on, the echo function is automatically switched on as well.

In the following all available commands and their meaning are described. The commands are ended with <CR>, respectively. The response of the LC2002 to each command is written indent.

Remark: The symbol <CR> is obtained by pressing the enter button (↵) on the keyboard. So, do not use the symbols 'C' and 'R'.

The response of the LC2002 is indented.

12.5.2 Request Commands (Requests)

Request commands always result in a response of the LC2002. They are characterised by a question mark at the end of the command, followed by an end symbol.

- Request the device ID number

  IDN?<CR>

  LC2002A

- Request the firmware version

  VER?<CR>

  1.04

- Request the configuration

  CONF?<CR>

  4 1E BE 13 0 0 0 1 0 0 5 1C
  CC 77 FF A7 0 0 A 0 0 89 D 15
  F A 3C 6

The response values shown here are examples and can vary with respect to the configuration of the device. The meaning of the bytes can be obtained from the following table. The bytes specify user-specific as well as device-internal configurations.

Byte No.	Meaning	intern. symbol
0	Most significant byte PLL-Factor	
1	Less significant byte PLL-Factor	
2	HPOS, image position horizontal	
3	VPOS, image position vertical	
4	Internal configuration	HDN
5	SHP, pixel synchronicity of image playback	
6	Internal configuration	HCKP
7	Internal configuration	HSTP
8	Internal configuration	CLPP
9	Internal configuration	SHD
10	Internal configuration	SH
11	Internal configuration	MBK

12	MODE, image format switching	
13	DIR, e. g. scanning direction	
14	GCB (***G***amma ***C***ontrol ***B***lack), RGB signal common black side voltage gain change point control	
15	BRT (***BR***igh***T***ness), RGB signal common main brightness control	
16	BLIM (***B***lack ***LIM***iter), Limiter control for limiting the output amplitude of the RGB signal	
17	WLIM (***W***hite ***LIM***iter), RGB signal white peak limiter control	
18	GGW (***G***amma ***G***ain ***W***hite), RGB signal common white side voltage gain control	
19	GCW (***G***amma ***C***ontrol ***W***hite), RGB signal common white side voltage gain change point control.	
20	GGB (***G***amma ***G***ain ***B***lack), RGB signal common black side voltage gain control	
21	CON (***CON***trast), Gain control for RGB signal common variable gain amplifier	
22	Internal configuration	SBRT
23	Internal configuration	SID
24	Internal configuration	VCOM
25	Internal configuration	CENT
26	ID number, Most significant byte	
27	ID number, Less significant byte	

12.5.3 Configuration Commands (Configs)

Configuration commands consist of a command name and a parameter value that is separated from the name by a colon. The parameter value must be given as an integer.

- Image width

Command name	Parameter	
	min.	max.
PLLP	**848**	**2045**

Example:

PLLP:1054<CR>

OK

The parameter influences the pixel synchronicity of the image playback. For the image format SVGA (800 x 600 image pixels) usually 1054 is the correct value.

- Horizontal image position

Command name	Parameter	
	min.	max.
HPOS	**0**	**255**

Example:

HPOS:207<CR>

OK

- Vertical image position

Command name	Parameter	
	min.	max.
VPOS	**0**	**255**

Example:

VPOS:19<CR>

OK

- Pixel phase (pixel synchronicity)

Command name	Parameter	
	min.	max.
SHP	**0**	**15**

Example:

SHP:1<CR>

OK

- Image format

Command name	Parameter	Meaning
MODE	**204**	SVGA 800x600 (CCh)
	201	PC-98 640x400 (C9h)
	206	VGA 640x480 (CEh)

Example:

MODE:204<CR>

OK

Remark: When setting the image format using the MODE command, the pixel-synchronised playback is preserved. Image formats that that do not fill up the display are automatically centred and surrounded by a black frame.

- Entry point of gamma correction white

Command name	Parameter	
	min.	max.
GCW	**0**	**255**

Example:

GCW:1<CR>

OK

- Intense of gamma correction white

Command name	Parameter	
	min.	max.
GGW	**0**	**255**

Example :

GGW:1<CR>

OK

- Entry point of gamma correction black

Command name	Parameter	
	min.	max.
GCB	**0**	**255**

Example:

GCB:1<CR>

OK

- Intense of gamma correction black

Command name	Parameter	
	min.	max.
GGB	**0**	**255**

Example:

GGW:254<CR>

OK

- Contrast

Command name	Parameter	
	min.	max.
CON	**0**	**255**

Example:

CON:196<CR>

OK

- Brightness

Command name	Parameter	
	min.	max.
BRT	**0**	**255**

Example:

BRT:183<CR>

OK

12.5.4 Other Commands

- Echo switching on/off

The command **ECHO:OFF**<CR> suppresses the mandatory response with **OK** on each correctly decoded command or error code messages. The command **ECHO:ON**<CR> can be used to switch the echo on again.

12.6 Error Messages

The meaning of error messages is given in the following list:

ERR 1	Overflow of the symbol-receiving buffer	RS-232 handshake does not work, internal or external error
ERR 2	Unexpected symbol in command (neither letter, digit, nor underscore)	Command incorrect
ERR 3	Unknown command	Command incorrect
ERR 4	Parameter of preceding command not allowed	Parameter incorrect
ERR 5	Unknown parameter	Parameter incorrect
ERR 6	Unexpected symbol in parameter (neither letter, digit, nor underscore)	Parameter incorrect
ERR 7	Digit was expected but a different symbol received	
ERR 8	Command did not end correctly; instead of end symbol another symbol was received	
ERR 9	Command parameter missing	
ERR 10	Internal error (EEPWR)	LC2002 defect
ERR 11	Internal error (EEPRD)	LC2002 defect
ERR 12	Internal error (DACWR)	LC2002 defect
ERR 13	Internal error (EPTWR)	LC2002 defect
ERR 14	Internal error (RESTORE)	LC2002 defect

12.7 Assembly Drawing

In order to assemble the LC2002 device on one side four drill-holes M2 are provided. The assembly screws must not go deeper than 8mm into the box!

The dimension values are given in mm.

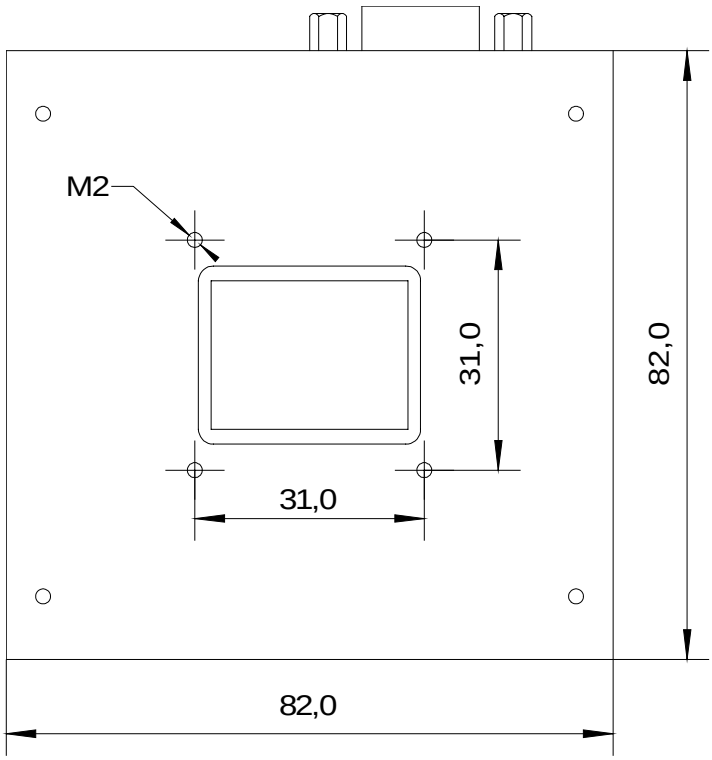

Figure 63: Assembly drawing

13 Laser module

13.1 Technical data

Wavelength:	650 nm
Operating voltage:	5 V (DC)
Current:	≤ 120 mA
Operating voltage power supply:	100-230 V AC + 10% 50-60 Hz
Current power supply:	max. 180 mA
Aperture:	d = 20 mm
Output power laser light:	8 mW
Beam diameter:	focus adjustable
Beam magnification:	> 8-fold magnification
Working distance:	max. 30m
Operating temperature:	-10°C ~ +40°C
Storage temperature:	-40°C ~ +80°C

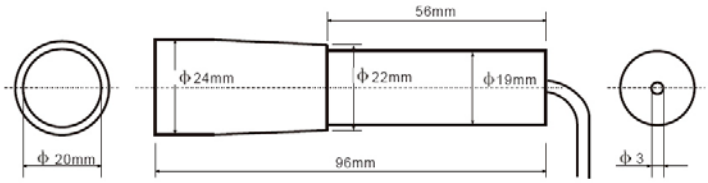

Figure 64: Geometrical size of the provided laser module.

class 3B laser

13.2 Connecting the Laser Module for Usage

For using the laser module connect the 5V-power supply with the laser module and plug the power supply to the electrical outlet

13.3 Laser Safety

The provided laser is a class 3B laser module.

Class 3B laser products can emit up to 500 mW of accessible laser emission. Class 3B lasers are capable of causing a permanent eye injury with brief exposure, can cause minor skin burns, and can ignite many materials with sustained or focused exposure.

Do not watch into the laser beam or on any reflections!

Some basic guidelines for Laser Safety:

1. Never look into the beam of any laser.
2. Be aware of the hazards posed by your laser.
3. Aim the laser well away from others.
4. Use an appropriate target.
5. Do not allow the beam to inadvertently reflect from metal or glass surfaces.
6. Use protective eyewear.

Certain preventive measurements have to be done before the usage of the provided laser. Inform yourself about applicable regulations with laser products of the class 3B and consider these before and during application of the laser.

HOLOEYE assumes no liability for any damage caused by the laser.

14 Polarising Filters

Transmission:	~ 30 % at 400 nm - 700 nm
Transmission for crossed polarisers:	~ 0,15 % at 400 nm - 700 nm
Polarisation efficiency:	95 %
Operating temperature:	-15°C to +70°C

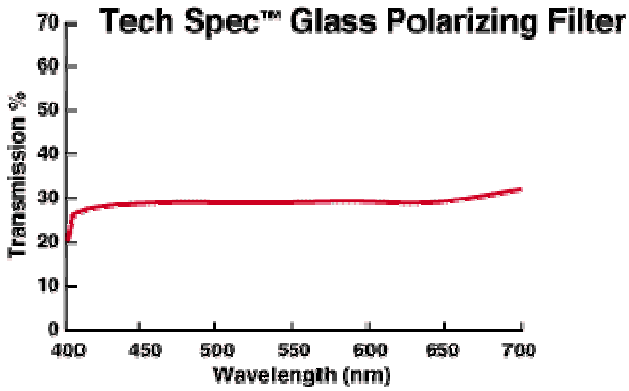

Figure 65: Transmission of a single polariser

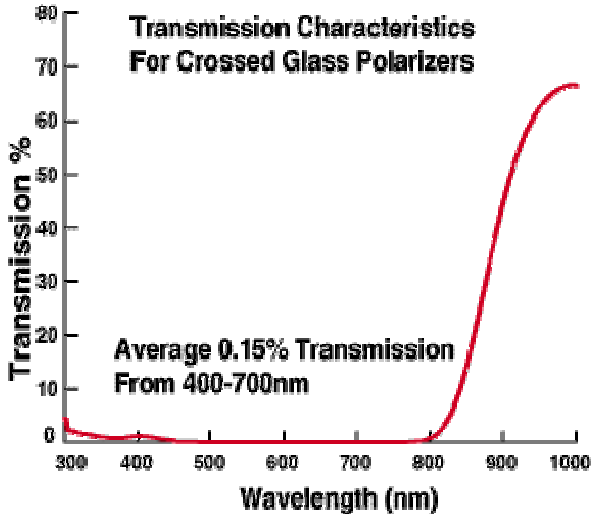

Figure 66: Transmission of two crossed polarisers

IV OPERATING INSTRUCTIONS SOFTWARE

15 LC2002 Control Software

The LC2002 control program uses RS-232 commands to perform its tasks on the LCD. In principle, these commands can be also send by another control device. This makes it possible to integrate the LC2002 in prototype systems where the control unit may be a different device than a PC. The RS-232 commands are described in section 12.5.

15.1 System Requirements

- IBM- or compatible PC
- 32 MB main memory or more
- VGA graphics board
- Free RS-232 port (COM1 or COM2)
- Operating systems: Microsoft Windows 95, Windows 98, Windows NT 4.0, Windows 2000, Windows XP

15.2 Installation

For installing the control software execute the program SETUP.EXE on CD-ROM. This program requests for all information required for the installation process.

After the installation has been completed successfully, the LC2002 control software can be started from the Microsoft *Windows* 'Start menu' as shown in the next section.

15.3 Start of the LC2002 Control Program

You can start the LC2002 control program by selecting **Programs > LC2002 Control Program** in the Microsoft *Windows* 'Start menu'.

After starting the program the user dialog 'LC2002' as shown in Figure 67 appears. At the same time the program tries to identify automatically the LC2002 display that should be connected to the RS-232 port (COM1 or COM2). If the identification succeeds, the coloured 'Connected' sign appears in the lower right corner of the dialog window.

In the title of the dialog window the version of the LC2002´s firmware and its individual series number are displayed

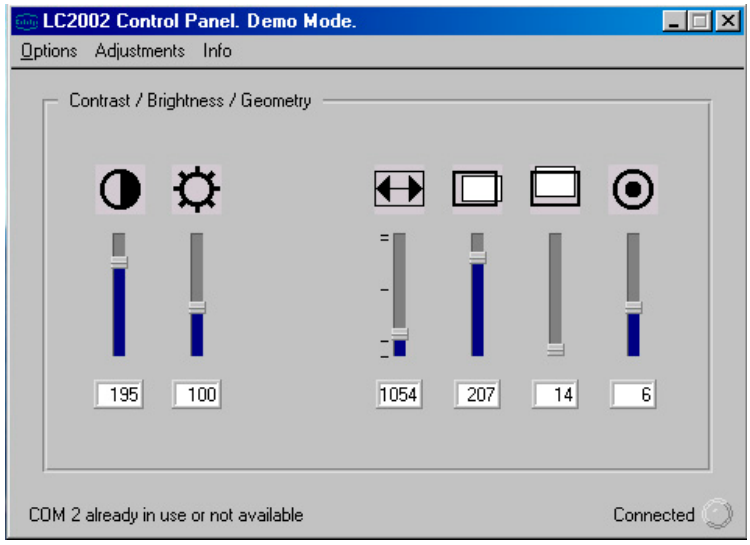

Figure 67: User dialog of the control program after start-up

If no LC2002 device is found to be connected to the RS-232 interface, the error message in Figure 68 will be displayed.

Figure 68: Error message if no LC2002 device has been recognised

In this case, confirm the message to make the program change into the demonstration mode. In this mode no commands are directed to RS-232 port. Then, check if all cables are properly connected to their corresponding ports.

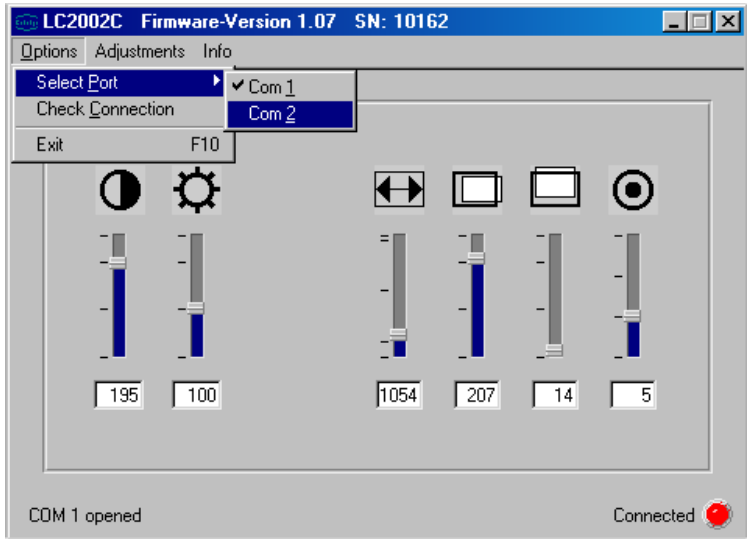

Figure 69: Selection of a COM port

It is also possible to select the COM port from the user dialog. This is shown in Figure 69 where the COM2 port is selected from the menu **Options > Select Port > COM2**. The currently used COM port is marked by a tick

If the selected port is still free, then the status message

COM 2 opened

is displayed in the status bar in the bottom left of the dialog.

In case the selected COM port does not exist or is not free, the message in the status bar states

COM 2 already in use or not available.

Now, if the selected COM port is free, select from the menu **Options > Check Connection** to establish the connection to the LC2002. If the LC2002 is correctly, it is automatically identified and its configuration data are transmitted to the control program.

The user dialog displays the mostly used parameter controls in the field 'Contrast / Brightness / Geometry'.

15.4 Controls: Contrast, Brightness, Geometry

The field 'Contrast / Brightness / Geometry' is obtained by selection of **Adjustments > Video** from the menu and pushing the **F2** button. The controls are


Contrast Control

This control can be used to modify the image contrast.


Brightness Control

This control can be used to modify the image brightness.


Image Width Control

This control can be used to modify the image width. Many technical applications require a very exact control of the image width. For this purpose a test image with a fine stripe pattern is used. If the image width is not adjusted exactly, a Moiré pattern results from the stripe pattern and the pixel structure of the LCD matrix. This Moiré pattern can be seen in the projected test image and vanishes when the image width is correctly adjusted.


Horizontal Image Position Control

This control can be used to modify the horizontal image position.

Vertical Image Position Control

This control can be used to modify the vertical image position.

Image Sharpness Control

This control can be used to modify the image sharpness.

Many technical applications require a very exact control of the image width. For this purpose a test image with a fine vertical stripe pattern and a bright-dark transition is recommended to be used. If the image sharpness is not exactly adjusted, shadow effects (‘ghosts’) can appear. However, if the adjustment is corrected the stripe pattern is rich in contrast and sharpness, and no ghost patterns appear.

15.5 Controls in the Field ‘Gamma Correction’

The ‘Gamma Correction’ function of the LC2002 is supposed to be used in advanced experiments, as it requires experiences to be used in an effective manner. The ‘Gamma Correction’ controls, shown in Figure 70, can be accessed by the menu option **Adjustments > Gamma Control** or by pushing the **F3** key. These controls influence the linearity of the transmission of image brightness signals. Within certain limits, the ‘Gamma Correction’ can be used to equalise non-linearities in the LCD´s transformation of electrical signals into optical transparency signals.

There are four different controls the resulting effect of which is depicted by the image of the transfer function in the centre. Depending on which control is selected the image of the transfer function changes respectively. The grey-scale is used to visualise which video signals, corresponding to grey levels and image location, are influenced by a control

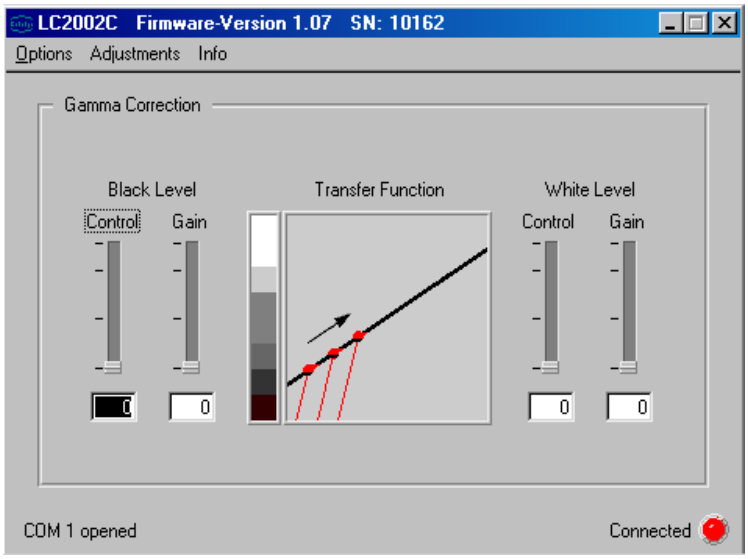

Figure 70: ‘Gamma Correction’ controls

Black Level Control

This control operates on the gamma correction of ‘darker’ image pixels. The control shifts the given correction entry-point onto a certain grey level. With respect to this point all ‘darker’ image pixels, and corresponding image locations, are gamma-corrected.

Black Level Gain

This control specifies the intense of the correction effect on dark image pixels, i.e. the increase of the intense beyond the correction entry-point.

White Level Control

This control operates on the gamma correction of ‘brighter’ image pixels. The control shifts the given correction entry-point onto a certain grey level. With respect to this point all ‘brighter’ image pixels, and corresponding image locations, are gamma-corrected.

White Level Gain

This control specifies the intense of the correction effect on bright image pixels, i.e. the increase of the intense beyond the correction entry-point.

Advice:

After first start-up of the control program all ‘gamma correction’ controls are set to zero, i.e., they have not effect. In order to use the gamma correction in a sensible manner suitable test images and optical instruments for measuring the LCD´s transmission properties are required.

15.6 Controls in the Field ‘Screen Format’

The screen format controls, shown in Figure 71, can be used to modify the image resolution and orientation. They can accessed by the menu option **Adjustments > Screen Format**.

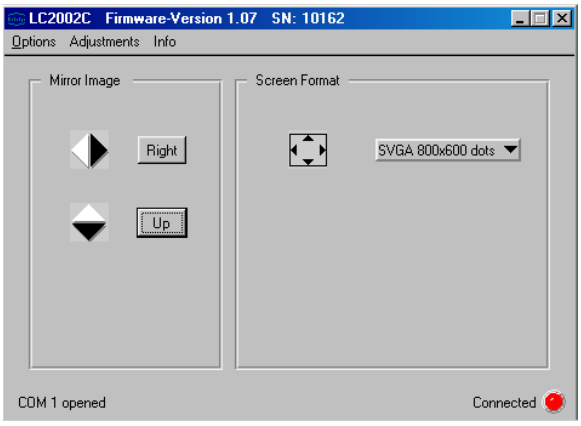

Figure 71: Image orientation and image format

You can use the buttons on the left hand side to mirror the image on the LCD in both directions. This is helpful to make optical experiments more comfortable.

Right Button

Pushing this button mirrors the image horizontally**.**

Up Button

Pushing this button mirrors the image vertically**.**

Format Button

Pushing this button you can select the image format to be applied. Three standard image formats, **SVGA**, **VGA** and **PC-98** are offered for selection. The image is always displayed in a pixel-synchronised manner. That means, images of formats with less than 800 x 600 pixels are centric positioned and have a surrounding black frame.

15.7 Factory Defaults

At every time the driver's configuration memory can be reset to the delivery state. To do this, select *Upload Factory Defaults...* from the *Adjustments* menu, shown in Figure 72.

As shown in Figure 73 a new user dialog appears. Just load the pre-selected *factory.ini*. This will reload the Factory Defaults.

The *lc2002.ini* is used for manufacturer's settings only and should not be utilised by customers.

Remark: The settings are immediately active but it takes up to 10 seconds to save these settings permanently.

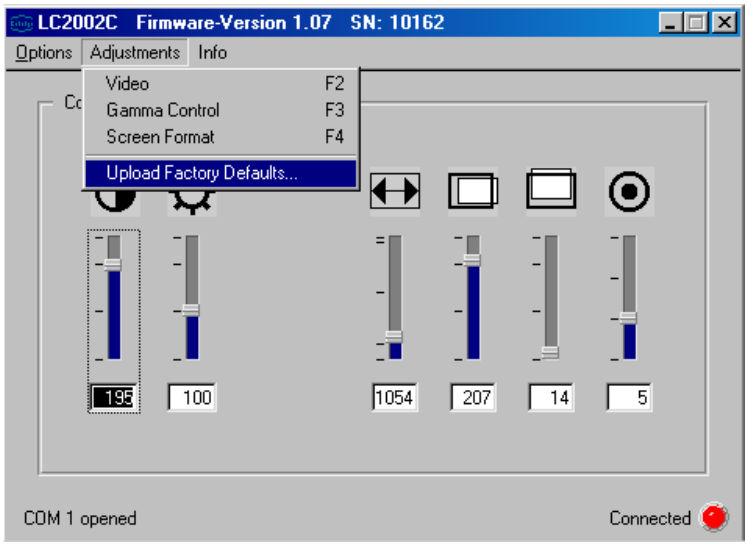

Figure 72: Upload Factory Default

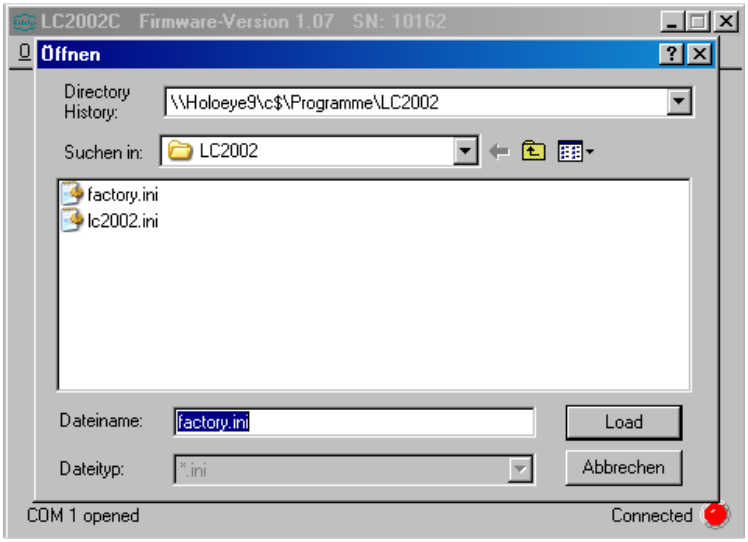

Figure 73: Factory Defaults Setting

16 'OptiXplorer' Software

16.1 System Requirements

- IBM- or compatible PC
- 32 MB main memory or more
- VGA graphics board
- Operating systems: Microsoft Windows 95, Windows 98, Windows NT 4.0, Windows 2000, Windows XP

16.2 Installation of the Software

Start 'installer.exe' and follow the instructions of the installation menu. Please accept the license agreement before choosing the required program components. Mark all checkboxes to install the complete version. Choose the destination folder as well as the start menu folder. Click 'Install' to start the installation procedure and click finally 'Close' to finish the installation.

16.3 Starting the Program

You can start the program by selecting **Programs > OptiXplorer Application Software** in the Microsoft *Windows* 'Start menu'.

If the entry does not exist in your start menu you can start the program by selecting the executable file (e. g. 'OptiXplorer_2.6.exe') from its installation directory.

Upon start-up, the software will determine the number of attached screens. Note that if available multiple screens are operated in a 'display clone mode' so that all attached screens display the same information, the software will recognize only *one* screen.

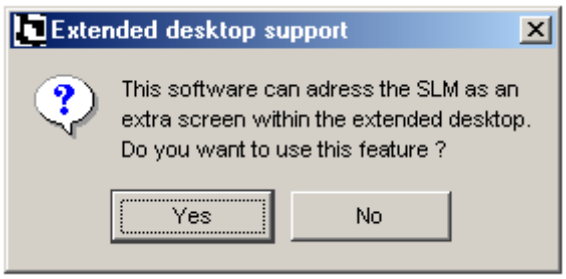

Figure 74: Choice for multiple attached screens

If the software detects more than one screen operated in an 'Extended desktop' configuration, it will determine whether *exactly one* of the non-primary screens has the pixel resolution of the SLM. If this is the case, it will display the message shown in 0

If 'Yes' is selected, the program will display the content of full-screen windows to the SLM with the correct resolution and display a monitor window on the primary screen for a convenient supervision of what is being displayed. Please see section 16.5 for details. If 'No' is selected, the user has to make sure that the signals are display on the SLM by e.g. dragging the windows to the part of the external desktop that corresponds to the SLM.

The operation of the SLM as an external monitor in a 'Display clone mode' of the operating system is of course the most straightforward option. However, there are a few disadvantages of the 'Display clone mode' which make using an 'Extended desktop' configuration attractive.

Firstly, the full-screen window has a boundary (and potentially a button toolbar) which somewhat distort the transmission function of the SLM. Secondly, the operation in 'clone

mode' is only easy if the primary display and the SLM are operated at the same pixel resolution, which may not be desirable. Third, if the PC that controls the SLM should be used for other tasks in parallel, the 'extended desktop mode' permits to do so without interrupting the operation of the SLM.

16.4 Opening an Image

Choose from the *File* menu the point 'Open Image File'. The supported image formats are BMP, PNG, JPEG, GIF, XBM, XPM, MNG and the different PNM formats: PBM (P1 or P4), PGM (P2 or P5), and PPM (P3 or P6). The loaded picture will be transformed to a picture with 256 grey-scale values. In order to display all 256 grey-scale values a monitor setting of minimum 16 Mio. colours (24bit) is required.

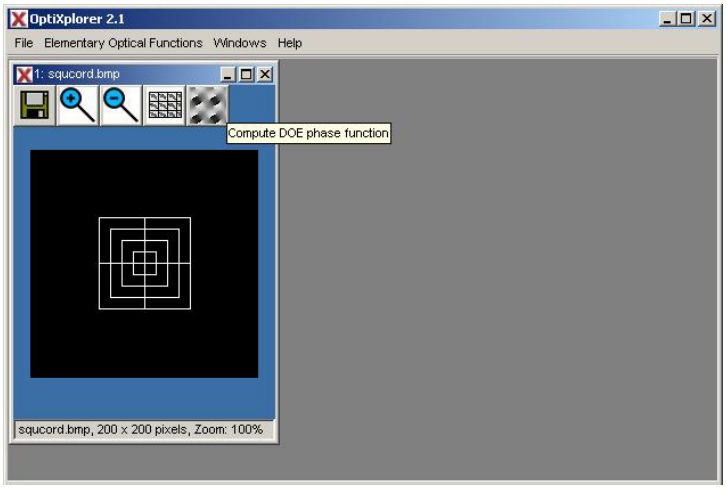

Figure 75: Image window of the application software

It is also possible to open an image by copying it to the clipboard with another application and inserting it into the application with the key combination CTRL-V.

The image window (see Figure 75) will have the following buttons:

'Zoom In' Button

Pushing this button will perform a fast 'zoom in' operation on the image.

'Zoom Out' Button

Pushing this button will perform a fast 'zoom out' operation on the image.

'Save' Button

Pushing this button will open a dialog in which a file name can be specified for saving the image in one of the supported formats (PNG or BMP Image, ASCII text file matrix of integer values representing the grey-scale values).

'Compute DOE' Button

This button will only appear if the displayed image (taking zoom operations into account) is no larger than 200x200 pixels.

When pushing this button a dialog will open in which one can select the number of quantization iteration steps and the number of the DOE phase quantization levels (2^1 to 2^8). 'OK' will start a computation of a Computer-generated hologram (CGH) phase function for the signal displayed in the image window. Please see section 16.6 for more information.

The result of the computation will be displayed in a full-screen window where it can be manipulated as explained in section 16.5.

'Replicate to full screen size' Button

Pushing this button will open a full-screen window in which the shown image is used as a single tile which is replicated until the whole screen is covered.

16.5 Full-Screen window functions

This full-screen image will display a task-bar immediately after its appearance. This taskbar will disappear but emerge again when the position of the mouse pointer of the PC is moved towards the right edge of the window (see Figure 76:).

The functions accessibly by the taskbar buttons offer the possibility to manipulate the 'basic tile' image by superposition of signals that represent optical elements (lens, prisms), by zooming and translating the image and by changing its grey scale values.

Some of the functions can be activated by pressing the buttons or by using a pressing a certain key combination on the keyboard, referred to as hotkeys in the forthcoming list.

The taskbar will have the following buttons:

'Zoom In' Button

Pushing this button will perform a fast 'zoom in' operation on the image that is the basic tile of the displayed image composition. Note that the zoom does **not** change superimposed optical functions, it will only be applied to the 'basic tile'.

'Zoom Out' Button

Pushing this button will perform a fast 'zoom out' operation on the image that is the basic tile of the displayed image composition. Note that the zoom does **not** change superimposed optical functions, it will only be applied to the 'basic tile'.

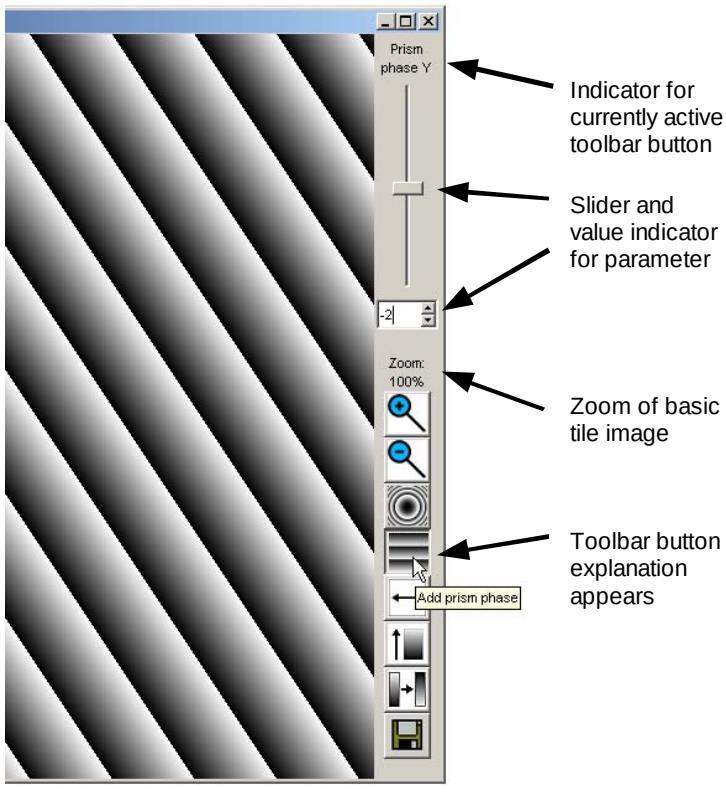

Figure 76: Toolbar of the full-screen window

'Save' Button (Hotkey: CTRL+S)

Pushing this button will open a dialog in which a file name can be specified for saving the full-screen image in one of the supported formats (PNG or BMP Image, ASCII text file matrix of integer values representing the grey scale values). The image will be saved as displayed, i.e. including effects by superposition of optical functions etc.

'Superimpose lens' Button (Hotkey: CTRL+L)

This button will superimpose the displayed image with a XY grey scale signal that resembles the optical phase function of a lens. This means that the focal plane of the light source incident on the LC Display is changed when such function is superimposed.

The focusing/defocusing strength of the optical lens function can be changed by adjusting the value given on the task bar by moving the slider or by directly entering a value.

'Superimpose prism in *X* direction' Button (Hotkey: CTRL+P)

Pushing this button will superimpose the displayed image with a grey scale signal that resembles the optical phase function of a prism in X direction. This means that all diffraction angles created by the signal on the LC Display are changed when such function is superimposed.

The strength of the optical prism function can be changed by adjusting the value given on the task bar by moving the slider or by directly entering a value.

In order to switch to a prism superposition in Y direction, click on the button again.

 **'Superimpose prism in *Y* direction' Button (Hotkey: CTRL+P)**

Pushing this button will superimpose the displayed image with a grey scale signal that resembles the optical phase function of a prism in Y direction. This means that all diffraction angles created by the signal on the LC Display are changed when such function is superimposed.

The strength of the optical prism function can be changed by adjusting the value given on the task bar by moving the slider or by directly entering a value.

In order to switch back to a prism superposition in X direction, click on the button again.

 **'Adjust Grey level 1' Button (Hotkey: CTRL+G)**

This button will only be accessible if the 'basic tile' image is binary, i.e. consists of only two different grey level values.

Pushing this button will than permit a change of one of the two grey scale values by moving the slider or by directly entering a value.

 **'Adjust Grey level 2' Button (Hotkey: CTRL+G)**

This button will only be accessible if the 'basic tile' image is binary, i.e. consists of only two different grey level values.

Pushing this button will than permit a change of the second of the two grey scale values by moving the slider or by directly entering a value.

 **'Adjust Gamma curve' Button (Hotkey: CTRL+G)**

This button will be accessible if either the 'basic tile' image is binary and a lens and/or prism functions are superimposed, or if the 'basic tile' image is not binary.

Pushing this button will than permit a simultaneous change of all grey scale values by moving the slider or by directly entering a value. The gamma curve is linear if the entered value is 0, and can be changed to concave and convex nonlinear curves by entering positive and negative values, respectively.

 **'Invert displayed bitmap' Button (Hotkey: CTRL+I)**

This toggle button will invert the grey scale value of the displayed full-screen image. This includes any superimposed lens and or prism functions. This inversion can be reversed simply by clicking the button again, which will cause the button to be no longer toggled.

 **'Translate in *X* direction' Button (Hotkey: CTRL+M)**

Pushing this button will move the shown image with respect to the X direction. This function can be used to align the displayed functions with respect to the incident beam.

Note that the translation does change the 'basic tile' **and** any superimposed optical functions (if present) simultaneously.

In order to switch to a translation in Y direction, click on the button again.

 **'Translate in *Y* direction' Button (Hotkey: CTRL+M)**

Pushing this button will move the shown image with respect to the X direction. This function can be used to align the displayed functions with respect to the incident beam. Note that the translation does change the 'basic tile' **and** any superimposed optical functions (if present) simultaneously.

In order to switch back to a translation in X direction, click on the button again.

 **'Connect to SLM' Button – Disconnected state**

This button is only visible if the software is operated in the 'extended desktop support mode' (see section 16.3 for details how to achieve this). Toggling this button will change the button to a green traffic light button, and the displayed bitmap of the full-screen window will be displayed as a frameless window on the SLM. If another full-screen window is already 'connected' to the SLM in this way when the button is toggled, it gets automatically disconnected.

 **'Connect to SLM' Button – Connected state**

This button is only visible if the software is operated in the 'extended desktop support mode' (see section 16.3 for details how to achieve this) and the button has been toggled before. In this case the 'bitmap content' of the window is currently displayed at the connected SLM. Toggling this button will change the button to a red traffic light button, and the SLM screen will be erased and reveal whatever is displayed underneath (other windows or the desktop background).

16.6 Calculating a diffractive optical element (DOE)

To compute a DOE, the signal image size needs to be smaller than 200x200 pixels. DOE computation for larger pictures is not supported by this software.

Load the image as described in section 16.4. If the image is not larger than the supported size pixels the **'Compute DOE' Button** will appear with the option to calculate a diffractive optical element (DOE) for this image.

By pressing the button a dialog window (see Figure 77) will open in which one can modify parameters for the calculation of the iterative Fourier Transformation Algorithm (IFTA) (see also section 4.6.1). One can modify the number of quantization iteration steps and the number of DOE phase quantization levels. More iteration steps improve the quality of the reconstructed image but increases the computing time. A phase DOE with 256 grey level only needs a small number of iteration steps. On the other hand a binary DOE needs significantly more iteration steps for a comparable quality of the reconstructed image. 'OK' starts the calculation. Note that the process of computing may take a while, depending strongly on the signal picture size.

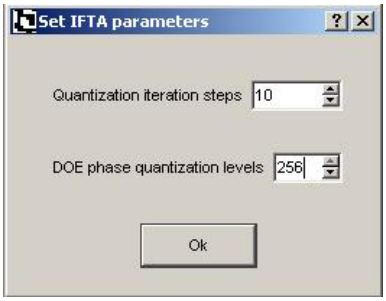

Figure 77: Dialog for entering IFTA parameters

When the process is finished, two windows will appear. They show the DOE phase function (in a full-screen window) and the calculated intensity of the diffraction pattern. This calculated intensity should look quite similar to the image in the original window, if the DOE calculation algorithm has properly converged.

16.7 Creating elementary optical functions

All optical functions from the menu point *Elementary Optical Functions* appear in a new window after input of the required parameters. Depending on the optical function, binary or multilevel, the task bar of the full-screen window will be slightly different (compare section 16.5)

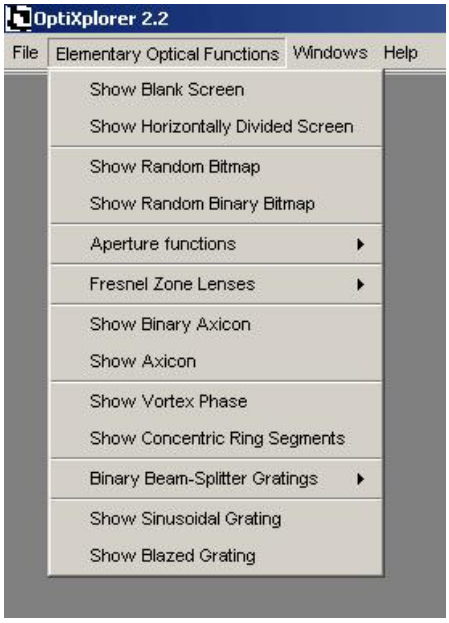

Figure 78: Menu entries for optical functions

- Blank screen

  With this function you can create a homogeneous grey level screen. If the mouse pointer is moved to the right edge of the window a taskbar for changing the addressed grey level occurs.

- Horizontally Divided Screen

  With this function you will create a horizontally divided screen, consisting of two homogeneous grey level partial screens. If the mouse pointer is moved to the right edge of the window a taskbar for changing the addressed grey levels occurs.

- Random Bitmap

  With this function you will create a random pixel distribution using 256 grey scale values. This function can be used to realize the optical function of a random phase plate.

- Random Binary Bitmap

  With this function you will create a random pixel distribution using only two grey scale values. This function can be used to realize the optical function of a random binary phase plate.

- Rectangular Aperture

  Use this function from the menu point *Aperture Functions* to create a rectangular aperture. The size of the aperture can be defined by specifying the aperture width and aperture height. With the sliders on the taskbar one can change the grey levels of the background and of the aperture.

- Circular Aperture

  Use this function from the menu point *Aperture Functions* to create a circular aperture. The radius of the aperture can be defined by specifying a numbers of pixels. With the sliders on the taskbar one can change the grey levels of the background and of the aperture.

- Single Slit and Double Slit

  To create a single slit choose the point 'Show Single Slit' from the menu point *Aperture Functions*. The slit width can be defined by the number of pixels in the dialog window.

  To create a double slit choose the point 'Show Double Slit' from the menu point *Aperture Functions.* Moreover the slit distance can also be defined. This refers to the gap between both slits.

- Binary Fresnel Zone Lens

  Use this function from the menu point *Fresnel Zone Lenses* to create a Binary Fresnel Zone Lens grey level image representation. In the dialogue field the lens function can be characterized by the radius of the smallest ring, which is defined by a number of pixels.

- Fresnel Zone Lens

  Use this function from the menu point *Fresnel Zone Lenses* to create a 256-level Fresnel Zone Lens grey level image representation. In the dialogue field the lens function can be characterized by the radius of the smallest ring, which is defined by a number of pixels. It can be specified whether the image representing the lens should be positive or negative.

- Cylindrical Fresnel Zone Lens

  Use this function from the menu point *Fresnel Zone Lenses* to create a 256-greylevel image representation of a Cylindrical Fresnel Zone Lens. In the dialogue field the lens function can be characterized by the width of the central zone, which is defined by a number of pixels. The angular orientation of the cylindrical lens can be entered in degrees (integer values only).

- Binary Axicon

  Use this function to create a Binary Axicon grey level image representation. In the dialogue field the lens function can be characterized by the radius of the smallest ring, which is defined by a number of pixels.

- Axicon

  Use this function to create a 256-level Axicon grey level image representation. In the dialogue field the axicon function can be characterized by the radius of the smallest ring, which is defined by a number of pixels. It can be specified whether the image representing the lens should be positive or negative.

- Vortex Phase

  Use this function to create a 256-greylevel image representation of a vortex phase. In the dialogue field the radius a central zone with constant phase can be specified as a number of pixels. The angular orientation of the line where the phase changes from 0 to 2π can be entered in degrees (integer values only).

- Concentric ring segments

  Use this function to create binary images consisting of concentric ring segments. In the dialogue field the image function can be characterized by the radius of the smallest ring, which is defined by a number of pixels, and the desired number of segments, which can be varied from two to 20 (even numbers only).

- Linear Gratings and Crossed Linear gratings

  Choose from the menu *Binary Beam-Splitter Gratings* the item 'Show Binary Linear or Separable 2D Grating' to create a grating. A dialog window opens in which the number of transition points (0 to 6) in vertical and horizontal direction can be selected. Depending on the number of transition points the pixel number of the ridges and grooves can be modified. Below the position of the transition points and the grating period in pixel is shown.

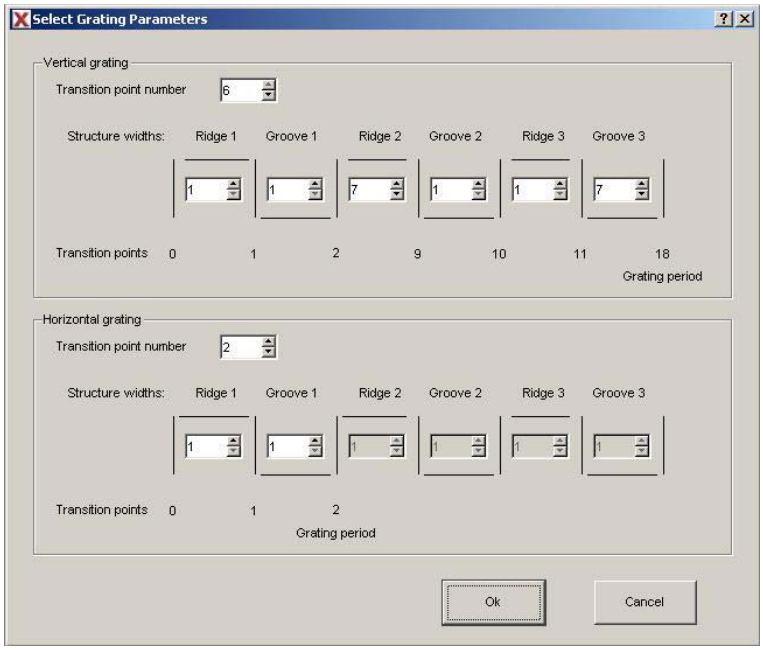

Figure 79: Window for creating two dimensional gratings

- Exemplary binary beam-splitter designs

  Choose from the menu *Exemplary Binary Beam-Splitter Designs* one of the menu items

- 'Show Binary Linear 1-to-5 Linear Beamsplitter Grating' (Grating period 26 Pixels)
- 'Show Binary 1-to-(2x2) Separable Array Beamsplitter Grating' (Grating period 18 Pixels)

- ‘Show Binary Array 1-to-(5x5) Separable Array Beamsplitter Grating’ (Grating period 26x26 Pixels)
- ‘Show Binary Array 1-to-(5x5) Non-separable Array Beamsplitter Grating’ (Grating period 26x26 Pixels)

to obtain a full-screen window with one of the mentioned diffractive elements.

The basic tiles of these gratings are fixed and usable as examples for separable and non-separable binary DOEs.

- Sinusoidal Grating

  Choose from the menu point Elementary Optical Functions ‘Show Sinusoidal Grating’ to create a sinusoidal grating. The size of the grating period can be specified by the number of pixels.

- Blazed Grating

  Choose from the menu point *Elementary Optical Functions* ‘Show Blazed Grating’ to create a blazed grating. The size of the grating period can be specified by the number of pixels.

16.8 The ‘Window’ Menu

The Menu ‘Windows’ contains the usual options for tiling, cascading and closing windows that are opened inside the main window.

When full-screen windows are open outside the main window, they can be closed via a separate menu point ‘Close all windows outside the main window’. Of course the menu item ‘Close all windows inside the main window’ does not affect full-screen windows outside and vice versa.

17 'PhaseCam' Software

The PhaseCam software is used for interferometrical determination of the phase shift of a display. The single software functions are described here, for the complete measuring procedure please refer to module INT.

17.1 System Requirements

- IBM- or compatible PC
- 32 MB main memory or more
- VGA graphics board
- Operating systems: Microsoft Windows 95, Windows 98, Windows NT 4.0, Windows 2000, Windows XP
- USB-camera, e. g. Webcam, CCD-camera with USB-converter

17.2 Installation of the Software

In order to make a successful installation, you should make sure that you have sufficient privileges in the computer's operating system. You should be permitted to create a directory in the directory that contains programs and copy files into that directory, and to write into the 'all users' section of the start menu of your operating system. Of course administrator privileges will be sufficient for all these operations.

Start 'setup.exe' in the PhaseCam folder and follow the instructions of the installation menu. Please accept the license agreement. Choose the destination folder as well as the start menu folder. Click 'Install' to start the installation procedure and click finally 'Close' to finish the installation

17.3 User Interface

Figure 80 shows the user interface of the software. It can be seen that it is basically divided into two parts. The part on the left hand side is used to set the measurement properties. On the right part the camera image will appear. The control part consists of 6 category groups which will be explained in this section.

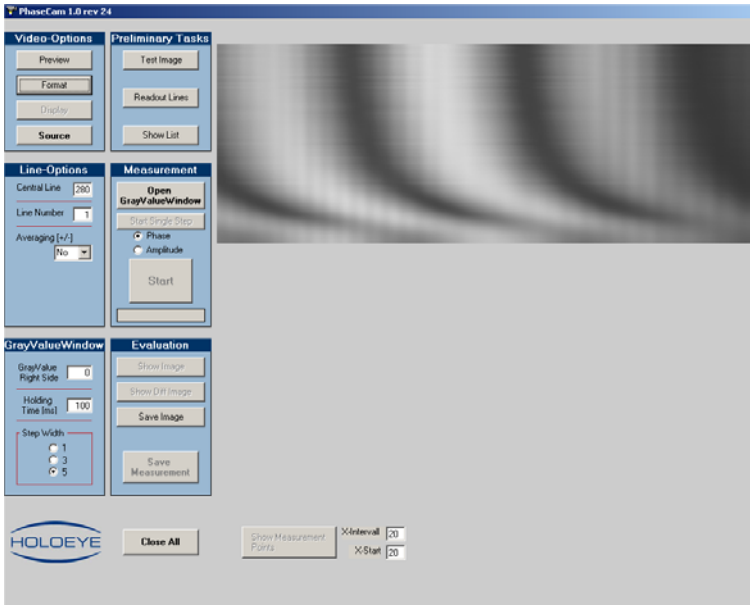

Figure 80: User interface

17.4 Video Options

Preview

This function displays the live stream of the used camera (web cam, CCD).

Format

This opens a dialog window where the screen resolution can be selected. If USB 1.1 is used the resolution will be limited to 320x240 pixel. This button as well as the 'Display' button is inactive if the camera does not provide this function.

Source

If the source button is pressed the user can control basic settings of the camera (e.g. brightness, contrast…) to get an optimal interference pattern.

17.5 Preliminary Tasks

Test image

With that function a stable test image will be recorded by the CCD camera and displayed on the right side of the user interface. This image is used for selecting the measurement line.

Readout Lines

If the 'test image' and the measurement line have been selected, the location of the minima and maxima as well as the period of the interference pattern can be determined. These values will appear on the lower right part of the user interface (see Figure 81). Pressing 'readout lines' the intensity distribution is shown in a graph (Figure 82).

The column where the software starts to search for a minimum can now be selected in the small window 'X-Start'. It should not exceed the value of 250. 'X-Interval' is the number of columns which are used by the program to search for a minimum around the 'X-Start' value.

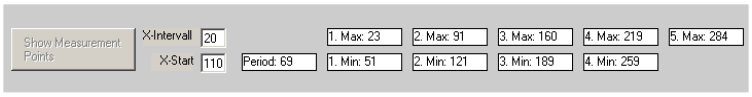

Figure 81: Min., max and period of the measurement line

Show List

This button lists the intensity distribution of the selected measurement line in a table.

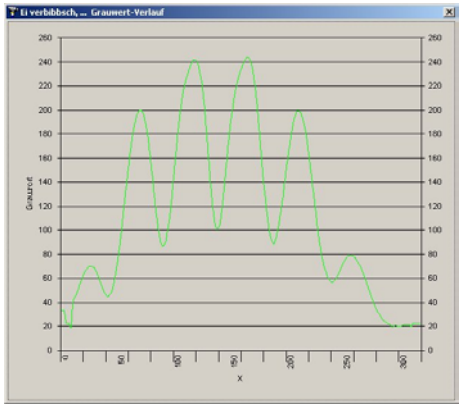

Figure 82: Greylevels for the selected measurement line

17.6 Line Options

Central line

By pressing the right mouse button inside of the ‘test image’ the measurement line will be selected. The selected line should have maximal interference contrast. The effective line number can be seen in the small window right beside ‘central line’.

Line number

Here the user can set the amount of measurement lines around the central line.

Averaging [+/-]

This function can be used to avoid saturation of the camera by averaging a certain amount of columns of the measurement line. This option also smoothes the interference pattern. Figure 83 shows the benefit of averaging.

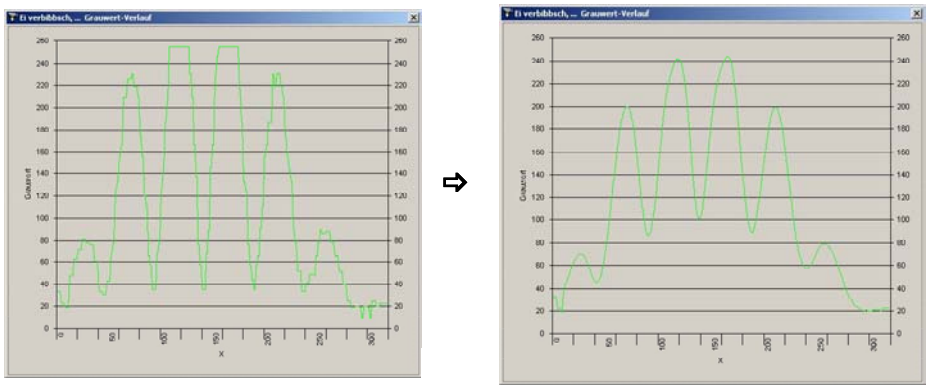

Figure 83: Averaging

17.7 Grey Value Window

Grey Value Right Side

This function enables the selection of the reference grey value.

Holding Time [ms]

This function belong to an earlier version of this software and is now obsolete.

Increment

Here one can choose the grey level increment of the measurement. Increasing the increment shortens the measurement time but on the other hand reduces the accuracy.

17.8 Measurement

Open Grey Value Window

This opens the grey value window which will be addressed onto the panel. Using the display as a second monitor (‘extended desktop’), one has to move the window to the corresponding part of the desktop and maximize it. The Windows screen magnifier can be used to control the correct position of the window.

Start Single Step

The user can increment the grey level of the active display half manually.

Phase/Amplitude

This option changes the mode of addressing. If phase mode is activated both display halves will be addressed independently.

If amplitude mode is active the display will be addressed with homogeneous grey level. All buttons which are only necessary for the evaluation of the interference pattern will be blocked.

Start

This starts the automatic measurement.

17.9 Evaluation

Show Image

If the measurement is finished, all lines per grey level will be displayed below each other (see Figure 84). By pressing ‘Show measurement points’ each measured minimum will be shown as a red point. Also a dialog will open to save the measurement.

Figure 84: Measurement image

Show Diff Image

A two coloured image of the upper image will be displayed (see Figure 85).

Figure 85: Differential image

Save Image

This function saves the shown measurement image.

Save Measurement

This saves the measurement values in a .txt file including the period of the interference pattern and the position of the measured line for each addressed grey level.

18 LabView™-Software ‘DynRon’

18.1 System Requirements

- IBM- or compatible PC capable for running LabView™
- LabView™ by National Instruments (version 8.2 or higher)
- VGA graphics board with two ports
- Detector with a PC interface to readout the measurement points
- Hardware used in the program:
  Photodiode with amplifier as the detector connected to an AD converter ‘LabJack U12’, which sends the voltage signal (which is proportional to the light power) via USB to the PC

18.2 Installation of the Software

Run the program DynRon with its SubVI’s as a virtual instrument in LabView™.

This program is written for the following measurement setup: A photodiode with amplifier is used as the detector. The ‘LabJack U12’ A/D converter sends the photovoltage values to the pc. The program can be adapted to different measurement setups. Therefore the SubVI ‘stream_photovoltages.vi’ for the data readout has do be modified or replaced.

18.3 User Interface

In Figure 86 the user interface is shown. The window is divided into two parts, the upper half is used for the input of the parameters, the lower half displays the measurement data.

18.4 Draw parameters

general

- display resolution

  Enter the resolution of the used display in these boxes. This will be the size of the grey level images drawn by the program.

- picture to be drawn

Select the grey level image to be drawn. ‘Blank Screen’ will display a homogeneous grey level image. ‘Ronchi grating: horizontal’ will display a horizontal Ronchi grating and ‘Ronchi grating: vertical’ a vertical Ronchi grating which create vertical and horizontal diffraction orders, respectively.

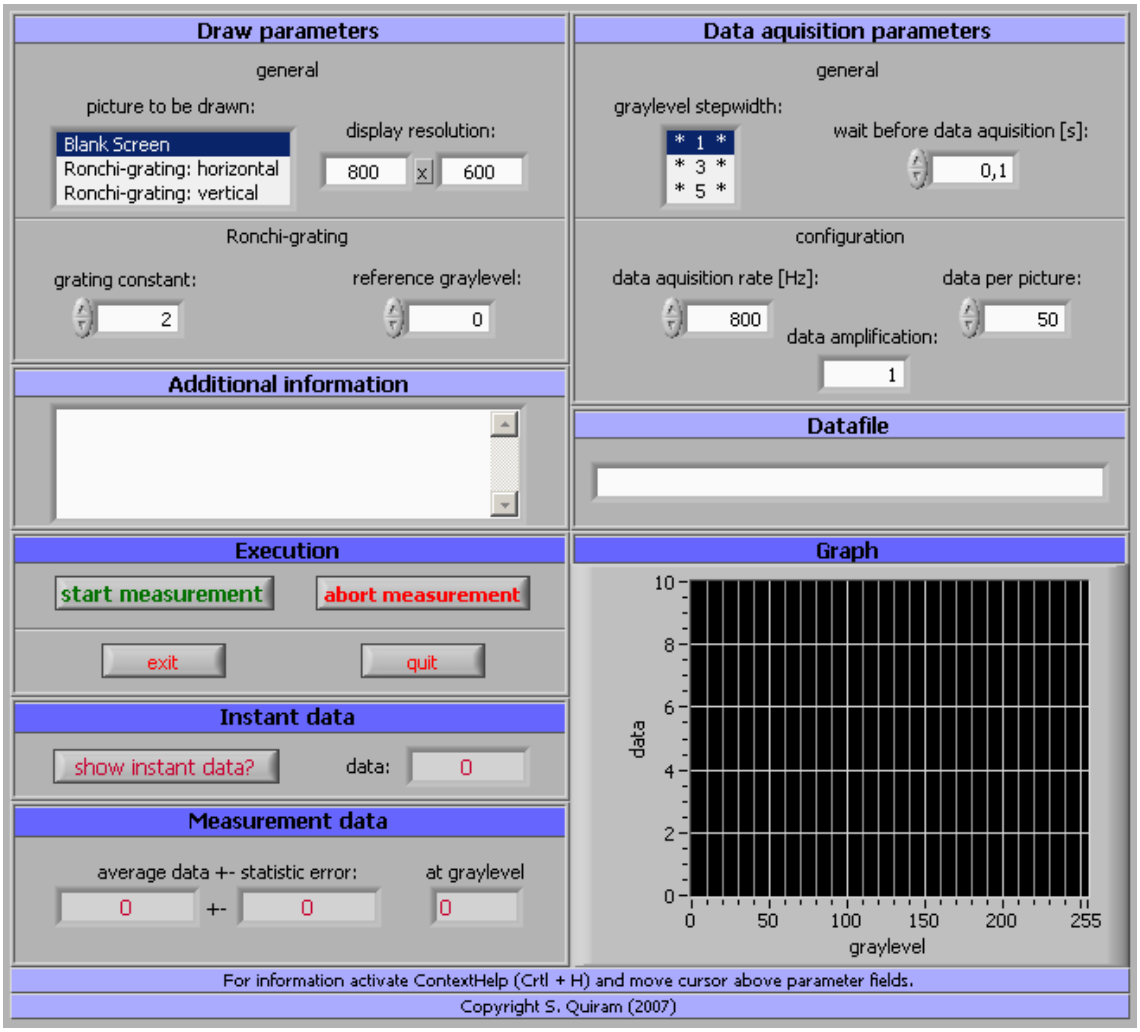

Figure 86: User interface of the program DynRon

grating

- grating constant

  This function defines the period of the Ronchi grating in pixel. Therefore the minimum is '2' corresponding to a grating period $g = 2 \cdot$pixel size of the display.

- reference grey level

  During the measurement one of the two grey level of the Ronchi grating will be constant while the other one will vary. Here the value for the constant grey level can be set.

18.5 Data acquisition parameters

general

- grey level step width

  Select the step width (1, 3 or 5) for the shifting of the grey level (from 0 to 255) during the measurement.

- wait before data acquisition

  This function defines the delay after addressing a new grey level before the data acquisition starts. The liquid crystal molecules needs a certain time to realign in the modified electrical field.

configuration

- data acquisition rate

  Select the frequency for the data acquisition for a single image. The frequency can vary between 200 Hz and 1200 Hz corresponding to a delay of 5 ms to 0.83 ms.

  This settings are fitted to the 'LabJack U12' setup. For a different setup this can be realized with a time delay. One has to have in mind the execution time for the data acquisition (i. e. the SubVI's). This defines the minimum time interval.

- data per picture

  Select the number of data points per addressed grey level image to average the measured power. For example, this can minimize the error caused by fluctuations of the laser. Also it is possible to characterize digital addressed light modulators which shows fluctuations because of a type depending over modulation.

  Here a special SubVI for the 'LabJack U12' is used, too. For different setups it is recommended to program a loop with a time delay fitted to the 'data acquisition rate'.

- data amplification

  This parameter is used to normalise the acquired data points if a detector with an adjustable amplification is used. It has no other influence to the program.

  Attention: This parameter does not modify the amplification in the circuit of the photodiode! Rather the amplification of the circuit is fed to the program.

18.6 Additional information and Datafile

- additional information

  Here one can enter comments before the measurement starts. These comments will be saved in the measurement file.

- datafile

  Here one can enter the desired name of the measurement file or the whole file path respectively. If necessary the program opens a dialog window to enter these parameters after the measurement is finished.

18.7 Execution

- start measurement

  Starts the measurement with the selected parameters.

- abort measurement

  Abort the measurement. The data which has been acquired until then will be saved in the file.

- exit

  Finishes the execution of the LabView™ VI.

  Note: This option is only active when no measurement is running.

- quit

  Finishes the program-VI and the main LabView™ program.

  Note: This option is only active when no measurement is running.

18.8 Instant data

- show instant data?

  This function displays the actual measured value without starting a measurement.

- data

  Here the actual data is displayed to align the setup. This can be an advantage, when the detector has no display of its own.

18.9 Measurement data

- average data ± statistic error

  During the measurement the actual mean and the statistical error are displayed. The displayed error offers to check e.g., if the number of data points per image is enough or if the power is fluctuating.

- grey level

  Displays the actual grey level used for the average data.

18.10 Graph

The graph shows the obtained data against the grey level. Here one can check the reproducibility of the measurement or compare the measured with the expected data.

18.11 Overview of the ‘DynRon’ software

If one is not familiar with LabView™ it is recommended to learn the basics with the ‘Getting started’ tutorial. In the following overview it is assumed that certain basic LabView™ terms are known.

A program created with LabView™ is called a VI (virtual instrument), it consists of two parts, a front panel and a block diagram.

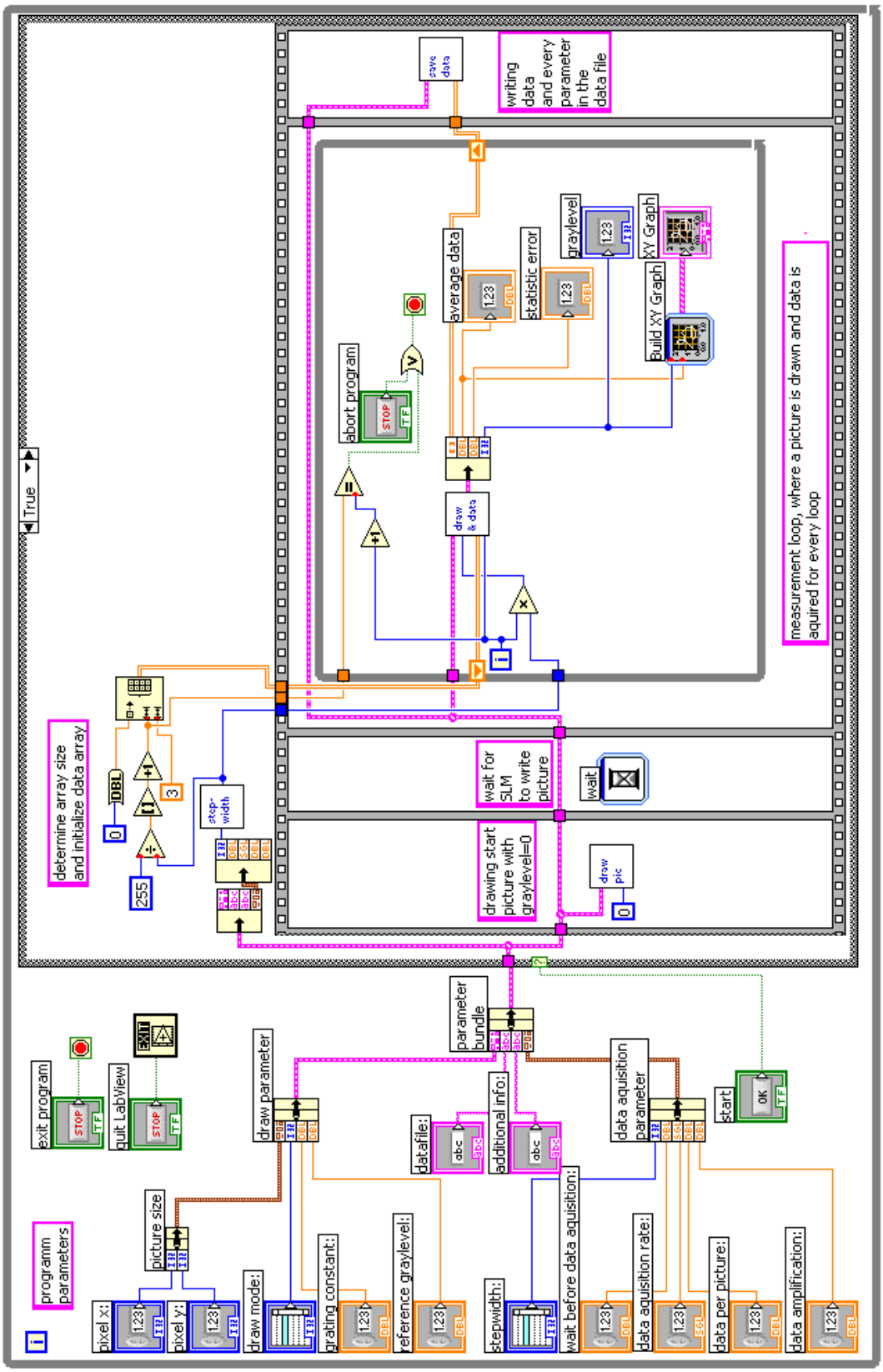

Figure 87: Block diagram of the LabView™ program ‘DynRon’ in the ‘true-case’

The front panel corresponds to the user interface of a program and is used to control the program and interact with the user (see Figure 86). For example, it can be used to display the measured data. Each element of the front panel corresponds to an element in the block diagram which contains the programming. In the block diagram elements are connected with wires. In Figure 87 the block diagram for the 'true-case' (i.e. the measurement has just started) is shown.

The block diagram illustrates the layout of the program 'DynRon'. In a VI further programs can be included as SubVI's. The handover of the parameters and the output of the results is realized via so called 'connectors' at the icon of a SubVI. On the left half of the block diagram are the input parameters located which are set by the front panel before the start of a measurement. When the measurement start these parameters are passed in a bundle. Until a measurement is started the program runs the 'false-case' sequence which contains the 'instant data' part. This is shown in Figure 88.

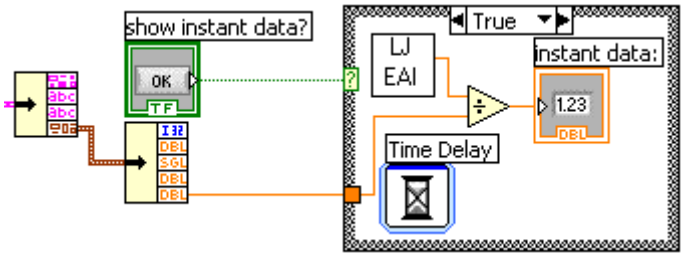

Figure 88: Part of the block diagram of the program for the 'false-case'

If the measurement is started, the program jumps into the 'true-case' as shown in Figure 87. The bundle with the parameters is passed to a 'flat sequence'. In the first part a starting image with the grey level 0 and in the case of the Ronchi gratings, the selected reference grey level. Therefore the SubVI 'draw_pictures.vi' is used. Depending on the input parameters from the front panel this SubVI, as shown in Figure 89, starts another SubVI which opens a second front panel on the second monitor, normally the light modulator, and addresses the selected grey level image.

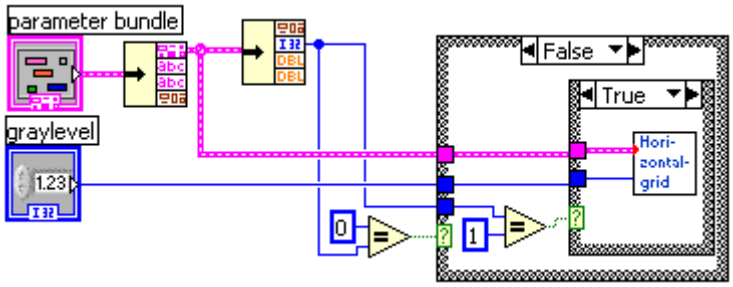

Figure 89: block diagram of the SubVI 'draw_picture.vi'

Here the SubVI 'draw_uniform_greylevel.vi' is introduced representing all the 'draw' SubVI's. Figure 90 shows the block diagram of this SubVI. It draws a rectangle filled with the selected grey level and the size corresponding to the selected display resolution. In the 'VI-Properties' it is selected that the front panel is addressed on the second monitor if one is connected.

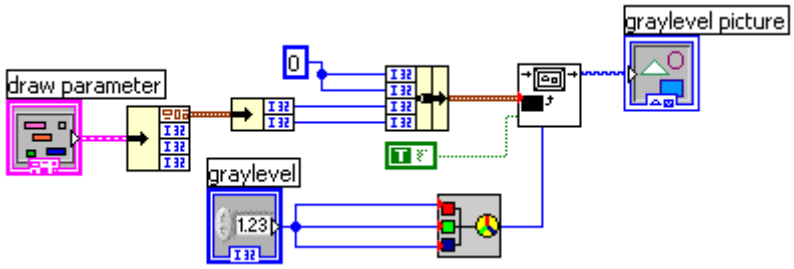

Figure 90: Block diagram of the SubVI ‘draw_uniform_greylevel.vi’

After drawing the first image the main program pauses the selected time before it starts the measuring loop. The parameter bundle, the step width, the calculated number of data points and an initialized array are passed to this loop. In the loop the data will be passed to the SubVI ‘measurement_sequence.vi’ with the icon ‘draw & data’ (see Figure 91)

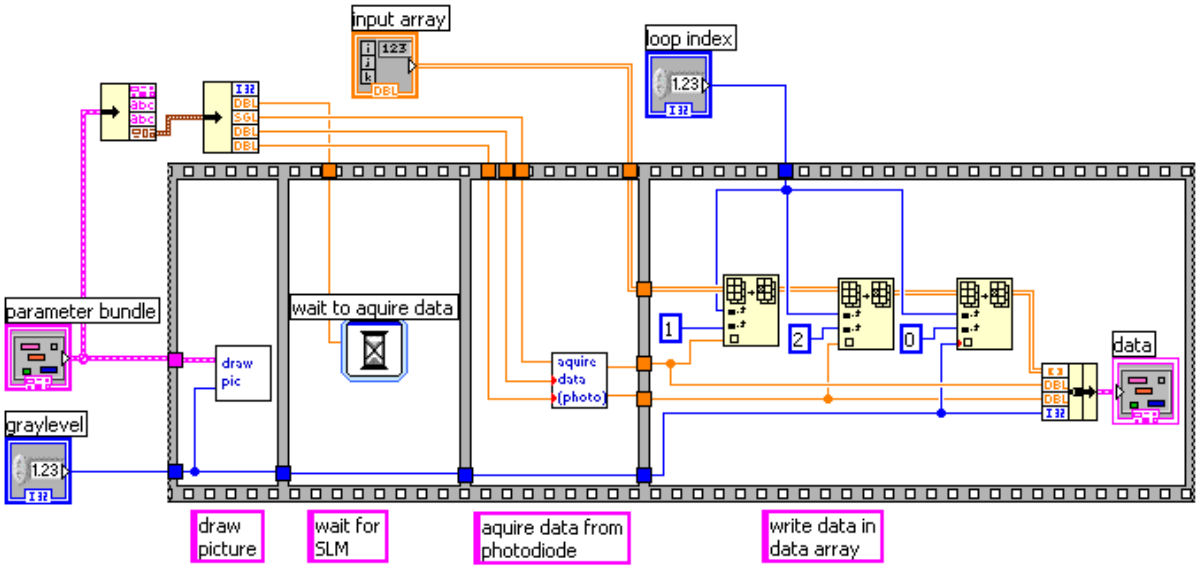

Figure 91: Block diagram of the SubVI ‘measurement_sequence.vi’

Corresponding to the loop index this SubVI first draws a grey level image using the SubVI ‘draw_pictures.vi’ and then waits the delay time which was defined on the front panel (‘wait to acquire data’). After that the data acquisition starts by calling the SubVI ‘aquire_data.vi’, which calculates the mean and the statistical error from the acquired data points. The SubVI ‘measurement_sequence.vi’ puts these results into the initialized array.

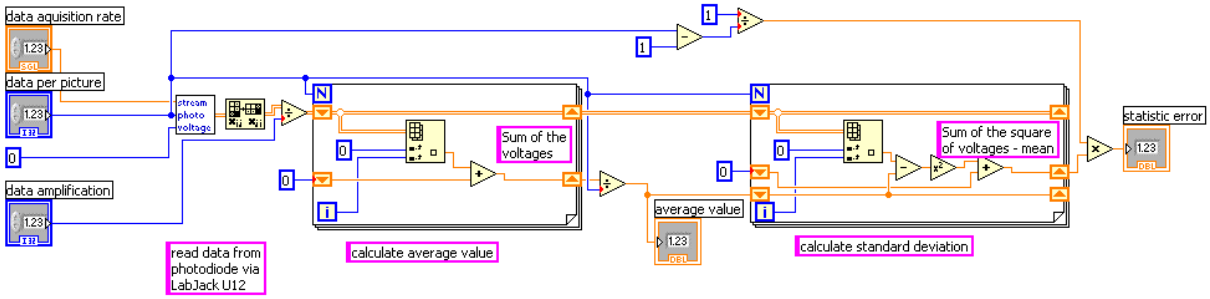

Figure 92: Block diagram of the SubVI ‘aquire_data.vi’

The SubVI ‘aquire_data.vi’ (see Figure 92) uses the SubVI ‘stream_photovoltages.vi’ which is particular designed for the used setup based on a virtual ‘LabJack U12’ instrument. When using a different setup this SubVi has to be modified or replaced.

In the main program the acquired data will be shown on the front panel using indicators for each loop. The graph is realized with the SubVI's ‘Build XY Graph’ and ‘XY Graph’ included in the LabView™ software.

After finishing or after aborting the measuring loop in the main program the acquired data will be saved using the SubVI ‘save_data.vi’, see Figure 93.

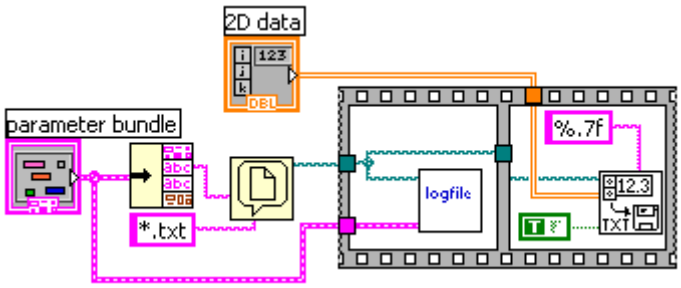

Figure 93: Block diagram of the SubVI ‘save_data.vi’

As seen in the block diagram, ‘save_data.vi’ contains a request for the path if no path is selected on the front panel, a SubVI ‘logfile.vi’ and a slightly modified version of the LabView™ VI ‘write spreadsheet to file.vi’ to write the data into a .txt file. The SubVI ‘logfile.vi’ saves all input parameter selected on the front panel in the measuring file.

After finishing the ‘true-case’ the program is ready to start a new measurement.

Remarks

If you have technical questions about the device, please get in contact with HOLOEYE at:

optixplorer@holoeye.com

HOLOEYE Photonics AG
Albert-Einstein-Str. 14
D-12489 Berlin

contact@holoeye.com
www.holoeve.com